University of La Laguna

Departament of Biochemistry, Microbiology, Cellular Biology and Genetics and Departament of Internal Medicine, Dermatology and Psichiatry.

PhD in Biomedical Sciences

ALTERATIONS IN GENE EXPRESSION INDUCED BY OXALIPLATIN-BASED CHEMOTHERAPY IN COLORECTAL CANCER

by Deborah Rotoli

Director: Dr. Pablo Martín Vasallo

Co-directors:

Dr. Julio Ávila Marrero, Dr.Manuel Morales González

.

May 2017

Cover image:
Double immunofluorescent staining
of AmotL2 protein (green) and the
pan-macrophage and endothelial/
pericyte marker CD31 (red) on
human CRC tissue section.

Universidad de La Laguna

Doctorado Ciencias Biomédicas

Biomedicina · Biotecnología · Másteres

Titulaciones Verificadas por ANECA
(BOE 305, 16-12-2010; BOE 47, 24-2-2011)

PhD in Biomedical Sciences.

ALTERATIONS IN GENE EXPRESSION INDUCED BY OXALIPLATIN-BASED CHEMOTHERAPY IN COLORECTAL CANCER

Author: Deborah Rotoli

A dissertation submitted to the University of La Laguna to obtain the PhD degree in *Biomedical Sciences.*

Director: Dr. Pablo Martín Vasallo

Co-directors:

Dr. Julio Ávila Marrero

Dr. Manuel Morales González.

La Laguna, may 2017

APPROVAL OF THESIS DIRECTORS

Pablo Martín Vasallo and Julio Ávila Marrero, both Professors of the Department of Biochemistry, Microbiology, Cellular Biology and Genetics of La Laguna University, and Dr. Manuel Morales González, Head of the Service of Medical Oncology, Hospital Universitario Nuestra Señora de Candelaria and Associate Professor of the Department of Internal Medicine , Dermatology and Psichiatry, University of La Laguna.

CERTIFY:

Deborah Rotoli has carried out under our supervision the research works in order to obtain the degree of Doctor. The thesis presented is entitled:

"ALTERATIONS IN GENE EXPRESSION INDUCED BY OXALIPLATIN-BASED CHEMOTHERAPY IN COLORECTAL CANCER"

Revised the present report, we estimate it meets the requirements to qualify for PhD degree and, consequently, authorize the presentation to public defence.

This certification is issued in La Laguna 22 of May 2017.

Dr. Pablo Martín Vasallo

Dr. Julio Ávila Marrero

Dr. Manuel Morales González

To my beloved father

ANKNOWLEDGMENTS

In this five years of my PhD course I had the opportunity to meet and interact with special people whom now I would like to thank:

My PhD Directors, Pablo Martín Vasallo, Manolo Morales and Julio Ávila, for giving me the possibility to achieve this goal, for their trust in me, for their support and for sharing with me their knowledge. A special thanks to Pablo, not only because of its ability to get the best out of people and for his advices, as well as his availability, even in holidays, but also for all the amazing canary food tasted during these years. Yummy!!!! 😋

Dr. Mari Carmen Maeso, for sharing with me her knowledge in pathological anatomy, for selecting and providing the tissue samples used in this study, for her availability in times of need, for her precious advices on how to manage the samples and on the analysis of the data obtained.

Professors Lucio Díaz Flores and Ricardo Gutierrez, for sharing with me their long experience and knowledge in pathological anatomy and for all the precious advices and help.

Professors Nélida Brito Alayón and Celedonio González Díaz, for their availability, advices and kindness.

All the friends and colleagues of the lab, Rebeca, Rita, Oscar, Elisa, for their help and advises and for their kindness. A special thanks to Rebeca for making me feel comfortable in the lab since the first days of my arrival, for all the help given, for being always ready to offer suggestions and for all the discussions, not only in the field of science.

All the friends and colleagues of the Department of Biochemistry, Microbiology, Cellular Biology and Genetics, especially Marcos and Mario, always available when I needed help, and for the good times spent in the several "guachinches" that Mario suggested. I really appreciated.😉

My children, Francesca, Yuri and Andrea, and my husband, Maurizio, for their patience and their support during these years. I'm sorry for all the nights spent writing articles and thesis. Thank you for understand my passion. I Love You .

My mother and my brother and sisters, for their unconditional support during these years. Despite the distance, I constantly felt your love.

Deborah

Thesis Structure

This thesis has been structured according to the rules of presentation as a compendium of publications approved by the Doctoral Committee of the University of La Laguna. The thesis is based on 4 articles related to and framed in the thesis topic, which have been published in journals indexed in international databases of recognized prestige.

1. ***Rotoli, D.**; Morales, M.; Maeso Mdel C; García Mdel P; Gutierrez, R.; Valladares, F; Avila, J.; Díaz-Flores, L.; Mobasheri, A. and Martin-Vasallo, P.* **Alterations in IQGAP1 expression and localization in colorectal carcinomas and liver metastases following oxaliplatin based chemotherapy.** *Onc. Lett. 14: 2621-2628, 2017 doi: 10.3892/ol.2017.6525.*
   Journal Citation Report I.F. 2015: 1,482
2. ***Rotoli D**, Morales M, Maeso Mdel C, García Mdel P, Morales A, Ávila J, Martín-Vasallo P.* **Expression and localization of the immunophilin FKBP51 in colorectal carcinomas and primary metastases, and alterations following oxaliplatin-based chemotherapy.** *Oncol Lett. 2016 Aug;12(2):1315-1322. Epub 2016 Jun 23.*
   Journal Citation Report I.F. 2015: 1,482
3. ***Rotoli D**, Morales M, Ávila J, Maeso Mdel C, García Mdel P, Mobasheri A, Martín-Vasallo P.* **Commitment of Scaffold Proteins in the Onco-Biology of Human Colorectal Cancer and Liver Metastases after Oxaliplatin-Based Chemotherapy.** *Int J Mol Sci. 2017 Apr 22;18(4). pii: E891. doi: 10.3390/ijms18040891.*
   Journal Citation Report I.F. 2015: 3,257.
4. *Baker Bechmann M*, **Rotoli D***, Morales M, Maeso Mdel C, García Mdel P, Ávila J, Mobasheri A, Martín-Vasallo P.* **Na,K-ATPase Isozymes in Colorectal Cancer and Liver Metastases.** *Front Physiol. 2016 Jan 29;7:9.* *These authors contributed equally to this work
   Journal Citation Report I.F. 2015: 4,031

The structure of the thesis consists of the following chapters:

Introduction.

Objectives & Background

Materials & Methods.

Results & Discussion.

Conclusions.

Reference list.

Appendix A-D: Articles published.

List of Abbreviations

5-FU	5-FluoroUracil
AJ	Adherence Junction
Akt	Serine/Threonine Kinase 1
AmotL2	Angiomotin-like 2
APC	Adenomatous Polyposis Coli
BMPs	Bone Morphogenetic Proteins
BMPR1	Bone Morphogenetic Protein Receptors type I
BMPR2	Bone Morphogenetic Protein Receptors type II
CAFs	Cancer Associated Fibroblasts
CLIP-170	Cytoplasmic Linker Protein 170
Crb3	Crumbs 3
CRC	Colo- Rectal Adenocarcinoma
CSCs	Cancer Stem Cells
CT	ChemoTherapy
DLT	Dose-Limiting Toxicity
ECS	Endothelial cells
EMT	Epithelia to Mesenchymal Transition
FKBP51	FK506 Binding Protein 5
FOLFOX	FOL-Folinic acid (leucovorin) F-Fluorouracil, 5-FU, OX-Oxaliplatin
HGF	Hepatocyte Growth Factor
HH	Hedgehog
HSP90	Heat Shock Protein 90
IQGAP1	IQ-motif containing GTPase activating protein 1
LV	Levamisole

MMPs	Matrix Metalloproteases
MT	MicroTubules
MTOC	MicroTubule Organizing Centre
NE	Nuclear Envelope
NF-kB	Nuclear factor k B
OPN	Osteopontin
Par3	Par-3 family cell polarity regulator
PI3K	Phosphatidylinositol 3-kinase
PPIs	Peptidyl-Prolyl Isomerases
PTEN	Phosphatase and Tensin homolog
PWCs	Peripheral White Cells
SCs	Stem cells
SMT	Somatic Mutation Theory
SRC	SRC proto-oncogene, non-receptor tyrosine kinase
TAMs	Tumour Associated Macrophages
TGF-β	Transforming Growth Factor β
TOFT	Tissue Organization Field Theory
TPR	TetratricoPeptide Repeat
Wnt	Wingless-related integration site
YAP	Yes Associated Protein

TABLE OF CONTENT

INTRODUCTION

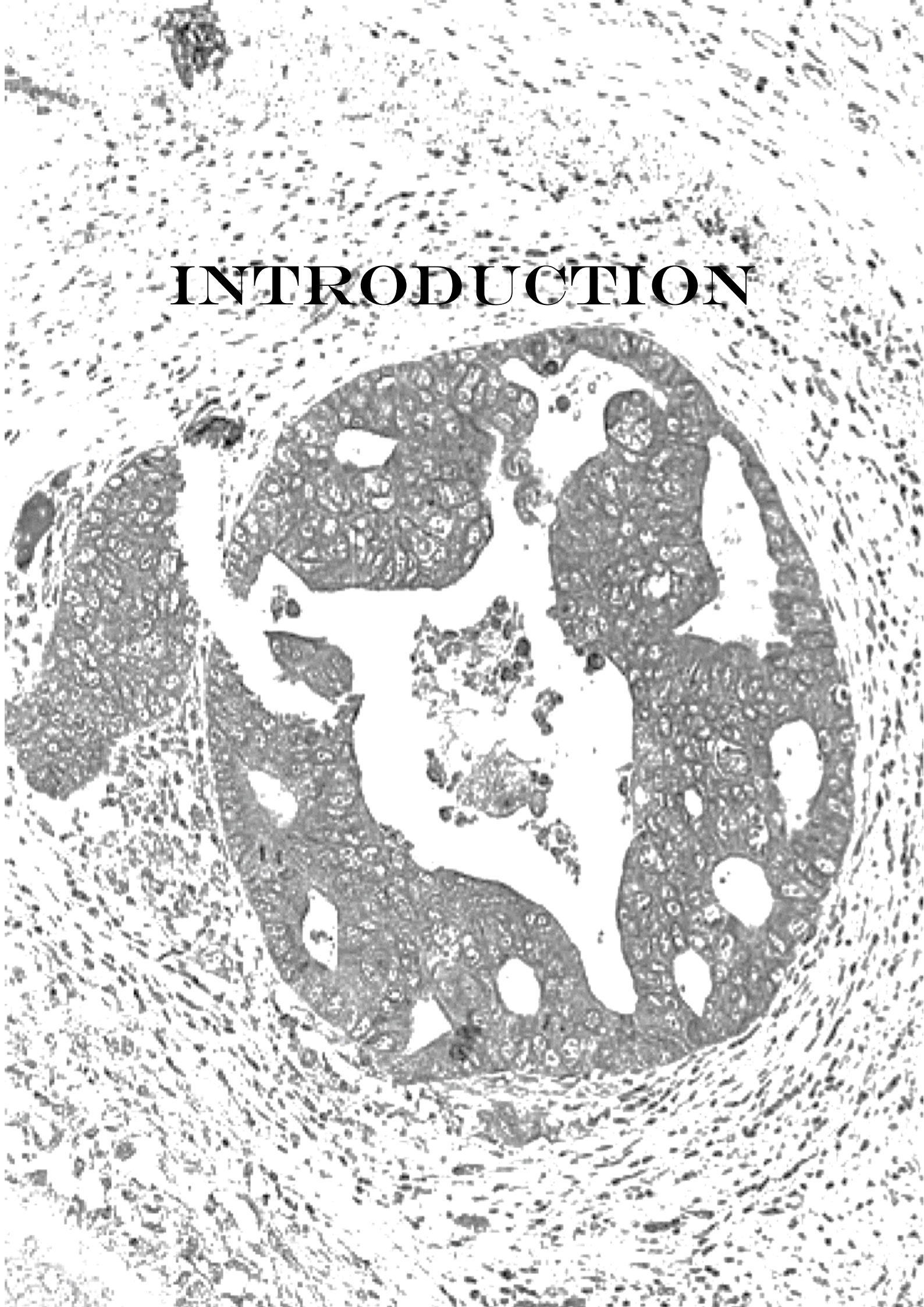

Carcinogenesis arises from cells which have accumulated genetic and epigenetic alterations that affect the strictly monitored growth control. These uncontrolled growing cells acquire the ability to invade and damage the organ where they have arisen and to spread to other organs through the bloodstream and lymphatic fluid. The cell that acquires tumorigenic mutations (e.g. the cell origin of the tumor) is different from the cells responsible for the propagation of the tumor after the onset [1]. Stem cells, progenitor cells or differentiated cells can gather mutations that lead to its malignant transformation and become the cell of origin [2]. After tumor inception, the processes of carcinogenesis and tumor progression can be explained accordingly to the two proposed models, the Stochastic or the Cancer Stem Cell models.

1.1 The Stochastic Model.

The stochastic theory postulates that every cell can accumulate mutations that lead to its transformation allowing the initiation and propagation of the tumor. Further mutations can be acquired following transformation, giving rise to different populations of sub-clones. According to this model, the accumulation of stochastic genetic abnormalities and the microenvironmental niche impact may account for the intrinsic heterogeneity of the tumor [1,3]. Not all the clones can acquire the properties to migrate and form metastasis, however the cancer cells that acquire these features can migrate, gather more mutations and give rise to a metastatic lesion with distinct characteristics compared to the parental tumor [4].

1.2 The Cancer Stem Cell (CSC) Model.

The CSC theory, conversely, postulates that a very low percentage (1%) of tumor cells have the potential to propagate the tumor, and though classified as Cancer Stem Cells (CSCs) [5]. Only these cells own the competence of self-renewal, multipotency, unlimited proliferation capacity, immune evasion properties and angiogenic characteristics as normal tissue stem cells (SCs) [6]. Other common features of CSCs and SCs are the active expression of the telomerase, the increase of the active membrane transports, the anti-apoptotic pathways activation and the capacity of metastasis migration and colonization [7]. To explain tumor heterogeneity, the CSC model postulates that, alike normal tissues, cancers are hierarchically arranged. The high proliferative multipotent CSCs produce a broad variety of progenitor cells, characterized by a medium proliferative capacity, and of non-proliferative differentiated cells [4,8]. CSCs are highly resistant to current systemic therapies, which only induce partial or incomplete remission, due to the expression of DNA repair machine, detoxifying enzymes and drug transporters. Surgical resection is, at the moment, the only effective arm against CSCs. Thus, new therapies for targeting this distinct group of cancer cells are urgently required. Unluckily, SCs form a core unit in the human body, and try to selectively target CSCs is, actually, extremely hard due to the lack of biomarkers that unequivocally discriminates between them [9].

1.3 Somatic Mutation Theory vs Tissue Organization Field Theory.

In the last decades, the Tissue Organization Field Theory (TOFT) has been proposed as a new theory for cancer neo-genesis, in contrast to the classical Somatic Mutation Theory (SMT) [10]. The core of the SMT is that cancer develops from a single somatic cell that accumulated sequential multiple DNA mutations in genes controlling cell proliferation and cell cycle [11]. According to this theory, neoplastic lesions that overwhelm normal tissue architecture are the results of DNA-level events [11]. On the contrary, the TOFT theory arguments that carcinogenesis is mainly a question of tissue organization. Carcinogens (chemicals, viruses, inflammation) alters the normal tissue architecture, destroying cell-to-cell signaling and affecting genome integrity [11–14]. According to this theory, the DNA mutations are the effect of the tissue-level events, and not the cause [15]. In recent years, there is a heated debate between the supporters of either theories. Several arguments have been proposed to sustain one or the other theory [13–18]. However, it can't be excluded that the two theories might be confluent and complementary [11].

1.4 Tumor progression and metastasis.

Concerning tumor progression, metastasis accounts for over 90% of mortality in cancer patients [19].

A pathologic based point of view depicts a series of determined events leading to metastatic colonization (Fig.1):

1. An epithelial-to-mesenchymal transition (EMT) leads to increased motility and invasive potential of a primary tumor cell [20]; transforming growth factor β (TGF-β) and Wnt pathways play key roles in this process [21,22].
2. Proteolysis of the basement membrane and extracellular matrix, which involves the action of Matrix Metalloproteases (MMPs) family proteins, allow the cell to enter the stroma [23].
3. A crosstalk between tumor cells and the surrounding stroma cells (e.g. fibroblasts, macrophages, telocytes, pericytes, endothelial cells) leads to modifications of the tumor microenvironment that facilitates the intravasation of malignant cells in the bloodstream and lymphatic system [24].
4. Extravasation and invasion of a distant tissue are achieved once the circulating cancer cell acquires the capacity to survive and evade the immune system attack [25].
5. Metastatic colonization is gained if the malignant cell is able to adapt to the new foreign microenvironment and to crosstalk with it to create a suitable environment for micro and macro-metastasis development [25].

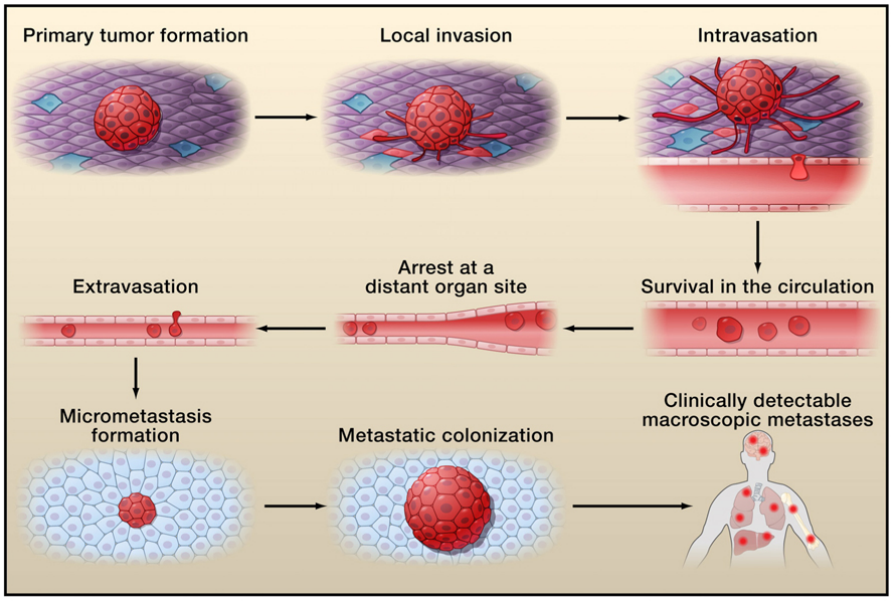

Fig.1: From primary tumor to metastatic colonization.
©Valastyan and Weinberg [25].

Depending on the targeted organ and the genetic profile of the primary cancer, the abovementioned steps may vary and involve different and defined genetic alterations.

1.5 Tumor microenvironment.

Tumor microenvironment (Fig. 2) is critical in the process of metastatic colonization. Different cancer stromal elements (e.g. cancer associated fibroblasts, tumor associated macrophages, endothelial cells, pericytes, telocytes) express several factors that influence the epithelium to regulate epithelial CSC function. For example, *CAFs (cancer associated fibroblasts)* express BMP antagonists, MMPs, cytokines, hepatocyte growth factor (HGF) and osteopontin (OPN).

TAMs (tumor associated macrophages) tightly resemble M2-polarized macrophages that, in normal conditions, regulate the anti-inflammatory response and the wound healing process. TAMs play a key role in the regulation of tumor microenvironment, creating a suitable niche for cancer cell development and progression [26]. Accumulation of TAMs in tumors is correlated with poor prognosis [27].

ECs (endothelial cells) communicate with the epithelium through the expression of the Notch ligand Jagged1 to regulate Notch pathway, promoting the CSC phenotype in colorectal cancer cells [28] .

Pericytes are involved in blood flow regulation and vessel permeability, and play an important role in the stabilization of the vascular wall and in vessel remodeling and maturation [29–31]. Moreover, several studies hint a role for pericytes in the maintenance of adult SCs [32] and in immune-regulation [33]. For all these features,

pericytes, in carcinogenesis, are regarded as important regulators of illness progression, participating in tumor progression, metastatic process and resistance to therapy [34].

Telocytes are a recently identified interstitial cell type present in several tissues and organs [35]. Are characterized by a small cell body and 1 to 5 thin and very long moniliform prolongations (telopodes), with an alternation of thin segments (podomers) and dilated areas (podoms) [36]. Telocytes are interconnected, via their telopodes, creating a complex 3D interstitial network forming homo-cellular contacts as well as hetero-cellular contacts with other neighboring cell types [37]. They are also involved in paracrine signaling, indeed they can release extracellular vesicles such as exosomes and ectosomes [36]. Functionally, they are involved in the regulation of tissue homeostasis and renewal [36,38].

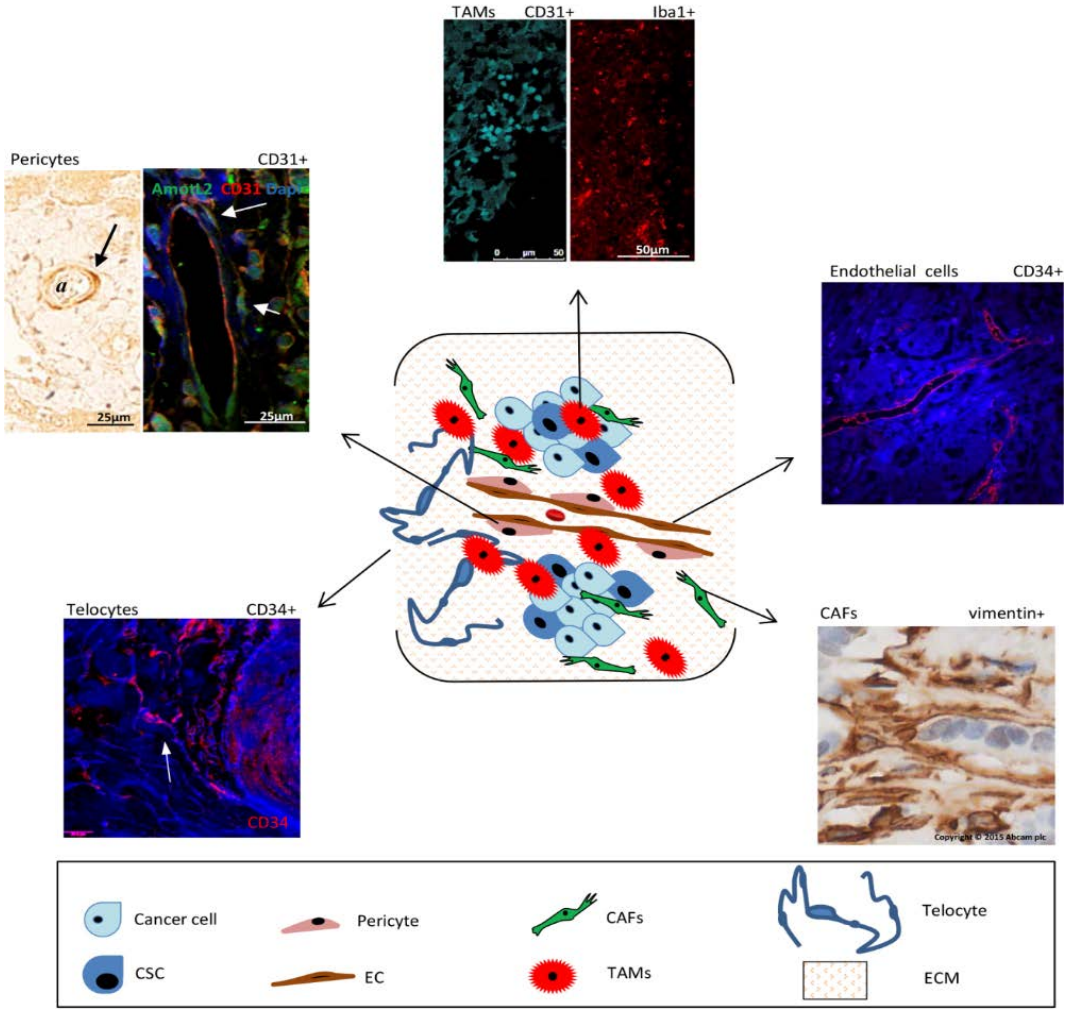

Fig.2: Tumor microenvironment. Schematic illustration of cancer stromal elements that influence tumor progression and growth and representative images from CRCs of immunohistochemical or immunofluorescent staining of typical markers for such cells. CAFs: cancer associated fibroblasts; CSC: cancer stem cell; EC: endothelial cell; ECM: extra cellular matrix; TAMs: tumor associated macrophagies.

1.6 Intestinal tissue homeostasis vs colorectal cancer: signaling pathways involved.

Colorectal cancer is among the leading causes of death in western world [39]. Over 95% of colorectal cancers are adenocarcinomas, namely epithelial-derived malignant tumors that arise from the cells that line the interior of the colon and rectum and that produce and release mucus and other fluids. The main risk factors are genetic factors (family history), low fiber and high fat diet and smoking. The development and progression from adenoma to cancer and metastatic disease implies the concurrently failure of protective mechanisms (e.g. adenomatous polyposis coli, p53 and transforming growth factor-β) and the induction of oncogenic pathways (e.g. Ras) [40,41].

Under normal conditions, intestinal homeostasis is controlled by a complex crosstalk network between several evolutionary conserved pathways that stringently regulates the balance among proliferation, differentiation, apoptosis, migration and renewal [42]. These pathways are: Wingless-related integration site (Wnt), Notch, transforming growth factor-β (TGF-β)/bone morphogenetic protein (BMP), Hedgehog (HH), Phosphatidylinositol 3-kinase (PI3K)/Akt, Hippo. Jointly, the TGF-β/BMP, Wnt and Hedgehog signaling pathways preserve the crypt-villus architecture, while Notch, Wnt and Hippo pathways connect to regulate the cellular fate of intestinal SCs [43]. Alterations in these key signaling pathways, due to oncogenic factors and/or genetic/epigenetic mutation may lead to malignant cell transformation. The interplay with microenvironmental and germ-line factors play an important role in this process leading to altered colonic mucosa phenotype [40,41].

The Wnt signaling pathway is a key regulator of embryonic development and tissue homeostasis [44]. It plays a pivotal role in intestinal stem cell preservation by regulating cell-fate decisions, proliferation and differentiation [45–51]. Apart from its critical role in tissue homeostasis, the Wnt signaling is abnormally activated in many human disorders, including metabolic diseases and cancers, especially in CRCs [52]. Mutations in the pathway negative regulator Adenomatous Polyposis Coli (APC) [53–55], or in β-catenin (the key transcription modulator of the pathway) [56] or in the proteins that regulate the pathway (e.g. AXIN1, AXIN2), cause its constant activation leading to uncontrolled proliferation and increased survival [57]. Wnt pathway is also implicated in the EMT and invasion processes [8,58].

Notch signaling has a crucial role in the normal maintenance and homeostasis of the intestinal epithelium [59,60], regulating the balance between cell differentiation, proliferation and apoptosis and controlling the cellular fate of intestinal SCs and the differentiation of Goblet cells [61,62]. In many human cancers, including CRCs, abnormally activated Notch pathway was correlated with increased progression, metastatic potential and relapse [63–65].

TGF-β/BMP pathway plays a key role in preventing cell proliferation and in the regulation of immune control, cell invasion and microenvironment adaptation [66]. TGF-β and BMP are members of a family of ligands whose receptors interact with the intracellular cascade of the SMAD proteins [67]. TGF-β inhibits intestinal epithelial cell proliferation and induces apoptosis in normal conditions, acting as a tumor suppressor [40,42,68]. Many colorectal cancers evade the tumor-suppressor action of TGF-β and are resistant to TGF-β-induced growth inhibition [69]. However, in the late stages of colorectal carcinogenesis, TGF-β is usually highly expressed and acts as an oncogene promoting the survival, invasion and metastasis of CRC [70]. Overexpression of TGFβ1 in the primary CRC is associated with advanced stages, poor prognosis and recurrence [71,72]. BMPs bind to Bone Morphogenetic Protein Receptors type I and II (BMPR1 and BMPR2) and phosphorylates the intracellular signal transducing factors SMAD 1, 5 or 8. Upon the formation of a heterodimer with SMAD4, the complex then translocates to the nucleus and activates the transcription of target genes [73]. BMP signaling is a well-known tumor suppressive pathway. The loss of SMAD4 in CRC cells determines a change in BMP signaling, that now acts as a metastasis promoter, instead that a tumor suppressor, by increasing EMT and invasiveness in CRC [74].

Hedgehog signaling pathway is essential for normal embryonic development and plays critical roles in adult tissue maintenance, renewal and regeneration [75]. It regulates progenitor cell fate in normal development and homeostasis. Although the lack of incontrovertible proofs, it seems that abnormal pathway activation might be involved in the maintenance of progenitor cell population in cancer. Recently, Varnat et al. [75] provided evidences that supported the crucial involvement of this pathway in human colon cancer growth, relapse, metastases and stem cell proliferation [75,76].

PI3K/Akt pathway leads to reduced apoptosis, stimulates cell growth and increases proliferation. The major player of this pathway is PI3K, that, upon activation, phosphorylates its substrate determining the activation of the Akt-kinase by PDK1. A negative regulator of this signaling pathway is PTEN (phosphatase and tensin homolog). In 60-70% of human CRCs, activation of Akt pathway and altered expression of PTEN has been reported [77].

Hippo pathway regulates cell proliferation, growth and apoptosis, and controls organ size, stem cell functions and tissue homeostasis. This pathway acts primarily through inhibition of TAZ and YAP1 kinases, which are its major nuclear effectors. Inhibition of Hippo signaling leads to stem cell expansion and neoplastic growth [78].

1.7 Current challenge to CRC: combined 5-fluorouracil/oxaliplatin chemotherapy.

In CRC, after curative surgery alone, the percentage of patients that subsequently relapse and die of metastatic disease ranges between 40-50%. This percentage falls to 33% when patients receive postoperative adjuvant chemotherapy (CT) with 5-fluorouracil and levamisole (5-FU/LV), and to 23% when the platinum-based drug oxaliplatin is added to this treatment (FOLFOX: FOL-Folinic acid, leucovorin, F-Fluorouracil, 5-FU, OX-Oxaliplatin) [79].

Fluorouracil has been used by more than half a century as a chemotherapeutic agent for colorectal cancer due to its action on multiple pathways, such as RNA metabolism and DNA signaling and repair. Folinic acid and/or levamisole improve the efficacy of 5-FU [80]. The addition of oxaliplatin to a regimen of 5FU/LV doubles the response rate and prolongs progression-free survival [80]. Interestingly, it has been reported that administration of oxaliplatin and 5-FU augments BMP4 antitumor action [2,42]. BMP4 is able to initiate a differentiation program and to drive apoptosis in colon CSCs by the reduction of β-catenin activation via the upregulation of Wnt-negative controllers and the inhibition of PI3K/Akt pathway [2]. Todaro et al. [81] demonstrated that the concomitant administration of oxaliplatin and 5-fluorouracil elicited BMP4 action and induced complete and long-term regression of colon CSCs-derived xenograft tumors [81].

Oxaliplatin (*trans*-1-diaminocyclohexane oxaliplatinum) is a third generation platinum derivative, containing the 1,2-diaminocyclohexane group (Fig. 1). It acts via the formation of cytotoxic cross-linked DNA adducts. The cyclic group is thought to be responsible for the greater resistance to DNA repair, in respect to other platinum-derivative drugs, such as cisplatin (*cis*-dichlorodiamine platinum II) or carboplatin, which lack this cyclic group. In particular, oxaliplatin forms both inter- and intra-strand cross links in DNA (Fig. 2), which prevent DNA replication and transcription, causing cell death.

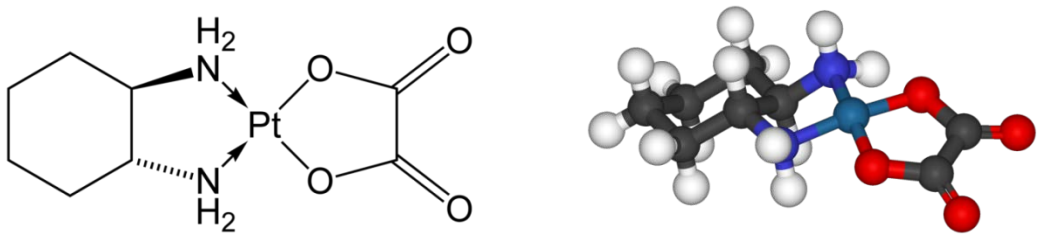

Fig.1 : Oxaliplatin structure showing the cyclic bulk group 1,2-diaminocyclohexane. (Wikipedia)

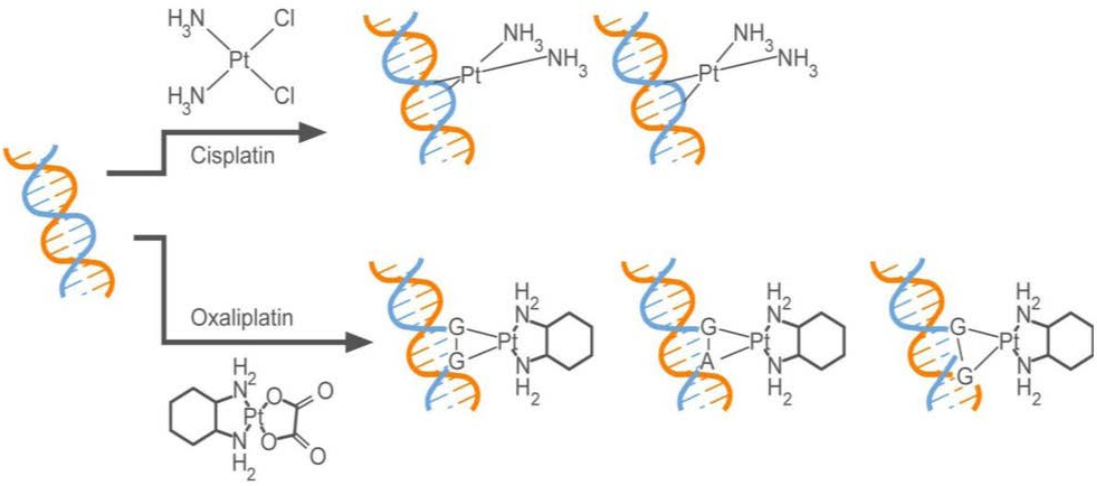

Fig.2: DNA adducts formed by cisplatin and oxaliplatin [80].

Unfortunately, beside the positive results obtained by the combination protocols of oxaliplatin with fluoropyrimidines (e.g. 5-fluorouracil) and folinic acid (leucovorin) in disease-free survival of stage II or III colon cancer [79], unwanted side effects are to be considered and monitored, as they can affect in various degrees the quality of patient's life. Several secondary effects have been reported for oxaliplatin, which include gastrointestinal toxicity, moderate hematologic toxicity, hypersensitivity and neurologic toxicity. This unpredictable neural toxicity has quite unique features and determines the dose-limiting toxicity (DLT) of this platinum-based drug [82].

The identification of biomarkers would be of great importance in order to avoid the onset of long term toxicity or permanent damage in patients at risk. A recent project from our laboratory has led to the identification of several genes which were significantly up- or down- regulated following oxaliplatin-based chemotherapy treatment (CT) [83]. More in details, the aim of the project was to study the differential expression of genes associated with neuropathy which expression was affected by oxaliplatin CT. Using peripheral white cells from patients suffering from colon adenocarcinoma before and after 3 CT cycles, a differential transcriptome profile of peripheral white cells (PWCs) was obtained. Among the differentially expressed genes obtained with this approach, we found genes coding for cellular component movement, metabolic proteins, response to drugs, cell morphogenesis and differentiation.

OBJECTIVES & BACKGROUND

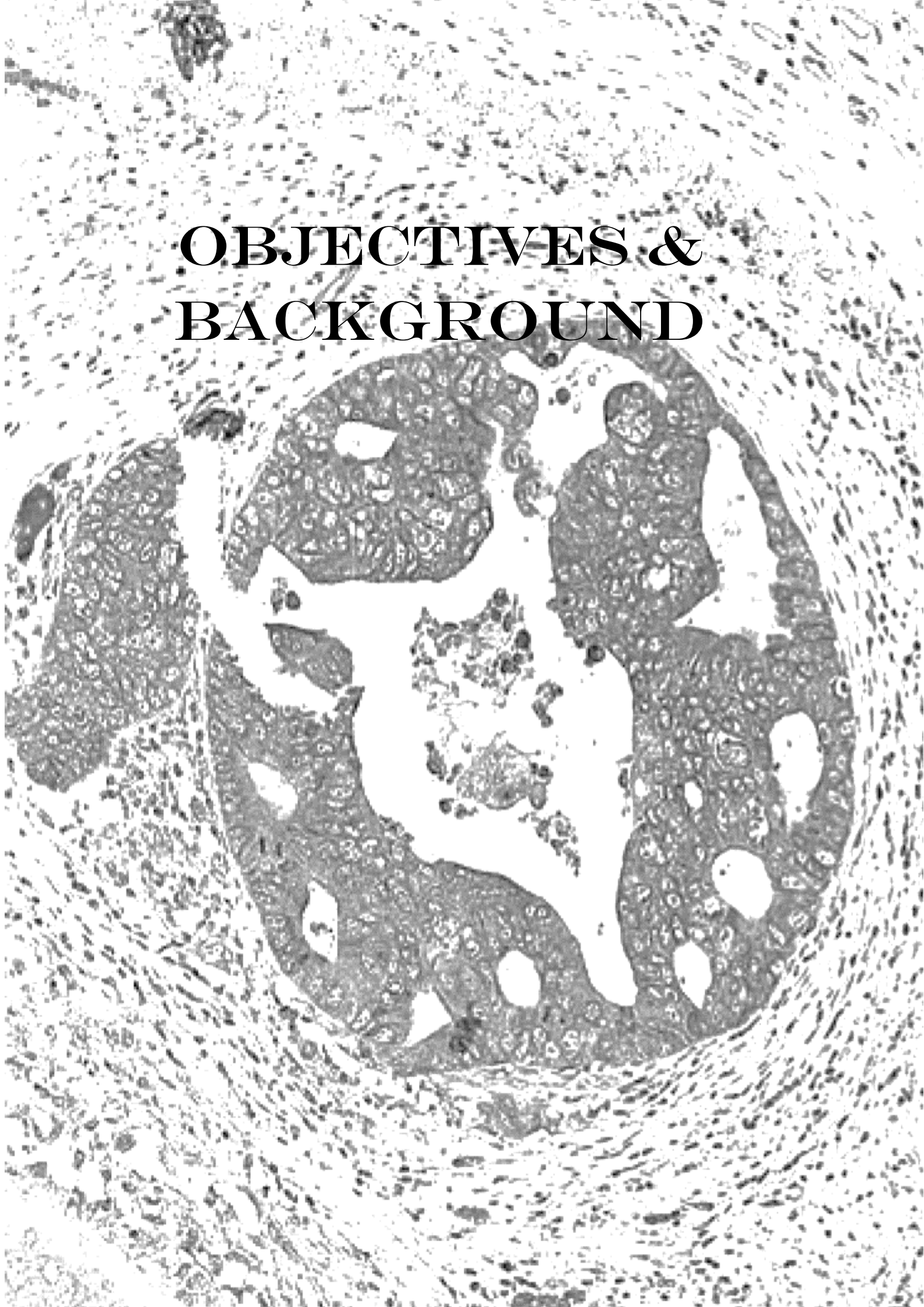

2.1 Objectives

The aim of the present study was to determine whether the alterations in gene expression observed in peripheral white cells (PWCs) [83] could be detected in CRC tumours and in metastasis after the administration of chemotherapy and whether these alterations had any role in tumour-pathogenesis and prognostic implications. To this end, we performed an immunohistochemistry analysis of the proteins encoded by the selected genes in CRC and metastases.

Specifically, genes which expression had been investigated were the scaffold proteins IQGAP1 (IQ-motif containing GTPase activating protein 1), FKBP51 (FK506 binding protein 5), AmotL2 (Angiomotin-like 2), and the proteins corresponding to the α1, α3, β1 and β2 subunits of Na,K-ATPase. Table 1 details selected genes and gene expression levels in PWCs before (PRE) and after (POST) 3 cycles of CT.

Genebank Acc. Nº	Gene	Symbol	PRE	POST
NM_003870.3	IQ motif containing GTPase activating protein	***IQGAP1***	0	229,5
NM_U71321.1	FK506 binding protein 5	***FKBP51***	3812	1383
NM_016201.3	Angiomotin-like 2	***AMOTL2***	15,4	68,1
NM_152296.4	ATPase, Na+/K+ transporting, α3polypeptide	***ATP1A3***	251	100

Table 1- Genes and gene expression levels in PWCs before (PRE) and after (POST) three cycles of FOLFOX CT.

2.2 Background

2.2.1 IQGAP1 (IQ motif containing GTPase activating protein 1)

IQGAP1 is a ubiquitously expressed scaffold protein that contains multiple protein interaction domains. The protein interacts with components of the cytoskeleton, cell adhesion molecules, and several signaling molecules to regulate cell morphology and motility, cell cycle and other cellular functions [84,85]. By regulating its binding partners, IQGAP1 integrates many signaling pathways, several of which contribute to tumorigenesis. For example, IQGAP1 is associated with actin dynamics through direct binding of actin and indirect regulation via Cdc42/Rac1 [86]. Through its poly-proline protein-protein domain (WW domain) it modulates the MAPK pathway which is associated with cell cycle control [87]. Hence, IQGAP1 can link MAPK signaling (e.g. decisions about cell fate) to the cytoskeleton or cellular adhesion, with important implications for cancer. Moreover, interactions of IQGAP1 with ERK1/2 and MEK1/2

can lead to activation of the mitogen-activated protein kinase (MAPK) signaling pathway, modulating cell differentiation and proliferation [87]. Thus, IQGAP1 plays pivotal roles in several cellular functions, such as control of cell adhesion, polarization, migration, proliferation and angiogenesis. Many immunohistochemical studies have demonstrated that in several cancer types IQGAP1 is over-expressed and an aberrant membrane accumulation is observed, especially at the invasive front [88,89]. The higher expression and the altered localization of IQGAP1 from the cytoplasm to the membrane correlate with the grading of the tumor and with poor prognosis. The presence of IQGAP1 in the cell membrane may decrease adherence junction function, favoring the dissociation of the tumor cells [90].

2.2.2 FKBP51 (FK506 binding protein 5)

The immunophilin protein FKBP51 (FK506 binding protein 5) is a member of the peptidyl-prolyl isomerases (PPIs) superfamily [91]. This superfamily includes three distinct classes: the FK506-binding proteins (FKBPs) (e.g. FKBP12, FKBP51, FKBP52); the CyclosporinA-binding proteins and the parvulin-like PPIs [92]. PPIs catalyze the cis-trans conversion of peptidylprolyl imide bonds in target proteins [93]. FKBP51 is a 51 kD FK506 binding protein with a C terminal tetratricopeptide repeat (TPR) domain, and an N terminal FK1 domain responsible for PPIase activity [93]. Through the TPR domain, FKBP51 binds to heat shock protein 90 (HSP90) complexes, such as those associated with steroid hormone receptors. The mechanisms underlying the regulation of steroid hormone receptor signaling by this immunophilin and its physiological roles in endocrine-related processes are very well studied. Research in this field has led to the identification of FKBP51 as a potential therapeutic target for several endocrine-related diseases, such as metabolic and stress-related diseases, prostate cancer and breast cancer [94]. Diseases associated with this protein include major depressive disorder and glucocorticoid resistance (Gene Ontology annotations).

FKBP51 protein is localized in mitochondria, cytoplasm and nucleus [93,95,96], is involved in the regulation of a variety of signaling pathways and is considered as a molecular integrant of the adaptation process [97]. Recently, a role for the immunophilins FKBP51 and FKBP52 in regulating microtubules has been suggested, acting via their interaction with Tau proteins [98]. Regulation of microtubule dynamics by FKBPs has been associated with neurite outgrowth [99]. Furthermore, FKBP51 has been identified as a regulator of cell death in response to gemcitabine and cytarabine treatment: high levels of FKBP51 expression were associated with sensitivity, while low levels of expression were associated with resistance to these drugs [100].

In many different tumors altered expression levels have been described [101,102]. Through its influence on steroid receptor maturation, and on the regulation of PKA [103], NF-kB [94], Akt [104] and the transforming growth factor β (TGF-β) [105] signaling

pathways, FKBP51 plays an important role in tumorigenesis and response to anti-neoplastic therapy [106,107]. It has been demonstrated, for example, that it plays a role in negatively regulating the Akt pathway. Acting as a scaffold protein, FKBP51 promotes the interaction of Akt and PHLPP, a phosphatase that specifically dephosphorylates Akt at Ser473 and inhibits its activity [104]. Recently it has been demonstrated that FKBP51 is key in promoting the activation of genes involved in melanoma progression [108], and modulates the transforming growth factor β (TGF-β) signal in malignant melanocytes, increasing the tumor-promoter potential of TGF-β [109]. FKBP51 expression is also decreased in pancreatic cancer tissues and in numerous cancer cell lines.

2.2.3 AmotL2 (angiomotin-like 2)

Is a member of the angiomotin protein family responsible for maintaining cell to cell interactions to keep asymmetrical apical-basal polarity avoiding endothelial detachment and promoting vascular tube formation. Human AmotL2 encodes two isoforms of a molecular mass of 100kDa and 60kDa [110]. Most human cancers have an epithelial origin and the assessment of malignancy is based on the loss of apical–basal polarity of the epithelial organization (epithelial mesenchymal transition -EMT), however, whether this is a cause or consequence of tumor progression has yet to be established [111]. Loss of polarity, EMT and angiogenesis are crucial in CRC.

2.2.4 The Na^+,K^+-ATPase genes family

One of the differentially expressed genes was the isoform α3 of the Na,K-ATPase; mRNA levels of Na,K-ATPase α3 subunit were down-regulated 2.6 fold. Moreover, an alteration in the intracellular location of Na,K-ATPase α3 isoform has been reported in human CRC tumor cells versus normal colon [112]. Additionally, other laboratories have shown differential expression in cells, altered subcellular localization and down regulation of the β subunit of the Na+/K+-ATPase in carcinoma cells [113–116].

Na,K-ATPase is an integral protein in the plasma membrane of all animal cells that transports three sodium ions out and two potassium ions into the cell, against electrochemical gradient [117,118]. This activity is necessary for the regulation of the cellular ionic homeostasis and maintaining the electrochemical gradient required for ion channel function and secondary active transport [119]. Recently, additional functions for the Na,K-ATPase in the cell have been proposed, as a signal transducer and transcription activator [120–124] affecting cell proliferation [125], cell motility [126], and apoptosis [127]. Besides this, the Na,K-ATPase is the receptor of cardiotonic glycosides. It is functionally composed of catalytic α (100–112kDa) and regulatory β (45–55kDa) subunit and an optional γ (6.5–10kDa) subunit belonging to the FXYD family of proteins [128]. Na,K-ATPase is expressed as several isozymes. Four different isoforms of the α subunit

have been found in humans [129]. The α1 isoform (*ATP1A1* gene) is expressed almost in all tissues. Isoform α2 (*ATP1A2* gene) is the predominant isoform in skeletal muscle [130], brain (astrocytes) [131], heart [132], and adipose tissue [133]. The α3 isoform (*ATP1A3* gene) is primarily found in the brain (neurons) [131,134] and isoform α4 (*ATP1A4* gene) is only expressed in testis [135]. In reference to the β subunit, three different isoforms have been identified: β1 (*ATP1B1* gene), β2 (*ATP1B2* gene) and β3 (*ATP1B3* gene). While β1 has a generalized expression in almost all tissues and cells, the expression of the other β isoforms are more restricted to certain tissues and cells. The β2 isoform is found in skeletal muscle [136], pineal gland [137], and nervous tissues [138], whereas β3 is present in testis, retina, liver and lung [139–142]. The expression pattern of the Na,K-ATPase subunit-isoforms is subjected to developmental and hormonal regulation and can be altered during disease [141,143–146].

MATERIALS & METHODS

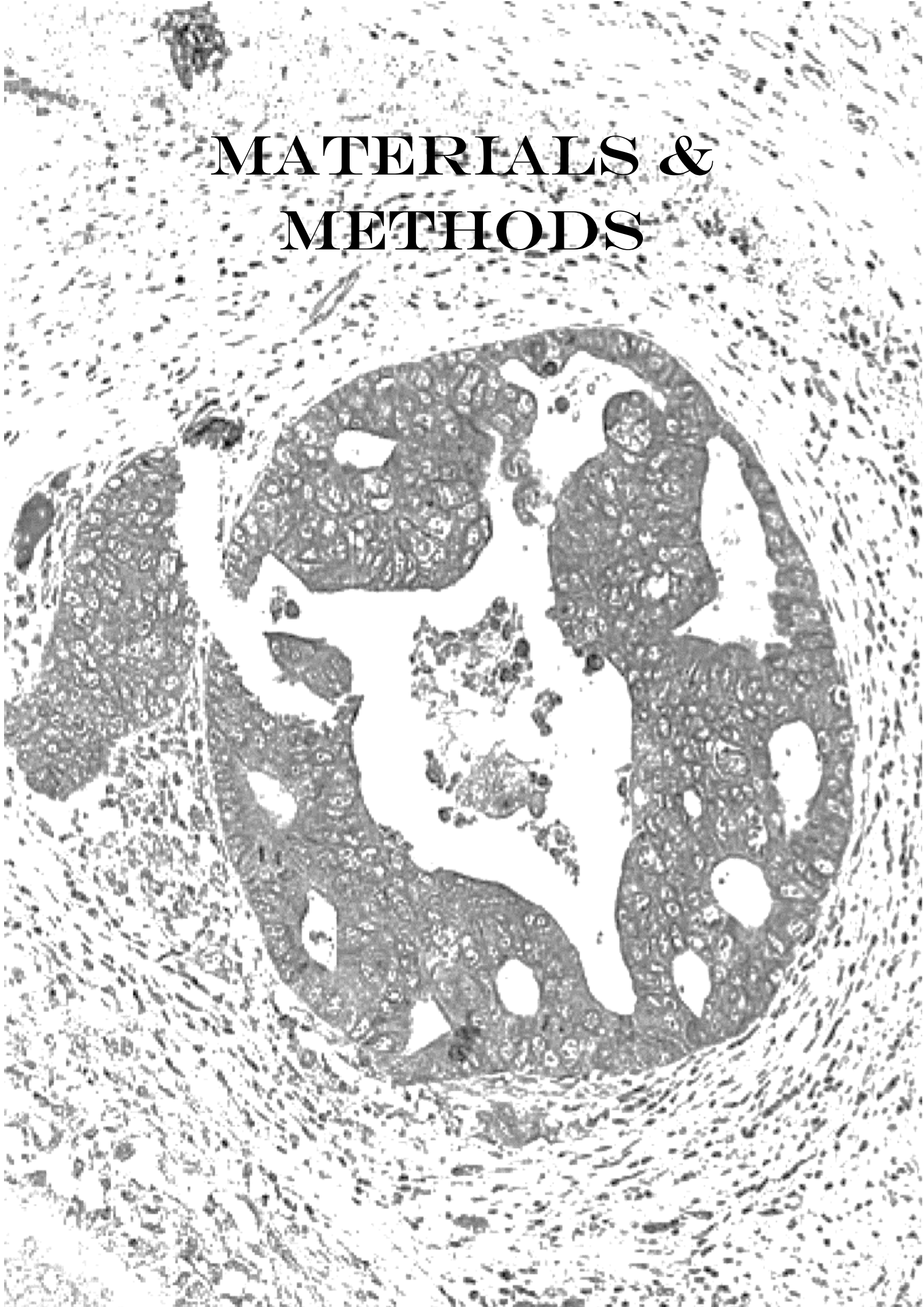

3.1 Patients.

The study was approved by the Ethics Committee of La Laguna University (La Laguna, Canary Islands, Spain) and the Ethical Committee of Nuestra Señora de Candelaria University Hospital (HUNSC); Santa Cruz de Tenerife, Canary Islands, Spain). All patients have been treated at HUNSC between years 2007-2015 and provided informed consent for the diagnosis and research of tissue specimens prior to entering the study. All patients had colonic cancer and liver metastasis, which had been treated with FOLFOX-CT, (day 1, oxaliplatin 100 mg/m2 iv over 2 h; leucovorin calcium 400 mg/m2 iv over 2 h; followed by 5-fluorouracil 400 mg/m2 iv bolus and by 5-fluorouracil 2400 mg/m2 iv over 46 h; every 14 days). All patients received the chemotherapy after the resection of the primary tumor. Thus, the primaries were chemotherapy naïve, while the liver metastases were chemotherapy-treated. Fifteen (27.8%) patients presented liver metastasis after CT. Curative resections of liver metastasis were performed following FOLFOX-CT. The average age of patients was 59 years old (range 35–78), with 29 (54%) males and 25 (46%) females. Eight patients (15%) were stage IV and underwent palliative surgery. The other patients, T3–T4, N1–N2 (85%) were stages partial response upon RECIST (Response Evaluation Criteria In Solid Tumors) criteria. The survival is 74% (40 patients), with a follow up of six years. Localization of tumors varied from cecum (4), ascending (13), transverse (8) colon, both flexures (7), sigmoid (16) colon and sigmo-rectal (3) area and rectum (3).

Paraffin-embedded tissue samples from 54 patients, ensuring patient anonymity, and the corresponding clinical data were obtained from the reference medical areas of HUNSC. Following the same ethics and consent rules, colon and liver samples were obtained from surgery partial exeresis pieces after trauma of three control males.

3.2 Antibodies

Table 2 at the end of this section, shows antibodies used in this thesis for the proteins object of the study and cell markers as well.

3.3 Immunohistochemistry.

Samples were fixed in 10% formalin, for 48–72 h at 4 ◦C. Immunoperoxidase staining of paraffin-embedded tissue sections was performed using the avidin-biotin reaction. Briefly, 5-µm-thick tissue sections, deparaffinized in xylene and hydrated in graded alcohol baths, were autoclaved at 120 ◦C for 10 min in sodium citrate buffer (pH 6.0) to uncover hidden antigenic sites (antigen retrieval). Samples were then incubated for 1 h at room temperature with 5% non-fat dry milk in Tris-buffered saline (TBS) to block non-specific sites. The Avidin/Biotin Blocking kit (Vector Laboratories Inc., Burlingame, CA, USA) was used to block endogenous biotin, according to the manufacturer‘s instructions. Primary antibodies were applied to slides overnight at 4 ◦C. Endogenous peroxidase activity was blocked by incubating the slides with 3% hydrogen peroxidase in methanol for 15 min. Biotin-conjugated anti-rabbit secondary antibody was incubated for 2 h at 37 ◦C, and the specific antibody staining was amplified with the ABC Peroxidase

Staining kit (Thermo Fisher Scientific, Inc.). 3,3'-diaminobenzidine substrate concentrate (#IHC-101F; Bethyl Laboratories Inc., Montgomery, TX, USA) was used to visualize immunohistochemical reactions. Samples incubated without primary antibodies were used as a negative control. Slides were counterstained with Harris hematoxylin solution DC (#253949, Panreac Química SLU, Barcelona, Spain) to visualize cell nuclei and mounted with Eukitt mounting medium (#253681, Panreac Química SLU, Barcelona, Spain). An optical light microscope (BX50; Olympus Corporation, Tokyo, Japan) was used to visualize the results of the immunostaining.

3.4 Double Immunofluorescence Simultaneous Staining.

Immunofluorescent staining of 10% formalin-fixed paraffin-embedded tissue sections was performed as previously described [47]. Briefly, 5-µm-thick tissue sections, deparaffinized in xylene and hydrated in a graded series of alcohol baths, were autoclaved at 120 ◦C for 10 min in sodium citrate buffer (pH 6.0) to uncover hidden antigenic sites (antigen retrieval). Samples were then incubated for 1 h at room temperature with 5% bovine serum albumin in Tris-buffered saline (TBS) to block non-specific sites. Tissue sections were then incubated simultaneously with a mixture of two distinct primary antibodies overnight at 4 ◦C. Slides were then incubated for 1 h at room temperature in the dark with a mixture of two secondary antibodies raised in different species and conjugated to different fluorochromes. Slides were mounted with ProLong® Diamond Anti-fade Mountant with DAPI (Molecular Probes®; Thermo Fisher Scientific, Inc.) to visualize cell nuclei. Slides were analyzed using Leica SP8 (Leica Microsystems, Wetzlar, Germany) confocal microscopes and Olympus FV1000 (Olympus Corporation, Tokyo, Japan).

3.5 Image Analysis and Statistical Analysis.

To compile tables, two independent observers evaluated the specimens blindly. After an initial examination of the whole blind-coded material, cut-offs were established by consensus between each investigator. Staining intensities were graded as strong (+++), moderate (++), weak (+) or absent (−). When scorings differed by more than one unit, the observers re-evaluated the specimens to reach consensus, otherwise means of the scorings were calculated.

For the semi-quantitative image analysis performed in publication nº2 (Rotoli et al. Oncol. Lett. 2016, 12, 1315–1322), the open resource digital image analysis software ImageJ was used, implemented with the IHC Profiler plug-in developed by Varghese *et al [147]*, which creates a pixel-by-pixel analysis profile of a digital IHC image, and further assigns a score in a four tier system: High positive (pixel intensity range, 0-60), positive (pixel intensity range, 61-120), low positive (pixel intensity range, 121-180), negative (pixel intensity range, 181-235). All images were captured at the same magnification (40x) and with the same levels of contrast and brightness. Pearson's Correlation

Coefficient and Student's *t*-test were performed using SPSS version 20 software (IBM SPSS, Madrid, Spain) in order to estimate the reliability of the study.

Table 2: Antibodies and cell markers used

Antibody	M/P	IHC-P	IH-F	Source	Cat.#
Anti-AMOTL2	Rabbit polyclonal	1:100	1:250	LifeSpan BioSciences	LS-C178611
Anti-FKBP51	Rabbit polyclonal	1,25:100	1:50	Abcam	ab46002
Anti-IQGAP1	Rabbit polyclonal	1:500	1:250	Millipore	ABT186
α1-isoform (620)	Rabbit polyclonal	1:1000	-	M.J. Kashgarian	-
α3-isoform	Mouse monoclonal	1:600	1:300	M. Caplan	-
α3 (XVIF9-G10)	Mouse monoclonal	1:5	1:5	Arystarkhova and Sweadner	-
SpETβ1 β1-isoform	Rabbit polyclonal	1:600	1:300	P. Martín-Vasallo	-
SpETβ2 β2-isoform	Rabbit polyclonal	1:600	-	P. Martín-Vasallo	-
anti-PCNA	Mouse monoclonal	-	1:100	Boehringer Mannheim	1486 772
anti-human CD34	Mouse monoclonal	-	Ready-to-use	Dako	IR632
anti-human CD31	Mouse monoclonal	-	Ready-to-use	Dako	IR610
anti-β tubulin	Mouse monoclonal	-	1:150	Santa Cruz Biotechnology	sc-101527
Anti-rabbit IgG (H+L), biotin conjugated	goat pAb against rabbit IgG	1:300		Pierce	31820
Anti-rabbit IgG (whole molecule), FITC-conjugated	goat pAb against rabbit IgG	-	1:200	Sigma-Aldrich	F9887
Anti-mouse IgG, DyLight®650-conjugated	goat pAb against mouse IgG	-	1:100	Abcam	ab97018

RESULTS & DISCUSSION

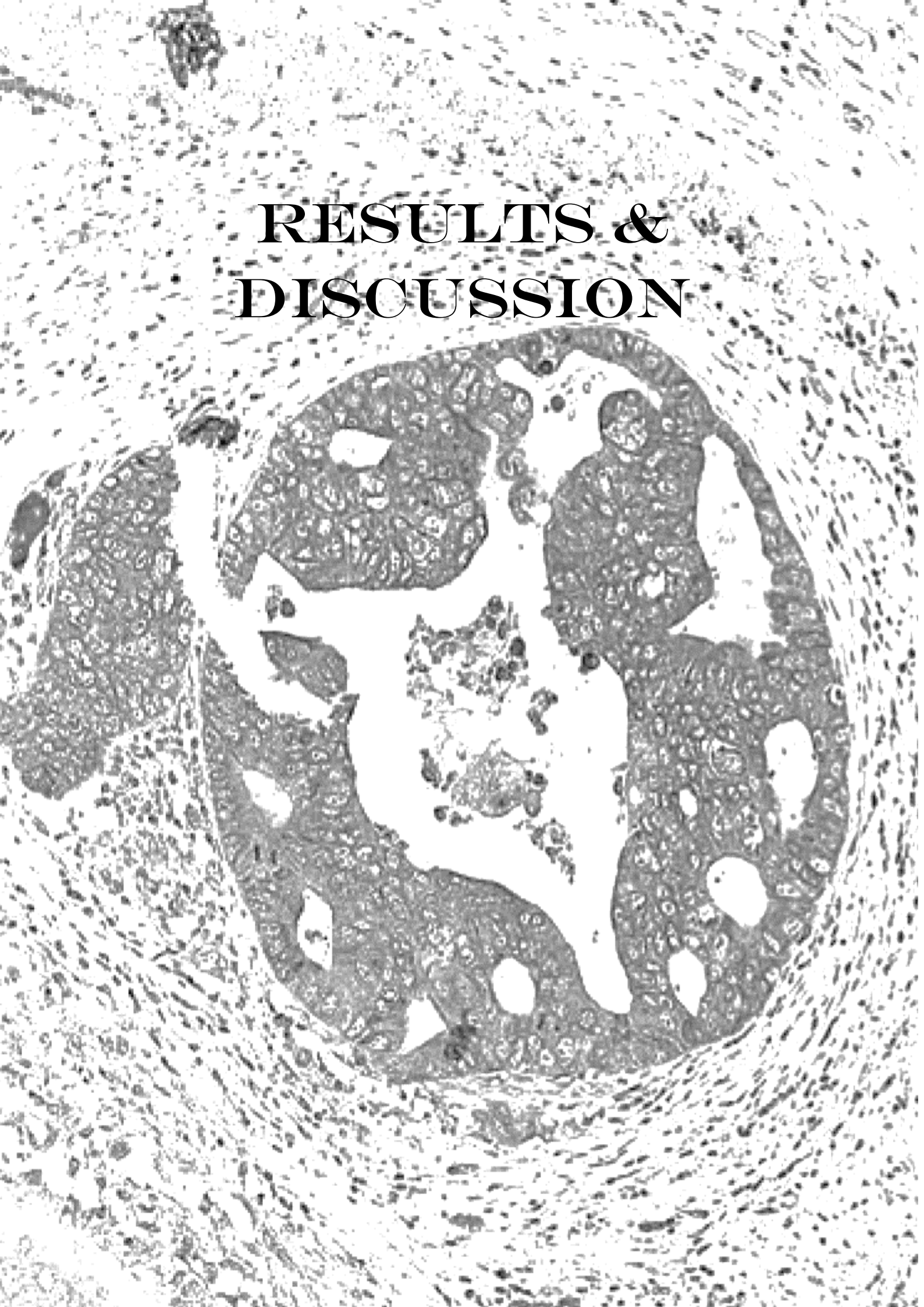

Research in the field of cancer is mainly focused on cell cultures to study the molecular basis of cancers, but to do so we must first consider tumours in their original environment and microenvironment, taking into account all the players involved in the process (cell of origin, macrophages, endothelial cells, pericytes, telocytes, fibroblasts, immune cells, ….), as the interactions between them are strictly related to the inception and propagation of malignancy.

The aim of my PhD project was to study, by immunohistochemistry immunolabelling, the expression of the scaffold proteins IQGAP1, FKBP51 and AmotL2 and the proteins corresponding to the α1, α3, β1 and β2 subunits of Na,K-ATPase, in CRC and liver metastases after the administration of adjuvant CT. The use of double fluorescent protein immunolocalization on human cancer tissue specimens, using different established markers to recognize such players, allowed us to see the macroscopic properties of the disease and gave us preliminary insights that open the way for more specific studies, including the use of experimental animal models and cell cultures, aimed to better understand the role of such players and the molecular basis of the tumorigenic process.

During the course of this PhD project, 4 scientific articles had been published in indexed international scientific journals, allowing the presentation of this PhD thesis as a compendium of publications. Hence, following the procedures that regulate this kind of thesis, the memory includes, in addition to the previous chapters, a report that summarizes the results and discussion of the published articles, and the final conclusions.

4.1 Article 1: Alterations in IQGAP1 expression and localization in colorectal carcinomas and liver metastases following oxaliplatinbased chemotherapy. *Oncol. lett. doi:10.3892/ol.2017.6525*

In healthy colon tissue samples, a homogeneous IQGAP1 pattern was observed in nuclear membrane and in lateral cell membrane and cytoplasm (Article 1, Fig.1A) Instead, the expression pattern and localization of IQGAP1 protein in CRC tissue sections was heterogeneous, both in the healthy glandular epithelium and in tumour glands and nests: strongly IQGAP1^{+} cells were intermixed with unstained tumour cells within a lesion (Article 1, Fig.1G, black arrow). The protein was found localized in the cytoplasm, nuclear envelope, cell junctions, plasma membrane, apical membrane, and this variable localization can be seen in the same structure concurrently (Article 1, Fig.1B,D-F). Cancer cell nests showing a variable positive perinuclear and cytoplasmic staining were often seen in the open-lumen lymphatic ducts present in the submucosa (Article 1, Fig.1B,E *black arrows*). Moreover, high levels of IQGAP1 expression were observed at the growing front of tumour glands (Article 1, Fig.1C).

In several lesions, we observed a strong apical cell membrane staining (Article 1, Fig.1G *arrowhead*) and a strong expression in areas where cells were detaching from the lesion into the lumen (*Article 1, Fig.1G asterisk*). This higher expression and the altered IQGAP1 localization from the cytoplasm to the membrane may lead to a decrease in adherence junctions (AJ) stability, allowing the dissociation of tumour cells [90].

Hepatocytes in healthy liver and in apparently healthy areas of CRC metastasized liver, as well as metastases, exhibited a heterogeneous positive IQGAP1 staining in cytoplasm, nuclear envelope and/or nucleus (Article 3, Fig.6D-E; Article 1 Fig.2 E-F).

Double immunofluorescent staining by IQGAP1 and β-tubulin allowed us to notice that in some tumour cells the co-localization of both proteins was lost (Article 1, Fig.4), showing clear points of EMT occurrence and confirming the proposed role of IQGAP1 in the regulation of membrane dynamics by connecting the cortical actin network to microtubules via plus-end binding proteins (e.g. Cytoplasmic linker protein CLIP-170 and Adenomatous Polyposis Coli -APC) [148–150]. All these findings point to a key role for IQGAP1 in the modulation of functions such as cell growth and survival, cell migration, and cytokinesis. Furthermore, some tumour cells exhibited a co-expression of IQGAP1 and β-tubulin in the nuclear envelope (NE) (Article 1, Fig.4 *arrowheads*), a co-localization that had already been described by Johnson et al. [151] in several epithelial cancer cell lines. The authors correlated these data with a possible role for IQGAP1 in cell polarization and migration processes and in cell-cycle-associated NE assembly/disassembly, suggesting that the interplay between IQGAP1 and the microtubules (MT) may tether MT network to perinuclear actin to modulate the microtubule organizing centre (MTOC) and nuclear positioning during cell migration, a crucial process in carcinogenesis.

To further characterize IQGAP1 expression pattern, we performed double immunofluorescent staining of IQGAP1 protein and the endothelial/ pericyte/macrophage marker CD31 or the endothelial/telocyte marker CD34. A colocalization of IQGAP1 with both markers had been observed in several vessels (Article 1, Fig.3A-E), implicating IQGAP1 in tumour angiogenesis and/or in vascular invasion processes. Moreover, we identified $CD31^+$ stromal cells and $CD34^+$ telocytes (TCs) co-expressing IQGAP1. Telocytes are involved in paracrine signaling and they can release extracellular vesicles such as exosomes and ectosomes from the cell body and from telopodes [36,152]. Increasing evidences point to a role for IQGAP1 in regulating protein trafficking by modulating the assembly-disassembly of actin filaments at the exocytic targets [153]. Interestingly, IQGAP1 labelling in telocytes was found along the plasma membrane of TC's cellular body and in telopodes (Article 3, Fig.6N-Q; *supplemental Fig.S2, panels I-P*).

4.2 Article 2: Expression and localization of the immunophilin FKBP51 in colorectal carcinomas and primary metastases, and alterations following oxaliplatin-based chemotherapy. Oncol. Let. 12: 1315-1322, 2016. doi:10.3892/ol.2016.4772

FKBP51 protein expression in healthy colon and in CRC tissue samples (Article 2, Fig.1) was detected in enterocytes nuclei (Article 2, Fig.1A), endothelial cells, in cells of the *lamina propria* (Article 2, Fig.1A), in the inflammatory and fibrous stromal cells surrounding the lesions (Article 2, Fig.1D-G), and in the cytoplasm and/or nucleus of tumour cells (Article 2, Fig.1D,F). In addition, FKBP51$^+$ telocyte-like cells were observed, forming a network that enveloped CRC tumour nests (Article 3, Fig.5G-H). Co-localization of FKBP51 and the telocyte marker CD34 was detected in such cells (Article 3, Fig.5J-L).
Among the stromal cells, not all the cells expressed FKBP51 (Article 2, Fig.1D-G, Fig.2), suggesting a potential role for this immunophilin protein as a stromal cell subtype marker; though further studies are needed to assess this hypothesis.
Notably, the phenotype of the connective tissue surrounding the lesions appeared variable and dependent on FKBP51 expression. Indeed, in those areas where no immunophilin expression was observed in tumour and stromal cells, stromal fibroblasts exhibited a mature phenotype, with thin, wavy and small spindle cell morphology (Article 2, Fig. 1E and G*, arrows*); by contrast, immature phenotype of stromal fibroblasts, with large, puffy, spindle-shaped morphology, was observed in areas where positive FKBP51 immunostaining was present in tumour and stromal cells (Article 2, Fig. 1F). An increased micro-vessel density and enhanced infiltration of tumour-associated macrophages (TAMs) was also detected in the connective tissue surrounding FKBP51$^+$ lesions (Article 2, Fig. 1F). All these findings support the idea of a role for FKBP51 in the EMT process in CRC.
Interestingly, in CRC tissue sections, several cells of the myenteric plexus were strongly positive (Article 2, Fig.1B), while in healthy colon the signal was fainter (Article 2, Fig.B), suggesting a role for this immunophilin in the development of oxaliplatin-induced neuropathy [154].
IHC analyses allowed the observation of changes in FKBP51 expression levels and localization in malignant liver compared with CRC, confirming the downregulation of this immunophilin in metastasized liver sections resected after oxaliplatin-CT. *ImageJ* software, implemented with the open source plug-in *IHC Profiler*, was used to compare the visual human interpretation to that of the computer-aided vision. In Fig. 5 of Article 2, a box-and-whisker plot illustrates the results obtained using IHC Profiler to compare the percentage of positive pixels (pixel intensity range, 61-120) in the tissue samples. This clearly demonstrates the downregulation of FKBP51 protein in malignant liver specimens vs. CRC tissue samples (7.5±4.3% in liver vs. 71.3±7.6% in CRC; $P<0.003$). The observed downregulation could be associated with the effect of CT on tumour cells, rather than with intrinsic changes of transformed cells. This hypothesis is further supported by the observation that the metastatic liver lesion of a patient with a predominantly negative FKBP51 immunolocalization, exhibited a complete CT resistance.

Lung metastases exhibited a similar expression pattern observed in liver metastases, with weak staining in tumour cells and a strong signal in inflammatory and fibrous stromal cells surrounding the metastases. Whether this weaker expression in the metastatic cells is related to CT or to their cell biology is to be determined by further studies. However, in liver, changes in FKBP51 expression detected in tissues surrounding the metastases, may be related with hepatic sinusoidal injury elicited by oxaliplatin-CT [155].

4.3 Article 3: Commitment of Scaffold Proteins in the Onco-Biology of Human Colorectal Cancer and Liver Metastases after Oxaliplatin-Based Chemotherapy. Int. J. Mol. Sci. 2017, 18, 891; doi:10.3390/ijms18040891

The purpose of this study was to report on the cellular and subcellular localization and dynamics of the scaffold proteins AmotL2, FKBP51 and IQGAP1 in CRC tissue samples and its related liver metastases, discussing the possible interactions between these three scaffoldings in tumour progression and in EMT process.

In the reports of the articles 1 and 2, the variations in the localization and expression of IQGAP1 and FKBP51 had been already described and discussed. To make the dissertation smoother, the new data obtained for IQGAP1 and FKBP51 in this article (Article 3) had been included in those sections.

Here I will describe briefly the results obtained for AmotL2 expression and localization, and will discuss on the possible interplay between the three proteins in CRC tumorigenesis.

AmotL2$^+$ staining had been observed virtually in all the type of cells reported in this study, but at different expression levels. High levels of expression had been observed in blood vessel cells of both healthy and malignant tissues: endothelial cells (Article 3, Fig.2, *v;* Fig.3C-D *v;* Fig.4A-G, *white arrows*), pericytes (Article 3, Fig.S1D, *arrow;* Fig. 4H-M, *white arrows*), monocyte-derived macrophages (Article 3, Fig.4E-G, *yellow arrows;* Fig.4H M, *white arrowhead*). Double immunolocalization of AmotL2 and CD31 or CD34 in serial CRC tissue sections, showed several cells in the perivascular area co-expressing the three proteins (Article 3, Fig.4N-O; Fig.4P-Q), suggesting a pre-commitment stage of the cells from which they could take different cell differentiation fates.

Compared to healthy tissues, in apparently healthy areas of malignant tissues (both CRC and liver metastases) a lower expression level of angiomotin-like 2 protein had been observed (Article 3, Fig.1A-E; Suppl. Fig.S1). In addition, in malignant liver sections, the grading of staining observed in healthy tissues, with a higher AmotL2 cytoplasmic expression in hepatocytes surrounding the central vein (the less oxygenated functional zone) was no further observed. If the gradient expression pattern disappears because of FOLFOX-CT, or if the metastasizing process also affects it, remains to be studied.

In tumour affected areas of the intestinal epithelium, a higher homogeneous AmotL2$^+$ staining had been observed in Lieberkühn Crypts (Article 3, Fig.2F). The expression pattern

observed in healthy tissue, with a higher grade of expression in the crypts facing the *muscularis mucosae* (Article 3, Fig.2A) was no longer visible (Article 3, Fig.2F).
CRC cells exhibited variable intensity of AmotL2 labelling in cytoplasm and nuclear envelope, with a higher grade in budding cells of the invasive front (Article 3, Fig.2F-G'). Metastases exhibited high levels of angiomotin-2 staining in cytoplasm, as well as in the nucleus of budding cells (Article 3, Fig.3B_2).
Deregulated AmotL2 expression in tumours and metastasized areas during tumour progression confirms the recent finding that AmotL2 expression is correlated with loss of polarity and with the EMT process, leading to loss of tissue architecture. Indeed, Mojallal *et al.* have recently demonstrated that hypoxic stress determines the hypoxia-activated c-Fos dependent expression of AmotL2 protein in human breast and colorectal cancer cell lines [111]. c-Fos/hypoxia-induced Amotl2 interacts with the Crb3 and Par3 complexes, involved in the establishment and maintenance of apical-basal cell polarity, retaining such complexes in large vesicles and preventing them to reach the apical membrane [111].
Changes in expression levels and in the subcellular redistribution of AmotL2 protein in CRC cells shown in this study are indicative of the involvement of this scaffold protein in CRC tumorigenesis and progression, as well as EMT process.
Scaffold proteins, such as AmotL2, IQGAP1 and FKBP51, bring together in touch multiple modular partners committed in a specific task, usually in a stable complex and in a peculiar subcellular localization manner. These superstructures integrate functions such as enzymatic pathways, cell motility, sorting, signaling, stabilization, localization of plasma membrane proteins, recycling or cell polarity; facts all pivotal in cell fate, tumorigenesis, migration, tumour progression and angiogenesis [156–158].
In this study, we show evidence that these three scaffold proteins exhibit changes in expression and localization in tissue samples of pre-CT treated CRC compared to its liver metastases, resected after FOLFOX-CT. The co-localization of CD34 and/or CD31 with these scaffoldins in several vessel cells, including expression in pericytes and/or telocytes, suggests their involvement in tumour angiogenesis and/or in vascular invasion. Taking into account the key role of these proteins in the dynamics of tumour cells, they represent an attractive group of interacting scaffold proteins that could be used as biomarkers for diagnostic staging and as targets for therapy, although further research is needed to confirm and to precise these findings.
Figure 7. Article 3, shows a model of inferred interactions of AmotL2, FKBP51, and IQGAP1 made upon integration of our data with the literature and data from databanks.
Scaffold proteins connect structural and signaling molecules in the spatiotemporal organization and activation in CRC tumorigenic cells [159,160]. The process takes place in different subcellular localizations and at variable expression levels depending on the status of the cell within the tumour. Further studies are needed to confirm the possible existence of the complex FKBP51-HSP90-SRC-YAP-AmotL2-IQGAP1, though String analysis [161] has shown experimental and database evidences of known functional interactions among AmotL2, IQGAP1 and FKBP51 in several physiological and pathological situations

through the transcriptional coactivator Yap1, the oncogene Src and the chaperone HSP90 (Article 3, Fig.1).

4.4 Article 4: Na,K-ATPase Isozymes in Colorectal Cancer and Liver Metastases. Front. Physiol. 2016 Jan 29;7:9

Our purpose for this study was to determine the cellular and subcellular localization of the α and β subunit isoforms of Na,K-ATPase in CRC and its liver metastasis using a panel of well-characterized isoform-specific antibodies. The primary hypothesis of this study was that metastatic cancer cells possess a unique expression phenotype of Na,K-ATPase isozymes, similar to that of CRC cells. Na,K-ATPase subunits are able to form different functional isozymes in a promiscuous association of α and β isoforms. These isozymes are characterized by distinctive enzymatic properties and a strictly modulated pattern of expression relying on cell type, developmental phase and hormone regulation [162]. The 4 human α isoforms define the kinetic properties of the different isozymes, while the 3 β subunits are able to influence the Na^+ and K^+ affinities [129,162–164]. The apparent affinities for cations have been determined by expressing recombinant enzymes in heterologous systems [163,165]. Affinities of human isozymes expressed in *Xenopus laevis* oocytes are α1β1>α2β1>α3β1 for Na^+ and α3β1=α1β1> α1β3>α1β2> α2β1>α3β3> α3β2> α2β3> α2β2 for K^+ [165].

Table 2 of this article summarizes the cell-specific Na,K-ATPase subunit-isoforms expression detected in healthy colon and liver tissue samples and in CRC and its related liver metastases.

As can be observed, α3 isoform expression was increased in several cell types of CRC tissue samples (e.g. CRC cells, mesenchymal cells, immune system cells, endothelial cells), and an altered pattern of expression has been detected in CRC cells, compared to healthy tissues. Indeed, while in healthy epithelial cells α3 subunit was mainly located in or near the plasma membrane (Article 4, Fig.1E), in CRC samples this isoform was localized in a perinuclear fashion in CRC cells and no staining was detected in the plasma membrane (Article 4, Fig.1F). More intriguingly, in healthy liver tissues, the α3 isoform was not detected (Article 4, Fig.4E), while in metastatic liver samples, this isoform was detected mainly at a perinuclear location and diffusely expressed across the cytoplasm of malignant cells (Article 4, Fig.4F) and hepatocytes (Article 4, Fig.4H), and in immune cells (Article 4, Fig.4G). Conversely, we found the α1 isoform along the plasma membrane of hepatocytes in healthy liver tissues (Article 4, Fig.4A), but not in apparently healthy areas of metastatic liver tissues. α1 expression was also observed in metastatic tumour cell niches within the liver, with variable localization (cytoplasm and/or plasma membrane) (Article 4, Fig.4C-D). More studies are needed to assess if these changes in expression and localization of the α1 and α3 isoforms observed in metastasized liver tissues, are due to FOLFOX-CT or to intrinsic changes related with malignancy.

The high levels of perinuclear and cytoplasmic α3 isoform detected in malignant liver tissues, suggests other *moonlighting* functions for this isoform besides ion transport.
Regarding the β1 and β2 isoforms, in metastasized liver, β1 was detected in disordered and semi-necrotic tumour tissue (Article 4, Fig.5C-D), while β2 was not detected (Article 4, Fig.5H). This may be related to the fact that these metastatic cells arise from CRC tumour cells, which did neither express β2 isoform or at a very insignificant level (Article 4, Fig.5).
In Table 3 of Article 4, are highlighted the possible cell-specific isozymes that may be present in healthy colon, CRC, healthy liver and metastasized liver, based on the data collected in this study. As can be observed, in mesenchymal cells surrounding the lesions, the predominant isozyme is α3β2, which have a low K^+ affinity. Conversely, in CRC and in metastatic cells, the predominant isozymes are α1β1 and α3β1. α1β1 isozyme have the highest Na^+ affinity, while α3β1 the lowest; and both isozymes have the highest K^+ affinity. These are the isozyme combinations that allow an optimal performance of the enzymes involved in protein synthesis and transfer of phosphor groups. In cancer, Na^+ and K^+ ions are likely to favor optimal conditions for the function of nuclear enzymes involved in mitosis, particularly high intra-nuclear K^+ concentration.
Double immunofluorescent labelling of α3 and β1 subunits in liver metastases tissue samples, confirms the co-localization of both isoforms in malignant cells (Article 4, Fig.S1), and suggests the possible role for this isozyme as a novel biomarker for CRC metastatic cells in liver.

CONCLUSIONS

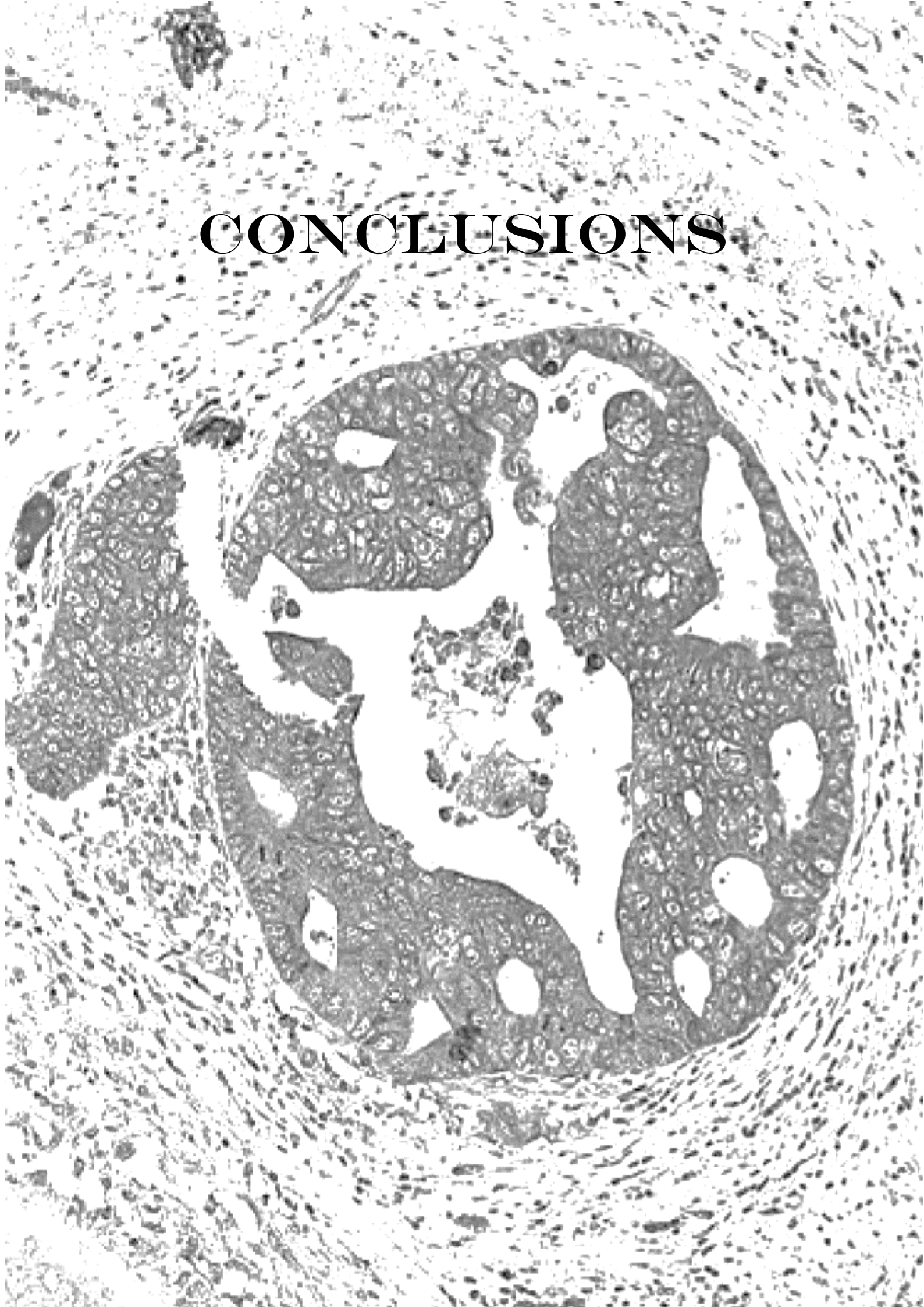

1. The analysis of IQGAP1 detailed expression in CRC tissue sections and metastasized liver tissue samples, resected after oxaliplatin-based CT-treatment, showed:

- The loss of β-tubulin and IQGAP1 co-localization in several tumour cells, detects clear points of EMT occurrence and confirm the already proposed role of IQGAP1 in the regulation of membrane dynamics, suggesting a key role for IQGAP1 in the modulation of cell growth and survival, cell migration, and cytokinesis.
- The co-expression of IQGAP1 and β-tubulin in the nuclear envelope (NE) of several tumour cells, correlates with a possible role for IQGAP1 in cell polarization and migration processes and in cell cycle-associated nuclear envelope assembly/disassembly.
- The colocalization of IQGAP1 with CD31 and CD34 markers observed in several vessels involves IQGAP1 protein in tumour angiogenesis and/or in vascular invasion processes.
- IQGAP1 labelling along the plasma membrane of telocyte's cellular body and in telopodes, sustains the idea of a role for IQGAP1 in the regulation of protein traffic by modulating the assembly-disassembly of actin filaments at the exocytic targets.

2. The immunohistochemistry for FKBP51 in tissue sections of metastasized liver resected after oxaliplatin-based chemotherapy confirms at the protein level the downregulation of FKBP51 gene expression elicited by FOLFOX chemotherapy in PWCs of CRC patients.

- The expression of FKBP51 in tumour and stroma cells correlates with the immature phenotype of stromal fibroblasts, suggesting a role for this protein in the EMT process in CRC.
- The observation that only certain cells in the tumour-associated stroma express FKBP51 suggests a potential role for this immunophilin as a stromal cell subtype marker.
- The high expression of FKBP51 in neural cells of the Auerbach's and Meissner's plexus in CRC, compared to a lighter signal in neural cells of healthy colon tissues, might be related with the development of oxaliplatin-induced autonomic neuropathy.

3. The expression levels and the subcellular redistribution of AmotL2 protein in CRC cells, as well as the altered pattern of protein expression detected in tumour affected areas of CRC and related metastases, are indicative of the involvement of this scaffold protein in CRC tumorigenesis and progression, as well as in the EMT and angiogenesis processes.

- The co-localization of IQGAP1, FKBP51 and AmotL2 with CD34 and/or CD31 in several cell vessels, including expression in pericytes and/or telocytes, suggests their involvement in tumour angiogenesis and/or in vascular invasion.
- Due to the key role that these scaffold proteins exert in the dynamics of tumor cells, they represent an attractive group of interacting proteins that could be used as biomarkers for diagnostic staging and as targets for therapy.

4. The α and β subunits of the Na,K-ATPase vary their pattern of expression and localization in CRC, in metastases and in metastasized liver tissue as follows:

- The α1, α3 and β1 isoforms are the most highly expressed in tumour cells and metastases.
- The high levels of perinuclear and cytoplasmic α3 isoform detected in malignant liver tissues, suggests other *moonlighting* functions for this isoform besides ion transport.
- Based on the data collected in this study, the possibly predominant isozymes present in tumour and metastatic cells are α1β1 and α3β1, which exhibit the highest and lowest Na^+ affinity respectively, and the highest K^+ affinity. These ions are likely to favor optimal conditions for the function of nuclear enzymes involved in mitosis.
- Double immunofluorescent labelling of α3 and β1 subunits in liver metastases tissue samples, confirms the co-localization of both isoforms in malignant cells, and suggests the possible role for this isozyme as a novel biomarker for CRC metastatic cells in liver.

REFERENCE LIST

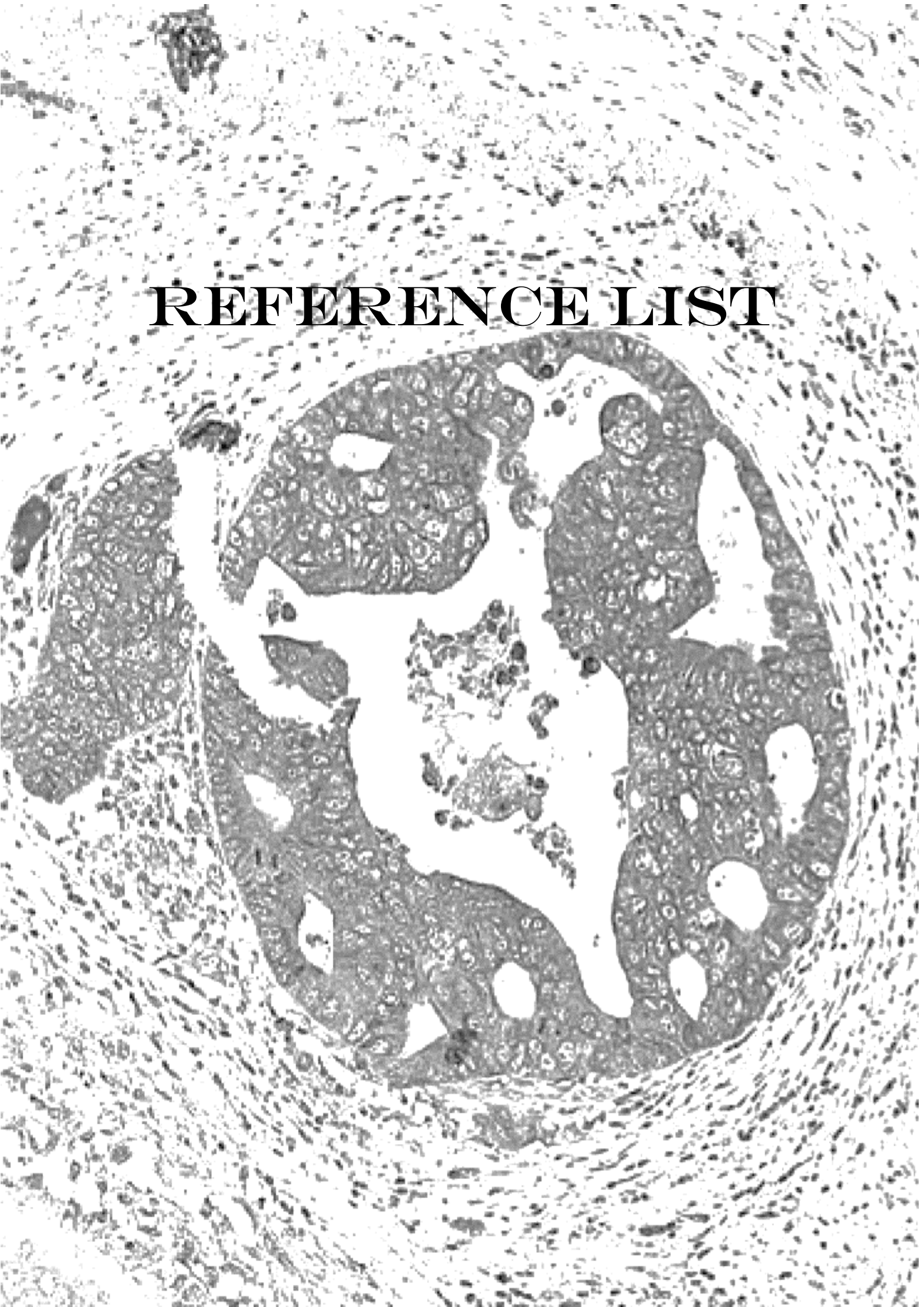

Reference List

1. Vries RG, Huch M, Clevers H. Stem cells and cancer of the stomach and intestine. *Mol. Oncol.* **2010,** 4, 373-384. S1574-7891(10)00034-7 [pii];10.1016/j.molonc.2010.05.001 [doi].

2. Todaro M, Francipane MG, Medema JP, Stassi G. Colon cancer stem cells: promise of targeted therapy. *Gastroenterology* **2010,** 138, 2151-2162. S0016-5085(10)00167-8 [pii];10.1053/j.gastro.2009.12.063 [doi].

3. Lobo NA, Shimono Y, Qian D, Clarke MF. The biology of cancer stem cells. *Annu. Rev. Cell Dev. Biol.* **2007,** 23, 675-699. 10.1146/annurev.cellbio.22.010305.104154 [doi].

4. Dalerba P, Cho RW, Clarke MF. Cancer stem cells: models and concepts. *Annu. Rev. Med.* **2007,** 58, 267-284. 10.1146/annurev.med.58.062105.204854 [doi].

5. Fabian A, Barok M, Vereb G, Szollosi J. Die hard: are cancer stem cells the Bruce Willises of tumor biology? *Cytometry A* **2009,** 75, 67-74. 10.1002/cyto.a.20690 [doi].

6. Frank NY, Schatton T, Frank MH. The therapeutic promise of the cancer stem cell concept. *J. Clin. Invest* **2010,** 120, 41-50. 41004 [pii];10.1172/JCI41004 [doi].

7. Wicha MS, Liu S, Dontu G. Cancer stem cells: an old idea--a paradigm shift. *Cancer Res.* **2006,** 66, 1883-1890. 66/4/1883 [pii];10.1158/0008-5472.CAN-05-3153 [doi].

8. Visvader JE, Lindeman GJ. Stem cells and cancer - the promise and puzzles. *Mol. Oncol.* **2010,** 4, 369-372. S1574-7891(10)00062-1 [pii];10.1016/j.molonc.2010.07.001 [doi].

9. Stoian M, Stoica V, Radulian G. Stem cells and colorectal carcinogenesis. *J. Med. Life* **2016,** 9, 6-11.

10. Smythies J. Intercellular Signaling in Cancer-the SMT and TOFT Hypotheses, Exosomes, Telocytes and Metastases: Is the Messenger in the Message? *J. Cancer.* **2015,** 6, 604-609.

11. Rosenfeld S. Are the Somatic Mutation and Tissue Organization Field Theories of Carcinogenesis Incompatible? *Cancer Inform.* **2013,** 12, 221-229. 10.4137/CIN.S13013 [doi];cin-12-2013-221 [pii].

12. Bedessem B, Ruphy S. SMT or TOFT? How the two main theories of carcinogenesis are made (artificially) incompatible. *Acta Biotheor.* **2015,** 63, 257-267. 10.1007/s10441-015-9252-1 [doi].

13. Sonnenschein C, Soto AM. Carcinogenesis explained within the context of a theory of organisms. *Prog. Biophys. Mol. Biol.* **2016,** 122, 70-76. S0079-6107(16)30088-8 [pii];10.1016/j.pbiomolbio.2016.07.004 [doi].

14. Soto AM, Sonnenschein C. The tissue organization field theory of cancer: A testable replacement for the somatic mutation theory. *Bioessays* **2011,** 33, 332-340. 10.1002/bies.201100025 [doi].

15. Sonnenschein C, Soto AM. Somatic mutation theory of carcinogenesis: why it should be dropped and replaced. *Mol. Carcinog.* **2000,** 29, 205-211. 10.1002/1098-2744(200012)29:4<205::AID-MC1002>3.0.CO;2-W [pii].

16. Vaux DL. Response to "The tissue organization field theory of cancer: a testable replacement for the somatic mutation theory". DOI: 10.1002/bies.201100025. *Bioessays* **2011,** 33, 660-661. 10.1002/bies.201100063 [doi].

17. Baker SG. TOFT better explains experimental results in cancer research than SMT (comment on DOI 10.1002/bies.201100025 and DOI 10.1002/bies.201100022). *Bioessays* **2011,** 33, 919-921. 10.1002/bies.201100124 [doi].

18. Maffini MV, Soto AM, Calabro JM, Ucci AA, Sonnenschein C. The stroma as a crucial target in rat mammary gland carcinogenesis. *J. Cell Sci.* **2004,** 117, 1495-1502. 10.1242/jcs.01000 [doi];jcs.01000 [pii].

19. Chaffer CL, Weinberg RA. A perspective on cancer cell metastasis. *Science.* **2011,** 331, 1559-1564.

20. Scheel C, Weinberg RA. Cancer stem cells and epithelial-mesenchymal transition: concepts and molecular links. *Semin. Cancer Biol.* **2012,** 22, 396-403.

21. Massague J, Blain SW, Lo RS. TGFbeta signaling in growth control, cancer, and heritable disorders. *Cell.* **2000,** 103, 295-309.

22. Derynck R, Akhurst RJ, Balmain A. TGF-beta signaling in tumor suppression and cancer progression. *Nat. Genet.* **2001,** 29, 117-129.

23. Shuman Moss LA, Jensen-Taubman S, Stetler-Stevenson WG. Matrix metalloproteinases: changing roles in tumor progression and metastasis. *Am. J. Pathol.* **2012,** 181, 1895-1899.

24. Pietras K, Ostman A. Hallmarks of cancer: interactions with the tumor stroma. *Exp. Cell Res.* **2010,** 316, 1324-1331.

25. Valastyan S, Weinberg RA. Tumor metastasis: molecular insights and evolving paradigms. *Cell.* **2011,** 147, 275-292.

26. Chanmee T, Ontong P, Konno K, Itano N. Tumor-Associated Macrophages as Major Players in the Tumor Microenvironment. *Cancers. (Basel)* **2014,** 6, 1670-1690. 10.3390/cancers6031670 [doi];cancers-06-01670 [pii].

27. Sica A, Mantovani A. Macrophage plasticity and polarization: in vivo veritas. *J. Clin. Invest* **2012,** 122, 787-795. 59643 [pii];10.1172/JCI59643 [doi].

28. Lu J, Ye X, Fan F, Xia L, Bhattacharya R, Bellister S, Tozzi F, Sceusi E, Zhou Y, Tachibana I, Maru DM, Hawke DH, Rak J, Mani SA, Zweidler-McKay P, Ellis LM. Endothelial cells promote the colorectal cancer stem cell phenotype through a soluble form of Jagged-1. *Cancer Cell* **2013,** 23, 171-185. S1535-6108(13)00031-7 [pii];10.1016/j.ccr.2012.12.021 [doi].

29. Bergers G, Song S. The role of pericytes in blood-vessel formation and maintenance. *Neuro. Oncol.* **2005,** 7, 452-464. 10.1215/S1152851705000232 [doi].

30. Gerhardt H, Betsholtz C. Endothelial-pericyte interactions in angiogenesis. *Cell Tissue Res.* **2003,** 314, 15-23. 10.1007/s00441-003-0745-x [doi].

31. Ribatti D, Nico B, Crivellato E. The role of pericytes in angiogenesis. *Int. J. Dev. Biol.* **2011,** 55, 261-268. 103167dr [pii];10.1387/ijdb.103167dr [doi].

32. Crisan M, Yap S, Casteilla L, Chen CW, Corselli M, Park TS, Andriolo G, Sun B, Zheng B, Zhang L, Norotte C, Teng PN, Traas J, Schugar R, Deasy BM, Badylak S, Buhring HJ, Giacobino JP, Lazzari L, Huard J, Peault B. A perivascular origin for mesenchymal stem cells in multiple human organs. *Cell Stem Cell* **2008,** 3, 301-313. S1934-5909(08)00337-8 [pii];10.1016/j.stem.2008.07.003 [doi].

33. Balabanov R, Washington R, Wagnerova J, Dore-Duffy P. CNS microvascular pericytes express macrophage-like function, cell surface integrin alpha M, and macrophage marker ED-2. *Microvasc. Res.* **1996,** 52, 127-142. S0026-2862(96)90049-7 [pii];10.1006/mvre.1996.0049 [doi].

34. Ribeiro AL, Okamoto OK. Combined effects of pericytes in the tumor microenvironment. *Stem Cells Int.* **2015,** 2015, 868475. 10.1155/2015/868475 [doi].

35. Popescu LM, Faussone-Pellegrini MS. TELOCYTES - a case of serendipity: the winding way from Interstitial Cells of Cajal (ICC), via Interstitial Cajal-Like Cells (ICLC) to TELOCYTES. *J. Cell Mol. Med.* **2010,** 14, 729-740.

36. Cretoiu SM, Popescu LM. Telocytes revisited. *Biomol. Concepts* **2014,** 5, 353-369. 10.1515/bmc-2014-0029 [doi];/j/bmc.2014.5.issue-5/bmc-2014-0029/bmc-2014-0029.xml [pii].

37. Edelstein L, Fuxe K, Levin M, Popescu BO, Smythies J. Telocytes in their context with other intercellular communication agents. *Semin. Cell Dev. Biol.* **2016,** 55, 9-13. S1084-9521(16)30071-4 [pii];10.1016/j.semcdb.2016.03.010 [doi].

38. Diaz-Flores L, Gutierrez R, Gonzalez-Gomez M, Diaz-Flores L, Jr., Valladares F, Rancel N, Saez FJ, Madrid JF. Telocyte Behaviour During Inflammation, Repair and Tumour Stroma Formation. *Adv. Exp. Med. Biol.* **2016,** 913, 177-191. 10.1007/978-981-10-1061-3_12 [doi].

39. Ferlay J, Shin HR, Bray F, Forman D, Mathers C, Parkin DM. Estimates of worldwide burden of cancer in 2008: GLOBOCAN 2008. *Int. J. Cancer.* **2010,** 127, 2893-2917.

40. Lampropoulos P, Zizi-Sermpetzoglou A, Rizos S, Kostakis A, Nikiteas N, Papavassiliou AG. TGF-beta signalling in colon carcinogenesis. *Cancer Lett.* **2012,** 314, 1-7. S0304-3835(11)00601-X [pii];10.1016/j.canlet.2011.09.041 [doi].

41. Markowitz SD, Bertagnolli MM. Molecular origins of cancer: Molecular basis of colorectal cancer. *N. Engl. J. Med.* **2009,** 361, 2449-2460. 361/25/2449 [pii];10.1056/NEJMra0804588 [doi].

42. Vaiopoulos AG, Kostakis ID, Koutsilieris M, Papavassiliou AG. Colorectal cancer stem cells. *Stem Cells* **2012,** 30, 363-371. 10.1002/stem.1031 [doi].

43. Jeon MK, Klaus C, Kaemmerer E, Gassler N. Intestinal barrier: Molecular pathways and modifiers. *World J. Gastrointest. Pathophysiol.* **2013,** 4, 94-99. 10.4291/wjgp.v4.i4.94 [doi].

44. Novellasdemunt L, Antas P, Li VS. Targeting Wnt signaling in colorectal cancer. A Review in the Theme: Cell Signaling: Proteins, Pathways and Mechanisms. *Am. J. Physiol Cell Physiol* **2015,** 309, C511-C521. ajpcell.00117.2015 [pii];10.1152/ajpcell.00117.2015 [doi].

45. Fevr T, Robine S, Louvard D, Huelsken J. Wnt/beta-catenin is essential for intestinal homeostasis and maintenance of intestinal stem cells. *Mol. Cell Biol.* **2007,** 27, 7551-7559. MCB.01034-07 [pii];10.1128/MCB.01034-07 [doi].

46. Sansom OJ, Reed KR, Hayes AJ, Ireland H, Brinkmann H, Newton IP, Batlle E, Simon-Assmann P, Clevers H, Nathke IS, Clarke AR, Winton DJ. Loss of Apc in vivo immediately perturbs Wnt signaling, differentiation, and migration. *Genes Dev.* **2004,** 18, 1385-1390. 10.1101/gad.287404 [doi];18/12/1385 [pii].

47. Ireland H, Kemp R, Houghton C, Howard L, Clarke AR, Sansom OJ, Winton DJ. Inducible Cre-mediated control of gene expression in the murine gastrointestinal tract: effect of loss of beta-catenin. *Gastroenterology* **2004,** 126, 1236-1246. S0016508504004500 [pii].

48. Korinek V, Barker N, Moerer P, van DE, Huls G, Peters PJ, Clevers H. Depletion of epithelial stem-cell compartments in the small intestine of mice lacking Tcf-4. *Nat. Genet.* **1998,** 19, 379-383. 10.1038/1270 [doi].

49. Pinto D, Gregorieff A, Begthel H, Clevers H. Canonical Wnt signals are essential for homeostasis of the intestinal epithelium. *Genes Dev.* **2003,** 17, 1709-1713. 10.1101/gad.267103 [doi];17/14/1709 [pii].

50. Wong MH, Huelsken J, Birchmeier W, Gordon JI. Selection of multipotent stem cells during morphogenesis of small intestinal crypts of Lieberkuhn is perturbed by stimulation of Lef-1/beta-catenin signaling. *J. Biol. Chem.* **2002,** 277, 15843-15850. 10.1074/jbc.M200184200 [doi];M200184200 [pii].

51. Wong MH, Rubinfeld B, Gordon JI. Effects of forced expression of an NH2-terminal truncated beta-Catenin on mouse intestinal epithelial homeostasis. *J. Cell Biol.* **1998,** 141, 765-777.

52. Comprehensive molecular characterization of human colon and rectal cancer. *Nature* **2012,** 487, 330-337. nature11252 [pii];10.1038/nature11252 [doi].

53. Mimori-Kiyosue Y, Shiina N, Tsukita S. The dynamic behavior of the APC-binding protein EB1 on the distal ends of microtubules. *Curr. Biol.* **2000,** 10, 865-868. S0960-9822(00)00600-X [pii].

54. Fearon ER. Molecular genetics of colorectal cancer. *Annu. Rev. Pathol.* **2011,** 6, 479-507. 10.1146/annurev-pathol-011110-130235 [doi].

55. Huels DJ, Cammareri P, Ridgway RA, Medema JP, Sansom OJ. Methods to assess Myc function in intestinal homeostasis, regeneration, and tumorigenesis. *Methods Mol. Biol.* **2013,** 1012, 237-248. 10.1007/978-1-62703-429-6_16 [doi].

56. Morin PJ, Sparks AB, Korinek V, Barker N, Clevers H, Vogelstein B, Kinzler KW. Activation of beta-catenin-Tcf signaling in colon cancer by mutations in beta-catenin or APC. *Science* **1997,** 275, 1787-1790.

57. Haegebarth A, Clevers H. Wnt signaling, lgr5, and stem cells in the intestine and skin. *Am. J. Pathol.* **2009,** 174, 715-721. S0002-9440(10)60932-7 [pii];10.2353/ajpath.2009.080758 [doi].

58. Medema JP, Vermeulen L. Microenvironmental regulation of stem cells in intestinal homeostasis and cancer. *Nature* **2011,** 474, 318-326. nature10212 [pii];10.1038/nature10212 [doi].

59. Noah TK, Shroyer NF. Notch in the intestine: regulation of homeostasis and pathogenesis. *Annu. Rev. Physiol* **2013,** 75, 263-288. 10.1146/annurev-physiol-030212-183741 [doi].

60. Pellegrinet L, Rodilla V, Liu Z, Chen S, Koch U, Espinosa L, Kaestner KH, Kopan R, Lewis J, Radtke F. Dll1- and dll4-mediated notch signaling are required for homeostasis of intestinal stem cells. *Gastroenterology* **2011,** 140, 1230-1240. S0016-5085(11)00039-4 [pii];10.1053/j.gastro.2011.01.005 [doi].

61. Fre S, Huyghe M, Mourikis P, Robine S, Louvard D, Artavanis-Tsakonas S. Notch signals control the fate of immature progenitor cells in the intestine. *Nature* **2005,** 435, 964-968. nature03589 [pii];10.1038/nature03589 [doi].

62. Zheng H, Pritchard DM, Yang X, Bennett E, Liu G, Liu C, Ai W. KLF4 gene expression is inhibited by the notch signaling pathway that controls goblet cell differentiation in mouse gastrointestinal tract. *Am. J. Physiol Gastrointest. Liver Physiol* **2009,** 296, G490-G498. 90393.2008 [pii];10.1152/ajpgi.90393.2008 [doi].

63. Sureban SM, May R, George RJ, Dieckgraefe BK, McLeod HL, Ramalingam S, Bishnupuri KS, Natarajan G, Anant S, Houchen CW. Knockdown of RNA binding protein musashi-1 leads to tumor regression in vivo. *Gastroenterology* **2008,** 134, 1448-1458. S0016-5085(08)00345-4 [pii];10.1053/j.gastro.2008.02.057 [doi].

64. Akiyoshi T, Nakamura M, Yanai K, Nagai S, Wada J, Koga K, Nakashima H, Sato N, Tanaka M, Katano M. Gamma-secretase inhibitors enhance taxane-induced mitotic arrest and apoptosis in colon cancer cells. *Gastroenterology* **2008,** 134, 131-144. S0016-5085(07)01807-0 [pii];10.1053/j.gastro.2007.10.008 [doi].

65. Santagata S, Demichelis F, Riva A, Varambally S, Hofer MD, Kutok JL, Kim R, Tang J, Montie JE, Chinnaiyan AM, Rubin MA, Aster JC. JAGGED1 expression is associated with prostate cancer metastasis and recurrence. *Cancer Res.* **2004,** 64, 6854-6857. 64/19/6854 [pii];10.1158/0008-5472.CAN-04-2500 [doi].

66. Bellam N, Pasche B. Tgf-beta signaling alterations and colon cancer. *Cancer Treat. Res.* **2010,** 155, 85-103. 10.1007/978-1-4419-6033-7_5 [doi].

67. Hardwick JC, Kodach LL, Offerhaus GJ, van den Brink GR. Bone morphogenetic protein signalling in colorectal cancer. *Nat. Rev. Cancer* **2008,** 8, 806-812. nrc2467 [pii];10.1038/nrc2467 [doi].

68. Abdul Khalek FJ, Gallicano GI, Mishra L. Colon cancer stem cells. *Gastrointest. Cancer Res.* **2010,** S16-S23.

69. Hoosein NM, McKnight MK, Levine AE, Mulder KM, Childress KE, Brattain DE, Brattain MG. Differential sensitivity of subclasses of human colon carcinoma cell lines to the growth inhibitory effects of transforming growth factor-beta 1. *Exp. Cell Res.* **1989,** 181, 442-453.

70. Xu Y, Pasche B. TGF-beta signaling alterations and susceptibility to colorectal cancer. *Hum. Mol. Genet.* **2007,** 16 Spec No 1, R14-R20. 16/R1/R14 [pii];10.1093/hmg/ddl486 [doi].

71. Friedman E, Gold LI, Klimstra D, Zeng ZS, Winawer S, Cohen A. High levels of transforming growth factor beta 1 correlate with disease progression in human colon cancer. *Cancer Epidemiol. Biomarkers Prev.* **1995,** 4, 549-554.

72. Robson H, Anderson E, James RD, Schofield PF. Transforming growth factor beta 1 expression in human colorectal tumours: an independent prognostic marker in a subgroup of poor prognosis patients. *Br. J. Cancer* **1996,** 74, 753-758.

73. von BA, Cho KW. Intracellular BMP signaling regulation in vertebrates: pathway or network? *Dev. Biol.* **2001,** 239, 1-14. 10.1006/dbio.2001.0388 [doi];S0012-1606(01)90388-4 [pii].

74. Voorneveld PW, Kodach LL, Jacobs RJ, Liv N, Zonnevylle AC, Hoogenboom JP, Biemond I, Verspaget HW, Hommes DW, de RK, van Noesel CJ, Morreau H, van WT, Offerhaus GJ, van den Brink GR, Peppelenbosch MP, Ten DP, Hardwick JC. Loss of SMAD4 alters BMP signaling to promote colorectal cancer cell metastasis via activation of Rho and ROCK. *Gastroenterology* **2014,** 147, 196-208. S0016-5085(14)00450-8 [pii];10.1053/j.gastro.2014.03.052 [doi].

75. Varnat F, Duquet A, Malerba M, Zbinden M, Mas C, Gervaz P, Altaba A. Human colon cancer epithelial cells harbour active HEDGEHOG-GLI signalling that is essential for tumour growth, recurrence, metastasis and stem cell survival and expansion. *EMBO Mol. Med.* **2009,** 1, 338-351. 10.1002/emmm.200900039 [doi].

76. Gulino A, Ferretti E, De SE. Hedgehog signalling in colon cancer and stem cells. *EMBO Mol. Med.* **2009,** 1, 300-302. 10.1002/emmm.200900042 [doi].

77. Colakoglu T, Yildirim S, Kayaselcuk F, Nursal TZ, Ezer A, Noyan T, Karakayali H, Haberal M. Clinicopathological significance of PTEN loss and the phosphoinositide 3-kinase/Akt pathway in sporadic colorectal neoplasms: is PTEN loss predictor of local recurrence? *Am. J. Surg.* **2008,** 195, 719-725. S0002-9610(08)00176-1 [pii];10.1016/j.amjsurg.2007.05.061 [doi].

78. Wierzbicki PM, Rybarczyk A. The Hippo pathway in colorectal cancer. *Folia Histochem. Cytobiol.* **2015,** 53, 105-119. VM/OJS/J/42583 [pii];10.5603/FHC.a2015.0015 [doi].

79. Andre T, Boni C, Mounedji-Boudiaf L, Navarro M, Tabernero J, Hickish T, Topham C, Zaninelli M, Clingan P, Bridgewater J, Tabah-Fisch I, de GA. Oxaliplatin, fluorouracil, and leucovorin as adjuvant treatment for colon cancer. *N. Engl. J. Med.* **2004,** 350, 2343-2351.

80. Kline CL, El-Deiry WS. Personalizing colon cancer therapeutics: targeting old and new mechanisms of action. *Pharmaceuticals. (Basel).* **2013,** 6, 988-1038.

81. Todaro M, Alea MP, Di Stefano AB, Cammareri P, Vermeulen L, Iovino F, Tripodo C, Russo A, Gulotta G, Medema JP, Stassi G. Colon cancer stem cells dictate tumor growth and resist cell death by production of interleukin-4. *Cell Stem Cell* **2007,** 1, 389-402. S1934-5909(07)00118-X [pii];10.1016/j.stem.2007.08.001 [doi].

82. Raymond E, Chaney SG, Taamma A, Cvitkovic E. Oxaliplatin: a review of preclinical and clinical studies. *Ann. Oncol.* **1998,** 9, 1053-1071.

83. Morales M, Avila J, Gonzalez-Fernandez R, Boronat L, Soriano ML, Martin-Vasallo P. Differential transcriptome profile of peripheral white cells to identify biomarkers involved in oxaliplatin induced neuropathy. *J. Pers. Med.* **2014,** 4, 282-296.

84. Johnson M, Sharma M, Henderson BR. IQGAP1 regulation and roles in cancer. *Cell Signal.* **2009,** 21, 1471-1478.

85. White CD, Brown MD, Sacks DB. IQGAPs in cancer: a family of scaffold proteins underlying tumorigenesis. *FEBS Lett.* **2009,** 583, 1817-1824.

86. Erickson JW, Cerione RA, Hart MJ. Identification of an actin cytoskeletal complex that includes IQGAP and the Cdc42 GTPase. *J. Biol. Chem.* **1997,** 272, 24443-24447.

87. Roy M, Li Z, Sacks DB. IQGAP1 is a scaffold for mitogen-activated protein kinase signaling. *Mol. Cell Biol.* **2005,** 25, 7940-7952.

88. McDonald KL, O'Sullivan MG, Parkinson JF, Shaw JM, Payne CA, Brewer JM, Young L, Reader DJ, Wheeler HT, Cook RJ, Biggs MT, Little NS, Teo C, Stone G, Robinson BG. IQGAP1 and IGFBP2: valuable biomarkers for determining prognosis in glioma patients. *J. Neuropathol. Exp. Neurol.* **2007,** 66, 405-417.

89. Nabeshima K, Shimao Y, Inoue T, Koono M. Immunohistochemical analysis of IQGAP1 expression in human colorectal carcinomas: its overexpression in carcinomas and association with invasion fronts. *Cancer Lett.* **2002,** 176, 101-109.

90. Takemoto H, Doki Y, Shiozaki H, Imamura H, Utsunomiya T, Miyata H, Yano M, Inoue M, Fujiwara Y, Monden M. Localization of IQGAP1 is inversely correlated with intercellular adhesion mediated by e-cadherin in gastric cancers. *Int. J. Cancer.* **2001,** 91, 783-788.

91. Erlejman AG, De Leo SA, Mazaira GI, Molinari AM, Camisay MF, Fontana V, Cox MB, Piwien-Pilipuk G, Galigniana MD. NF-kappaB transcriptional activity is modulated by FK506-binding proteins FKBP51 and FKBP52: a role for peptidyl-prolyl isomerase activity. *J. Biol. Chem.* **2014,** %19;289, 26263-26276.

92. Shaw PE. Peptidyl-prolyl isomerases: a new twist to transcription. *EMBO Rep.* **2002,** 3, 521-526.

93. Hubler TR, Denny WB, Valentine DL, Cheung-Flynn J, Smith DF, Scammell JG. The FK506-binding immunophilin FKBP51 is transcriptionally regulated by progestin and attenuates progestin responsiveness. *Endocrinology.* **2003,** 144, 2380-2387.

94. Storer CL, Dickey CA, Galigniana MD, Rein T, Cox MB. FKBP51 and FKBP52 in signaling and disease. *Trends Endocrinol. Metab.* **2011,** 22, 481-490.

95. Barik S. Immunophilins: for the love of proteins. *Cell Mol. Life Sci.* **2006,** 63, 2889-2900.

96. Galigniana MD, Radanyi C, Renoir JM, Housley PR, Pratt WB. Evidence that the peptidylprolyl isomerase domain of the hsp90-binding immunophilin FKBP52 is involved in both dynein interaction and glucocorticoid receptor movement to the nucleus. *J. Biol. Chem.* **2001,** 276, 14884-14889.

97. Rein T. FK506 binding protein 51 integrates pathways of adaptation: FKBP51 shapes the reactivity to environmental change. *Bioessays.* **2016,** 38, 894-902.

98. Jinwal UK, Koren J, III, Borysov SI, Schmid AB, Abisambra JF, Blair LJ, Johnson AG, Jones JR, Shults CL, O'Leary JC, III, Jin Y, Buchner J, Cox MB, Dickey CA. The Hsp90 cochaperone, FKBP51, increases Tau stability and polymerizes microtubules. *J. Neurosci.* **2010,** 30, 591-599.

99. Chambraud B, Sardin E, Giustiniani J, Dounane O, Schumacher M, Goedert M, Baulieu EE. A role for FKBP52 in Tau protein function. *Proc. Natl. Acad. Sci. U. S. A.* **2010,** 107, 2658-2663.

100. Li L, Fridley B, Kalari K, Jenkins G, Batzler A, Safgren S, Hildebrandt M, Ames M, Schaid D, Wang L. Gemcitabine and cytosine arabinoside cytotoxicity: association with lymphoblastoid cell expression. *Cancer Res.* **2008,** 68, 7050-7058.

101. Mukaide H, Adachi Y, Taketani S, Iwasaki M, Koike-Kiriyama N, Shigematsu A, Shi M, Yanai S, Yoshioka K, Kamiyama Y, Ikehara S. FKBP51 expressed by both normal epithelial cells and adenocarcinoma of colon suppresses proliferation of colorectal adenocarcinoma. *Cancer Invest.* **2008,** 26, 385-390.

102. Rotoli D, Morales M, Del Carmen MM, Del Pino GM, Morales A, Avila J, Martin-Vasallo P. Expression and localization of the immunophilin FKBP51 in colorectal carcinomas and primary metastases, and alterations following oxaliplatin-based chemotherapy. *Oncol. Lett.* **2016,** 12, 1315-1322.

103. Toneatto J, Guber S, Charo NL, Susperreguy S, Schwartz J, Galigniana MD, Piwien-Pilipuk G. Dynamic mitochondrial-nuclear redistribution of the immunophilin FKBP51 is regulated by the PKA signaling pathway to control gene expression during adipocyte differentiation. *J. Cell Sci.* **2013,** 126, 5357-5368.

104. Pei H, Li L, Fridley BL, Jenkins GD, Kalari KR, Lingle W, Petersen G, Lou Z, Wang L. FKBP51 affects cancer cell response to chemotherapy by negatively regulating Akt. *Cancer Cell.* **2009,** 16, 259-266.

105. Romano S, D'Angelillo A, D'Arrigo P, Staibano S, Greco A, Brunetti A, Scalvenzi M, Bisogni R, Scala I, Romano MF. FKBP51 increases the tumour-promoter potential of TGF-beta. *Clin. Transl. Med.* **2014,** 3, 1-3.

106. Gallo LI, Lagadari M, Piwien-Pilipuk G, Galigniana MD. The 90-kDa heat-shock protein (Hsp90)-binding immunophilin FKBP51 is a mitochondrial protein that translocates to the nucleus to protect cells against oxidative stress. *J. Biol. Chem.* **2011,** 286, 30152-30160.

107. Li L, Lou Z, Wang L. The role of FKBP5 in cancer aetiology and chemoresistance. *Br. J. Cancer.* **2011,** 104, 19-23.

108. Romano S, Staibano S, Greco A, Brunetti A, Nappo G, Ilardi G, Martinelli R, Sorrentino A, Di PA, Mascolo M, Bisogni R, Scalvenzi M, Alfano B, Romano MF. FK506 binding protein 51 positively regulates melanoma stemness and metastatic potential. *Cell Death. Dis.* **2013,** 4:e578. doi: 10.1038/cddis.2013.109., e578.

109. Romano S, Mallardo M, Romano MF. FKBP51 and the NF-kappaB regulatory pathway in cancer. *Curr. Opin. Pharmacol.* **2011,** 11, 288-293.

110. Bratt A, Wilson WJ, Troyanovsky B, Aase K, Kessler R, Van Meir EG, Holmgren L. Angiomotin belongs to a novel protein family with conserved coiled-coil and PDZ binding domains. *Gene.* **2002,** 298, 69-77.

111. Mojallal M, Zheng Y, Hultin S, Audebert S, van HT, Johnsson P, Lenander C, Fritz N, Mieth C, Corcoran M, Lembo F, Hallstrom M, Hartman J, Mazure NM, Weide T, Grander D, Borg JP, Uhlen P, Holmgren L. AmotL2 disrupts apical-basal cell polarity and promotes tumour invasion. *Nat. Commun.* **2014,** 5:4557. doi: 10.1038/ncomms5557., 4557.

112. Sakai H, Suzuki T, Maeda M, Takahashi Y, Horikawa N, Minamimura T, Tsukada K, Takeguchi N. Up-regulation of Na(+),K(+)-ATPase alpha 3-isoform and down-regulation of the alpha1-isoform in human colorectal cancer. *FEBS Lett.* **2004,** 563, 151-154.

113. Rajasekaran SA, Ball WJ, Jr., Bander NH, Liu H, Pardee JD, Rajasekaran AK. Reduced expression of beta-subunit of Na,K-ATPase in human clear-cell renal cell carcinoma. *J. Urol.* **1999,** 162, 574-580.

114. Rajasekaran SA, Palmer LG, Moon SY, Peralta SA, Apodaca GL, Harper JF, Zheng Y, Rajasekaran AK. Na,K-ATPase activity is required for formation of tight junctions, desmosomes, and induction of polarity in epithelial cells. *Mol. Biol. Cell.* **2001,** 12, 3717-3732.

115. Rajasekaran SA, Palmer LG, Quan K, Harper JF, Ball WJ, Jr., Bander NH, Peralta SA, Rajasekaran AK. Na,K-ATPase beta-subunit is required for epithelial polarization, suppression of invasion, and cell motility. *Mol. Biol. Cell.* **2001,** 12, 279-295.

116. Rajasekaran SA, Huynh TP, Wolle DG, Espineda CE, Inge LJ, Skay A, Lassman C, Nicholas SB, Harper JF, Reeves AE, Ahmed MM, Leatherman JM, Mullin JM, Rajasekaran AK. Na,K-ATPase subunits as markers for epithelial-mesenchymal transition in cancer and fibrosis. *Mol. Cancer Ther.* **2010,** 9, 1515-1524.

117. SKOU JC. The influence of some cations on an adenosine triphosphatase from peripheral nerves. *Biochim. Biophys. Acta* **1957,** 23, 394-401.

118. Jorgensen PL, Hakansson KO, Karlish SJ. Structure and mechanism of Na,K-ATPase: functional sites and their interactions. *Annu. Rev. Physiol* **2003,** 65, 817-849. 10.1146/annurev.physiol.65.092101.142558 [doi];092101.142558 [pii].

119. Mobasheri A, Avila J, Cozar-Castellano I, Brownleader MD, Trevan M, Francis MJ, Lamb JF, Martin-Vasallo P. Na+, K+-ATPase isozyme diversity; comparative biochemistry and physiological implications of novel functional interactions. *Biosci. Rep.* **2000,** 20, 51-91.

120. Aizman O, Uhlen P, Lal M, Brismar H, Aperia A. Ouabain, a steroid hormone that signals with slow calcium oscillations. *Proc. Natl. Acad. Sci. U. S. A* **2001,** 98, 13420-13424. 10.1073/pnas.221315298 [doi];221315298 [pii].

121. Miyakawa-Naito A, Uhlen P, Lal M, Aizman O, Mikoshiba K, Brismar H, Zelenin S, Aperia A. Cell signaling microdomain with Na,K-ATPase and inositol 1,4,5-trisphosphate receptor generates calcium oscillations. *J. Biol. Chem.* **2003,** 278, 50355-50361. 10.1074/jbc.M305378200 [doi];M305378200 [pii].

122. Harwood S, Yaqoob MM. Ouabain-induced cell signaling. *Front Biosci.* **2005,** 10, 2011-2017. 1676 [pii].

123. Zhang S, Malmersjo S, Li J, Ando H, Aizman O, Uhlen P, Mikoshiba K, Aperia A. Distinct role of the N-terminal tail of the Na,K-ATPase catalytic subunit as a signal transducer. *J. Biol. Chem.* **2006,** 281, 21954-21962. M601578200 [pii];10.1074/jbc.M601578200 [doi].

124. Yuan Z, Cai T, Tian J, Ivanov AV, Giovannucci DR, Xie Z. Na/K-ATPase tethers phospholipase C and IP3 receptor into a calcium-regulatory complex. *Mol. Biol. Cell* **2005,** 16, 4034-4045. E05-04-0295 [pii];10.1091/mbc.E05-04-0295 [doi].

125. Abramowitz J, Dai C, Hirschi KK, Dmitrieva RI, Doris PA, Liu L, Allen JC. Ouabain- and marinobufagenin-induced proliferation of human umbilical vein smooth muscle cells and a rat vascular smooth muscle cell line, A7r5. *Circulation* **2003,** 108, 3048-3053. 10.1161/01.CIR.0000101919.00548.86 [doi];01.CIR.0000101919.00548.86 [pii].

126. Barwe SP, Anilkumar G, Moon SY, Zheng Y, Whitelegge JP, Rajasekaran SA, Rajasekaran AK. Novel role for Na,K-ATPase in phosphatidylinositol 3-kinase signaling and suppression of cell motility. *Mol. Biol. Cell* **2005,** 16, 1082-1094. E04-05-0427 [pii];10.1091/mbc.E04-05-0427 [doi].

127. Wang XQ, Yu SP. Novel regulation of Na, K-ATPase by Src tyrosine kinases in cortical neurons. *J. Neurochem.* **2005,** 93, 1515-1523. JNC3147 [pii];10.1111/j.1471-4159.2005.03147.x [doi].

128. Mercer RW, Biemesderfer D, Bliss DP, Jr., Collins JH, Forbush B, III. Molecular cloning and immunological characterization of the gamma polypeptide, a small protein associated with the Na,K-ATPase. *J. Cell Biol.* **1993,** 121, 579-586.

129. Blanco G. Na,K-ATPase subunit heterogeneity as a mechanism for tissue-specific ion regulation. *Semin. Nephrol.* **2005,** 25, 292-303. S0270-9295(05)00047-1 [pii];10.1016/j.semnephrol.2005.03.004 [doi].

130. Hundal HS, Marette A, Mitsumoto Y, Ramlal T, Blostein R, Klip A. Insulin induces translocation of the alpha 2 and beta 1 subunits of the Na+/K(+)-ATPase from intracellular compartments to the plasma membrane in mammalian skeletal muscle. *J. Biol. Chem.* **1992,** 267, 5040-5043.

131. McGrail KM, Phillips JM, Sweadner KJ. Immunofluorescent localization of three Na,K-ATPase isozymes in the rat central nervous system: both neurons and glia can express more than one Na,K-ATPase. *J. Neurosci.* **1991,** 11, 381-391.

132. Zahler R, Brines M, Kashgarian M, Benz EJ, Jr., Gilmore-Hebert M. The cardiac conduction system in the rat expresses the alpha 2 and alpha 3 isoforms of the Na+,K(+)-ATPase. *Proc. Natl. Acad. Sci. U. S. A* **1992,** 89, 99-103.

133. Lytton J, Lin JC, Guidotti G. Identification of two molecular forms of (Na+,K+)-ATPase in rat adipocytes. Relation to insulin stimulation of the enzyme. *J. Biol. Chem.* **1985,** 260, 1177-1184.

134. Hieber V, Siegel GJ, Fink DJ, Beaty MW, Mata M. Differential distribution of (Na, K)-ATPase alpha isoforms in the central nervous system. *Cell Mol. Neurobiol.* **1991,** 11, 253-262.

135. Woo AL, James PF, Lingrel JB. Sperm motility is dependent on a unique isoform of the Na,K-ATPase. *J. Biol. Chem.* **2000,** 275, 20693-20699. 10.1074/jbc.M002323200 [doi];M002323200 [pii].

136. Lavoie L, Levenson R, Martin-Vasallo P, Klip A. The molar ratios of alpha and beta subunits of the Na+-K+-ATPase differ in distinct subcellular membranes from rat skeletal muscle. *Biochemistry* **1997,** 36, 7726-7732. 10.1021/bi970109s [doi];bi970109s [pii].

137. Shyjan AW, Cena V, Klein DC, Levenson R. Differential expression and enzymatic properties of the Na+,K(+)-ATPase alpha 3 isoenzyme in rat pineal glands. *Proc. Natl. Acad. Sci. U. S. A* **1990,** 87, 1178-1182.

138. Peng L, Martin-Vasallo P, Sweadner KJ. Isoforms of Na,K-ATPase alpha and beta subunits in the rat cerebellum and in granule cell cultures. *J. Neurosci.* **1997,** 17, 3488-3502.

139. Martin-Vasallo P, Wetzel RK, Garcia-Segura LM, Molina-Holgado E, Arystarkhova E, Sweadner KJ. Oligodendrocytes in brain and optic nerve express the beta3 subunit isoform of Na,K-ATPase. *Glia* **2000,** 31, 206-218. 10.1002/1098-1136(200009)31:3<206::AID-GLIA20>3.0.CO;2-1 [pii].

140. Arystarkhova E, Sweadner KJ. Tissue-specific expression of the Na,K-ATPase beta3 subunit. The presence of beta3 in lung and liver addresses the problem of the missing subunit. *J. Biol. Chem.* **1997,** 272, 22405-22408.

141. Zahler R, Gilmore-Hebert M, Sun W, Benz EJ. Na, K-ATPase isoform gene expression in normal and hypertrophied dog heart. *Basic Res. Cardiol.* **1996,** 91, 256-266.

142. Malik N, Canfield VA, Beckers MC, Gros P, Levenson R. Identification of the mammalian Na,K-ATPase 3 subunit. *J. Biol. Chem.* **1996,** 271, 22754-22758.

143. Book CB, Wilson RP, Ng YC. Cardiac hypertrophy in the ferret increases expression of the Na(+)-K(+)-ATPase alpha 1- but not alpha 3-isoform. *Am. J. Physiol* **1994,** 266, H1221-H1227.

144. Charlemagne D, Swynghedauw B. Myocardial phenotypic changes in Na+, K+ ATPase in left ventricular hypertrophy: pharmacological consequences. *Eur. Heart J.* **1995,** 16 Suppl C, 20-23.

145. Charlemagne D, Orlowski J, Oliviero P, Rannou F, Sainte BC, Swynghedauw B, Lane LK. Alteration of Na,K-ATPase subunit mRNA and protein levels in hypertrophied rat heart. *J. Biol. Chem.* **1994,** 269, 1541-1547.

146. Ewart HS, Klip A. Hormonal regulation of the Na(+)-K(+)-ATPase: mechanisms underlying rapid and sustained changes in pump activity. *Am. J. Physiol* **1995,** 269, C295-C311.

147. Varghese F, Bukhari AB, Malhotra R, De A. IHC Profiler: an open source plugin for the quantitative evaluation and automated scoring of immunohistochemistry images of human tissue samples. *PLoS. One.* **2014,** 9, e96801.

148. Fukata M, Kuroda S, Nakagawa M, Kawajiri A, Itoh N, Shoji I, Matsuura Y, Yonehara S, Fujisawa H, Kikuchi A, Kaibuchi K. Cdc42 and Rac1 regulate the interaction of IQGAP1 with beta-catenin. *J. Biol. Chem.* **1999,** 274, 26044-26050.

149. Fukata M, Watanabe T, Noritake J, Nakagawa M, Yamaga M, Kuroda S, Matsuura Y, Iwamatsu A, Perez F, Kaibuchi K. Rac1 and Cdc42 capture microtubules through IQGAP1 and CLIP-170. *Cell.* **2002,** 109, 873-885.

150. Watanabe T, Wang S, Noritake J, Sato K, Fukata M, Takefuji M, Nakagawa M, Izumi N, Akiyama T, Kaibuchi K. Interaction with IQGAP1 links APC to Rac1, Cdc42, and actin filaments during cell polarization and migration. *Dev. Cell.* **2004,** 7, 871-883.

151. Johnson MA, Henderson BR. The scaffolding protein IQGAP1 co-localizes with actin at the cytoplasmic face of the nuclear envelope: implications for cytoskeletal regulation. *Bioarchitecture.* **2012,** 2, 138-142.

152. Cretoiu D, Xu J, Xiao J, Cretoiu SM. Telocytes and Their Extracellular Vesiclesâ€"Evidence and Hypotheses. *Int. J. Mol. Sci.* **2016,** 17. 10.3390/ijms17081322 [doi];ijms-17-01322 [pii].

153. Osman MA. An Emerging Role for IQGAP1 in Regulating Protein Traffic. *ScientificWorldJournal.* 10, 944-953. 10.1100/tsw.2010.85 [doi].

154. Vandamme M, Pauwels W, Bleecker J. A case of delayed oxaliplatin-induced pseudo-obstruction: an atypical presentation of oxaliplatin neurotoxicity. *Acta Clin. Belg.* **2014,** %19:2295333714Y0000000110., 2295333714Y0000000110.

155. Nalbantoglu IL, Tan BR, Jr., Linehan DC, Gao F, Brunt EM. Histological features and severity of oxaliplatin-induced liver injury and clinical associations. *J. Dig. Dis.* **2014,** 15, 553-560.

156. Bendris N, Schmid SL. Endocytosis, Metastasis and Beyond: Multiple Facets of SNX9. *Trends Cell Biol.* **2016,** 10.

157. Garbett D, Bretscher A. The surprising dynamics of scaffolding proteins. *Mol. Biol. Cell.* **2014,** 25, 2315-2319.

158. Herrero-Garcia E, O'Bryan JP. Intersectin scaffold proteins and their role in cell signaling and endocytosis. *Biochim. Biophys. Acta.* **2017,** 1864, 23-30.

159. Malarkannan S, Awasthi A, Rajasekaran K, Kumar P, Schuldt KM, Bartoszek A, Manoharan N, Goldner NK, Umhoefer CM, Thakar MS. IQGAP1: a regulator of intracellular spacetime relativity. *J. Immunol.* **2012,** 188, 2057-2063.

160. White CD, Erdemir HH, Sacks DB. IQGAP1 and its binding proteins control diverse biological functions. *Cell Signal.* **2012,** 24, 826-834.

161. Szklarczyk D, Franceschini A, Wyder S, Forslund K, Heller D, Huerta-Cepas J, Simonovic M, Roth A, Santos A, Tsafou KP, Kuhn M, Bork P, Jensen LJ, von MC. STRING v10: protein-protein interaction networks, integrated over the tree of life. *Nucleic Acids Res.* **2015,** 43, D447-D452.

162. Blanco G, Sanchez G, Mercer RW. Comparison of the enzymatic properties of the Na,K-ATPase alpha 3 beta 1 and alpha 3 beta 2 isozymes. *Biochemistry.* **1995,** 34, 9897-9903.

163. Blanco G, Koster JC, Sanchez G, Mercer RW. Kinetic properties of the alpha 2 beta 1 and alpha 2 beta 2 isozymes of the Na,K-ATPase. *Biochemistry.* **1995,** 34, 319-325.

164. Jaisser F, Canessa CM, Horisberger JD, Rossier BC. Primary sequence and functional expression of a novel ouabain-resistant Na,K-ATPase. The beta subunit modulates potassium activation of the Na,K-pump. *J. Biol. Chem.* **1992,** 267, 16895-16903.

165. Crambert G, Hasler U, Beggah AT, Yu C, Modyanov NN, Horisberger JD, Lelievre L, Geering K. Transport and pharmacological properties of nine different human Na, K-ATPase isozymes. *J. Biol. Chem.* **2000,** 275, 1976-1986.

APPENDIX A
ARTICLE 1

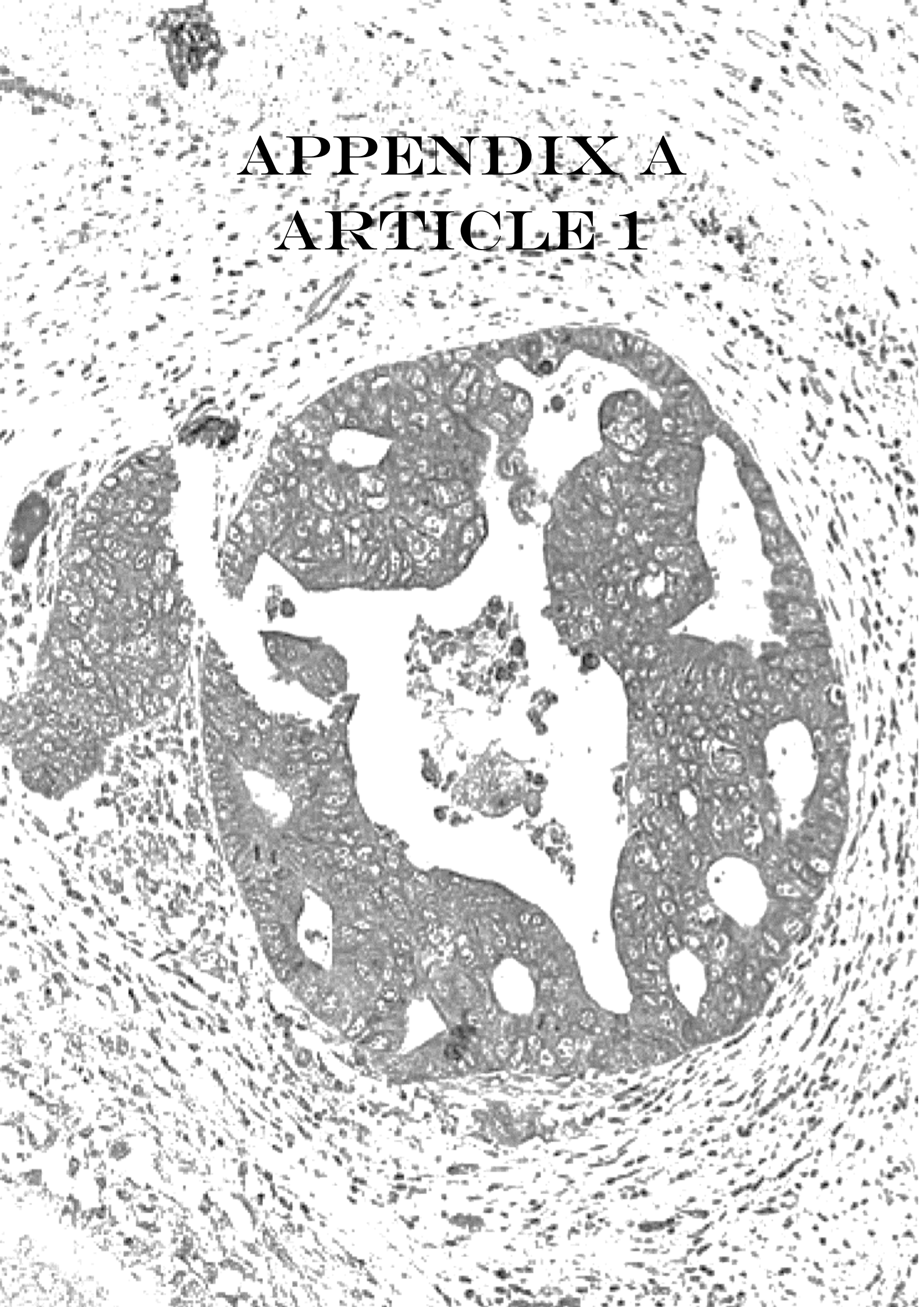

Alterations in IQGAP1 expression and localization in colorectal carcinoma and liver metastases following oxaliplatin-based chemotherapy

DEBORAH ROTOLI[1,2*], MANUEL MORALES[3,4*], MARÍA DEL CARMEN MAESO[5], MARÍA DEL PINO GARCÍA[6], RICARDO GUTIERREZ[7], FRANCISCO VALLADARES[7], JULIO ÁVILA[1], LUCIO DÍAZ-FLORES[7], ALI MOBASHERI[8,9] and PABLO MARTÍN-VASALLO[1]

[1]Laboratory of Developmental Biology, UD-Biochemistry and Molecular Biology and Centre for Biomedical Research of The Canary Islands, University of La Laguna, 38206 La Laguna, Canary Islands, Spain; [2]National Research Council, Institute of Endocrinology and Experimental Oncology, I-80131 Naples, Italy; [3]Service of Medical Oncology, University Hospital Nuestra Señora de Candelaria, 38010 Santa Cruz de Tenerife; [4]Medical Oncology, Hospiten Rambla, 38001 Santa Cruz de Tenerife; [5]Service of Pathology, University Hospital Nuestra Señora de Candelaria, 38010 Santa Cruz de Tenerife; [6]Department of Pathology, Hospiten Rambla, 38001 Santa Cruz de Tenerife; [7]Department of Pathology, School of Medicine, University of La Laguna, 38201 La Laguna, Canary Islands, Spain; [8]Department of Veterinary Preclinical Sciences, School of Veterinary Medicine, Faculty of Health and Medical Sciences, University of Surrey, Guildford GU2 7XH, UK; [9]Center of Excellence in Genomic Medicine Research, King Fahd Medical Research Center, Faculty of Applied Medical Sciences, King Abdulaziz University, Jeddah 21589, Saudi Arabia

Received July 21, 2016; Accepted October 11, 2016

DOI: 10.3892/ol.2017.6525

Abstract. IQGAP1 is a scaffolding protein that serves a key role in cell dynamics by integrating internal and external stimuli to distinct signal outputs. Previous studies have identified several genes that are significantly up- or downregulated in the peripheral white cells (PWCs) of patients with colorectal adenocarcinoma (CRC), who underwent oxaliplatin-based chemotherapy (CT). In addition, screening studies have reported that IQ-motif containing GTPase activating protein 1 (IQGAP1) transcriptional expression levels varied from 'off' to 'on' following oxaliplatin CT. In order to determine if variations previously described in PWCs are able to be observed at the protein level in tumors and in metastases following CT, the present study performed an immunohistochemical analysis of IQGAP1 in CRC and primary metastases. IQGAP1 expression was observed in the nuclear envelope and in lateral cell membranes and cytoplasm in normal colon tissue. However, in tumor tissue, cells exhibited a diffuse pattern, with variable expression levels of staining in the nuclear membrane and cytoplasm, with the highest expression intensity observed at the invasive front. In healthy and metastasized liver tissue and in the metastases themselves, expression levels varied from cell to cell from no expression to a high level. In the majority of cells, IQGAP1 co-localized with microtubules at the cytoplasmic face of the nuclear envelope. Strong positive expression was observed in areas of the lesion where cells were detaching from the lesion into the lumen. Despite the homogeneous IQGAP1 staining pattern observed in healthy colon tissue sections, CRC demonstrated heterogeneity in staining, which was more marked in metastasized liver tissue resected following CT. However, the most notable findings were the observed effects on the cellular and subcellular distribution and its implications for cancer biology. These results suggest that IQGAP1 may be a putative biomarker, a candidate for clinical diagnostics and a potential novel target for anti-cancer therapeutics.

Correspondence to: Professor Pablo Martín-Vasallo, Laboratory of Developmental Biology, UD-Biochemistry and Molecular Biology and Centre for Biomedical Research of The Canary Islands, University of La Laguna, Avenue Astrofísico Sánchez s/n, 38206 La Laguna, Canary Islands, Spain
E-mail: pmartin@ull.es

[*]Contributed equally

Abbreviations: AJ, adherens junction; APC, adenomatous polyposis coli; CRC, colorectal adenocarcinoma; CT, chemotherapy; EMT, epithelial mesenchymal transition; FOLFOX, folinic acid, leucovorin, 5-fluorouracil and oxaliplatin; IQGAP1, IQ-motif containing GTPase activating protein 1; MAPK, mitogen-activated protein kinase; PCNA, proliferating cell nuclear antigen; PWCs, peripheral white cells

Key words: colorectal cancer, oxaliplatin, IQGAP1, scaffold protein

Introduction

Folinic acid, leucovorin, 5-fluorouracil and oxaliplatin (FOLFOX)-based chemotherapy (CT) is widely used in the

treatment of colorectal adenocarcinoma (CRC). The addition of the platinum-containing compound oxaliplatin to the standard adjuvant treatment with 5-fluorouracil plus leucovorin enhances the efficacy of CT, doubling the response rate and prolonging progression-free survival of patients with stage II-III CRC (1,2). Despite positive results obtained from this chemotherapeutic regimen, unwanted side effects are significant and require monitoring, as they affect, to various degrees, the quality of patient.

In an attempt to identify biomarkers that may predict the onset of these secondary effects, a recent study investigated the differential gene expression of peripheral leukocytes in patients with CRC prior to and following 3 cycles of oxaliplatin-based CT (3). The study identified 502 differentially-expressed genes that were significantly up- or downregulated in the peripheral white cells (PWCs) of patients following CT treatment (3).

To determine whether the changes in gene expression observed in PWCs may be detected in tumors following the administration of adjuvant CT, the present study performed immunohistochemical analysis of a selected number of genes that had previously been identified in the differential transcriptome profile (4). The study observed that one gene among four, whose transcriptional expression levels varied from 'off' to 'on', was that coding for IQ-motif containing GTPase activating protein 1 (IQGAP1) (3).

IQGAP1 is a ubiquitously expressed scaffold protein, which contains a number of protein interaction domains (5). The protein interacts with cell adhesion molecules, components of the cytoskeleton, and various signaling molecules to regulate cell motility and morphology, cell cycle and other cellular functions (5,6). By regulating its binding partners, IQGAP1 integrates a number of signaling pathways, several of which contribute to tumorigenesis. For example, IQGAP1 is associated with actin dynamics by direct binding to actin or indirect regulation via cell division cycle 42/Rac1 (7). Through its polyproline protein-protein domain (WW domain), the protein modulates the mitogen-activated protein kinase (MAPK) pathway, which is associated with cell cycle control (8). Therefore, IQGAP1 links MAPK signaling (for example, decisions regarding cell fate) to the cytoskeleton or cellular adhesion, with important implications for cancer.

Furthermore, interactions of IQGAP1 with extracellular signal-regulated kinases 1/2 and MEK1/2 may lead to activation of the MAPK signaling pathway, thus modulating cell differentiation and proliferation (8). Therefore, IQGAP1 serves pivotal roles in several cellular functions, including control of polarization, cell adhesion, migration, proliferation and angiogenesis.

Numerous immunohistochemical studies have demonstrated that IQGAP1 is overexpressed in several forms of cancer and an aberrant membrane accumulation is observed, particularly at the invasive front (9,10). Higher expression and altered localization of IQGAP1 from the cytoplasm to the membrane correlates with tumor grade and poor prognosis (11). The presence of IQGAP1 in the cell membrane may decrease adherens junction (AJ) function, favoring dissociation of the tumor cells (12).

The present study reports the alteration of IQGAP1 expression in CRC and liver metastases following CT administration at the protein level by performing an immunohistochemical analysis.

Patients and methods

Patients. The study was approved by the Ethics Committee of La Laguna University (La Laguna, Canary Islands, Spain) and the Ethical Committee of Nuestra Señora de Candelaria University Hospital (HUNSC; Santa Cruz de Tenerife, Canary Islands, Spain). All patients were treated at University Hospital of the Nuestra Señora de Candelaria, Santa Cruz de Tenerife, Spain between May 2007 and September 2015 and provided informed consent for the diagnosis and research of tissue specimens prior to enrollment in the study. All patients had colonic cancer and liver metastasis, which had been treated with FOLFOX-CT, (day 1, oxaliplatin 100 mg/m^2 iv over 2 h; leucovorin calcium 400 mg/m^2 iv over 2 h; followed by 5-fluorouracil 400 mg/m^2 iv bolus and by 5-fluorouracil 2400 mg/m^2 iv over 46 h; every 14 days). All patients received CT following resection of the primary tumor. Therefore, the primary tumors were CT-naïve, while the liver metastases were CT-treated.

Tumor tissue. Paraffin-embedded tissue samples from 15 patients (7 males and 8 females), ensuring patient's anonymity, and the corresponding clinical data were obtained from the reference medical areas of HUNSC.

Antibodies. The following antibodies were used: Rabbit anti-human polyclonal antibody against IQGAP1 (dilutions, 1:500 for immunohistochemistry and 1:250 for immunofluorescence; cat. no. ABT186; EMD Millipore, Billerica, MA, USA); mouse monoclonal antibody clone PC10 against anti-proliferating cell nuclear antigen (PCNA; dilution, 1:100; cat. no. 1486772; Roche Diagnostics GmbH, Mannheim, Germany); mouse monoclonal anti-human cluster of differentiation (CD)34 class II clone QBEnd 10 (ready-to-use; cat. no. IR632; Dako; Agilent Technologies GmbH, Waldbronn, Germany); and mouse monoclonal anti-β tubulin (dilution, 1:150; cat. no. sc-101527; Santa Cruz Biotechnology, Inc., Dallas, TX, USA). Secondary antibodies: Biotin-conjugated anti-rabbit secondary antibody (dilution, 1:300; cat. no. 31820; Pierce; Thermo Fisher Scientific, Inc., Waltham, MA, USA); fluorescein isothiocyanate (FITC)-conjugated goat polyclonal antibody against rabbit IgG (cat. no. F9887; Sigma-Aldrich, Merck Merck Millipore, Darmstadt, Germany; dilution, 1:200); goat polyclonal antibody against mouse IgG (DyLight® 650; cat. no. ab97018; Abcam, Cambridge, UK; dilution, 1:100).

Immunohistochemistry. Immunoperoxidase staining of paraffin-embedded tissue sections (fixed in 10% formalin, for 48-72 h at 4˚C) was performed using the avidin-biotin reaction. Briefly, 5-μm-thick tissue sections were deparaffinized in xylene and hydrated in a graded series of alcohol baths. Heat-induced epitope retrieval was achieved by heating samples in sodium citrate buffer (pH 6.0) at 120˚C for 10 min in an autoclave. Once non-specific sites were blocked with 5% non-fat dry milk in TBS for 1 h at room temperature, endogenous biotin was blocked using the Avidin/Biotin Blocking kit (Vector Laboratories Inc., Burlingame, CA, USA). The primary antibody against IQGAP1 was applied (dilution, 1:500) to

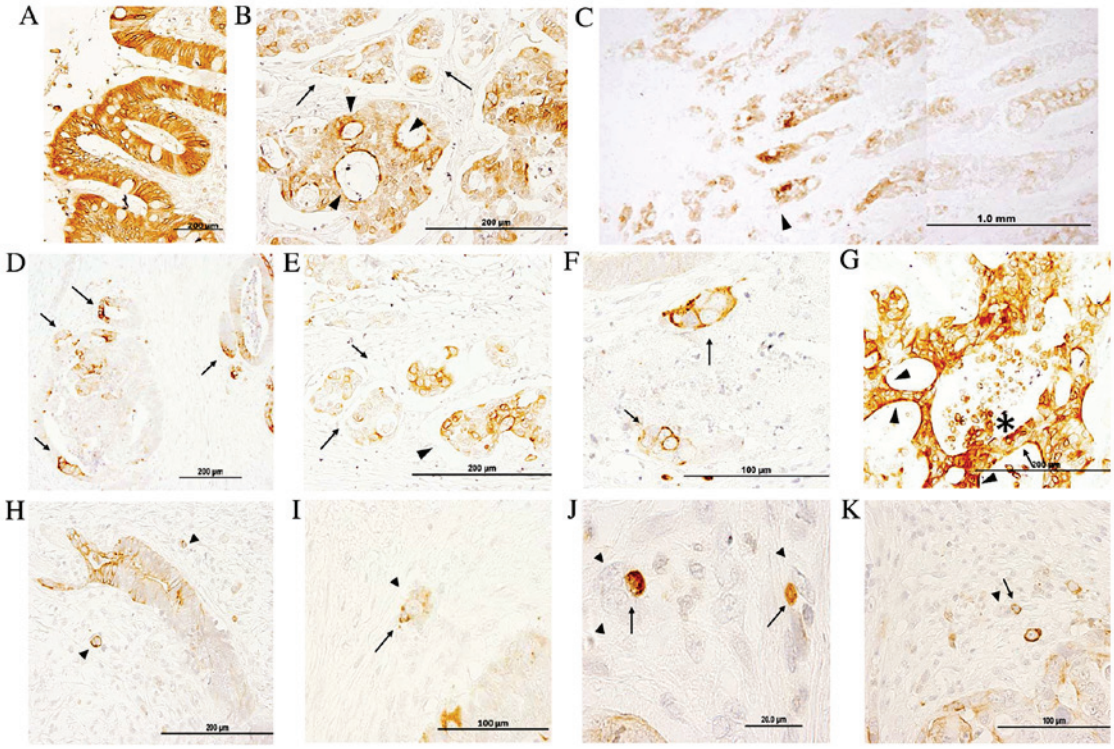

Figure 1. Immunohistochemical analysis of IQGAP1 protein expression in normal colon and colon adenocarcinoma tissue sections. (A) In normal colon tissue, positive staining was observed in the nuclear membrane, and in the lateral cell membrane and cytoplasm. (B) Tumor exhibiting heterogeneous IQGAP1 localization in the cytoplasm, nuclear membrane and plasma membrane. Arrowheads point to intense apical cell membrane staining, while arrows indicate budding tumor cells. (C) Low magnification of a CRC tumor section demonstrating a higher grade of IQGAP1 expression at the invasive front (arrowhead). (D) Tumor glands exhibiting a polarized positive signal. Cells located at the invasive front exhibited a strong membranous staining (arrows). (E) Tumor budding at the invasive front. Arrows identify open lumen lymphatic ducts with disseminated cancer cell nests. Nests demonstrated variable staining in the cytoplasm and nuclear envelope. Arrowhead points to the invasive lesion. (F) Cancer cell clusters with intense membranous staining (arrows) and lighter staining in cytosol. (G) Intense immunopositivity in a tumor gland exhibiting diffused localization (cytoplasm and nuclear membrane). Note the strong apical localization (arrowheads). Arrow points to unstained cells intermixed with IQGAP1$^+$ cells. (H-K) Arrowheads identify budding tumor cells. Arrows point to IQGAP1$^+$ immune cells associated with budding cells. Micrographs in the assembled figure were selected from different CRC cases. IQGAP1, IQ-motif containing GTPase activating protein 1; CRC, colorectal adenocarcinoma.

slides over night at 4˚C. To block endogenous peroxidase activity, the slides were incubated with 3% hydrogen peroxidase in methanol for 15 min. Biotin-conjugated anti-rabbit secondary antibody (dilution, 1:300; Pierce; Thermo Fisher Scientific, Inc., Waltham, MA, USA) was incubated for 2 h at 37˚C, and ABC Peroxidase Staining kit (Thermo Fisher Scientific, Inc.) was used to amplify the specific antibody staining. 3,3'-diaminobenzidine substrate concentrate (no. IHC-101F; Bethyl Laboratories Inc., Montgomery, TX, USA) was used to visualize immunohistochemical reactions. Samples incubated without primary antibodies were used as a negative control. Slides were counterstained with Harris hematoxylin solution DC (Panreac Química SLU, Barcelona, Spain) to visualize cell nuclei and mounted with Eukitt mounting medium (Panreac Química SLU). An optical light microscope (BX50; Olympus Corporation, Tokyo, Japan) was used to visualize the results of the immunostaining.

Image analysis and statistical analysis. To compile tables, two independent observers evaluated the specimens blindly. Staining intensities were graded as absent (-), weak (+), moderate (++) or strong (+++). These cut-offs were established by consensus between each investigator following an initial survey of the entire blind-coded material. In cases where scorings differed by more than one unit, the observers re-evaluated the specimens to reach a consensus. In other cases, means of the scorings were calculated.

Double immunofluorescence simultaneous staining. Following deparaffinization, hydration and a heat-induced epitope retrieval procedure (as described above), tissue sections were incubated simultaneously with a mixture of two distinct primary antibodies (rabbit anti-human polyclonal antibody against IQGAP1 and mouse monoclonal antibody anti-PCNA, anti-CD34 or anti-β-tubulin) overnight at 4˚C. Slides were then incubated for 1 h at room temperature in the dark with a mixture of two secondary antibodies raised in different species and conjugated to two different fluorochromes [anti-rabbit fluorescein isothiocyanate-conjugated antibody (Sigma-Aldrich; Merck Millipore) and anti-mouse DyLight®650-conjugated antibody (Abcam)]. Slides were mounted with ProLong® Diamond Anti-fade Mountant with DAPI (Molecular Probes®; Thermo Fisher Scientific, Inc.) to visualize cell nuclei. Slides were analyzed using a confocal microscope (FV1000; Olympus Corporation).

Results

IQGAP1 expression and localization in healthy colon and CRC tissue sections. Fig. 1 demonstrates IQGAP1 immunoreactivity

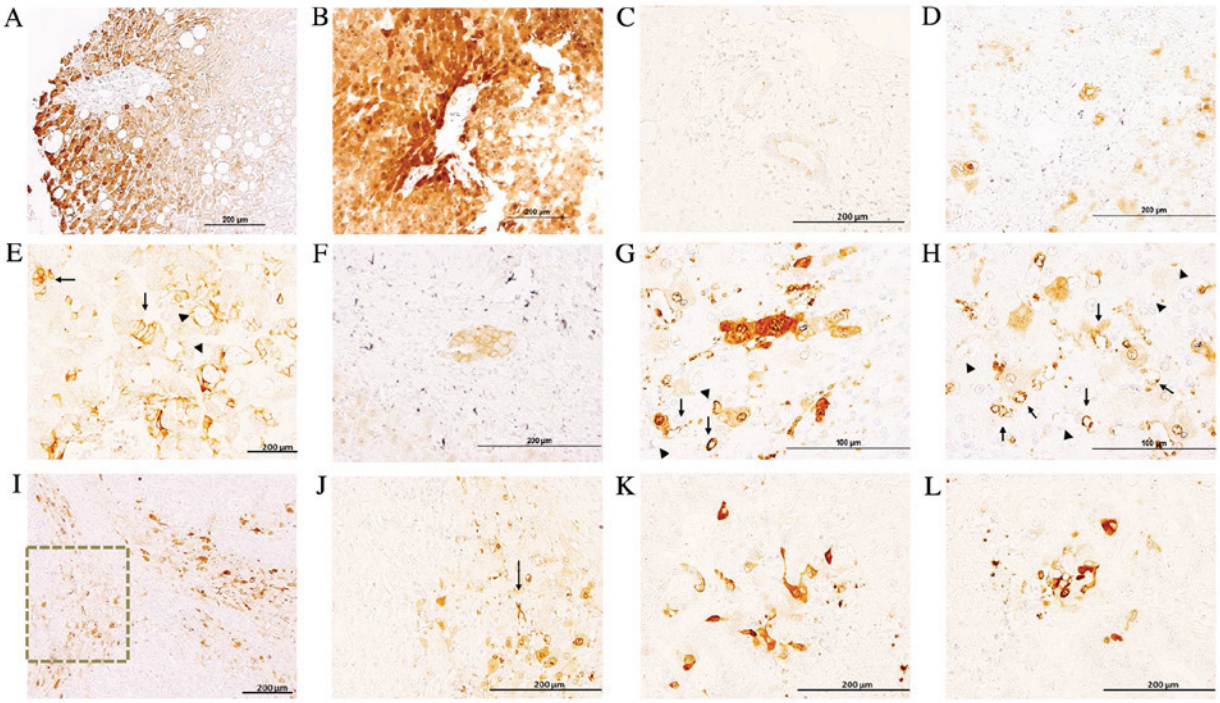

Figure 2. Immunohistochemical analysis of the expression of IQGAP1 in liver tissues. (A and B) Immunohistochemical staining demonstrated variable expression of IQGAP1 in hepatocytes in (A) healthy tissues and (B) a healthy area of metastasized liver tissue. Note that neighboring hepatocytes exhibited significantly different levels of expression. (C) Normal liver bile ducts with weak apical staining. (D) Metastasized liver portal trial with an intense positive membranous staining in bile ducts. (E) Metastases exhibited variable positive staining. Arrows point to malignant cells with strong membranous staining, while arrowheads point to areas of apical cell region staining. (F) Tumor glands demonstrated IQGAP1$^+$ membranous staining. (G and H) Several microvessels exhibited a strong positive signal (arrows), while other vessels appeared negative (arrowheads). (I) Several stromal cells and microvessels located between lesions exhibited intense positive staining. (J) Higher magnification of the inset in (I); arrow points to an IQGAP1$^+$ tumor-associated microvessel. (K and L) IQGAP1$^-$ tumor cells with tumor-associated fibroblast-like cells exhibited strong IQGAP1 staining. IQGAP1, IQ-motif containing GTPase activating protein 1.

in paraffin-embedded sections of normal colon and in healthy areas of adenocarcinoma sections. The signal revealed positive staining in enterocytes (nuclear membrane, cytoplasm, apical and lateral cell membrane) (Fig. 1A); the majority of cells were stained and only a few exhibited a lighter level of staining. IQGAP1 protein was localized in cytoplasm, nuclear envelope, cell junctions, plasma membrane and apical membrane, and this variable localization could be observed in the same structure concurrently (Fig. 1B and D-F). Within the tumor, tumor cells exhibited a diffuse pattern with a variable level of staining (from no staining to high intensity) in the nuclear envelope and in the cytoplasm. The intensity of staining was higher at the invasive front (Fig. 1C). Cancer cell nests exhibited variable positive perinuclear and cytoplasmic staining in the open-lumen lymphatic ducts located in the submucosa (Fig. 1B and E, black arrows). In Fig. 1D, the intense membranous IQGAP1 staining appeared polarized in several tumor glands, while the other cells of the lesion were negative or exhibited only weak reactivity. Thus, the expression pattern and localization of IQGAP1 protein in the CRC tissue sections was heterogeneous, both in the normal glandular epithelium and in tumor glands and nests. Strongly IQGAP1-positive cells were intermixed with unstained tumor cells within tumor lesions (Fig. 1G, black arrow); in several carcinoma cell clusters located in close proximity to tumor glands, a strong and diffuse membranous immunolocalization was observed, while nuclei were negative (Fig. 1F, black arrows). In several lesions, strong apical cell membrane staining was observed (arrowhead in Fig. 1G); in addition, strong IQGAP1 expression was observed in areas of the lesion where cells were detaching into the lumen (asterisk in Fig. 1G).

Fig. 1H-K shows representative images of budding tumor cells (arrowheads) either as small clusters of cells (<5 cells) or as single cells. IQGAP1 expression was variable, with certain cells exhibiting a strong positive signal all along the cell membrane, while others were completely negative. The presence of IQGAP1$^+$ immune cells (arrows) was associated with budding cells.

IQGAP1 expression and localization in healthy and metastasized liver tissue sections. In healthy liver and the healthy region of metastasized liver tissues, hepatocytes exhibited a clearly delimitated labeling in the plasma membrane, cytoplasm and nuclear envelope, exhibiting non-homogenous IQGAP1$^+$ immunostaining, with neighboring hepatocytes demonstrating variable levels of expression (Fig. 2). Along the tissue sections, there were areas with no signal and areas exhibiting variable positive staining. The intensity of the signal was higher in the metastasized tissue sections compared with normal liver sections (Fig. 2A and B). Bile ducts exhibited weak apical staining in normal liver sections (Fig. 2C), while in metastasized liver sections they demonstrated intense membranous positive staining (Fig. 2D).

Metastases exhibited variable levels of IQGAP1 expression, and were heterogeneous in terms of intensity and localization (Fig. 2E-G). Positive immunostaining was observed in several

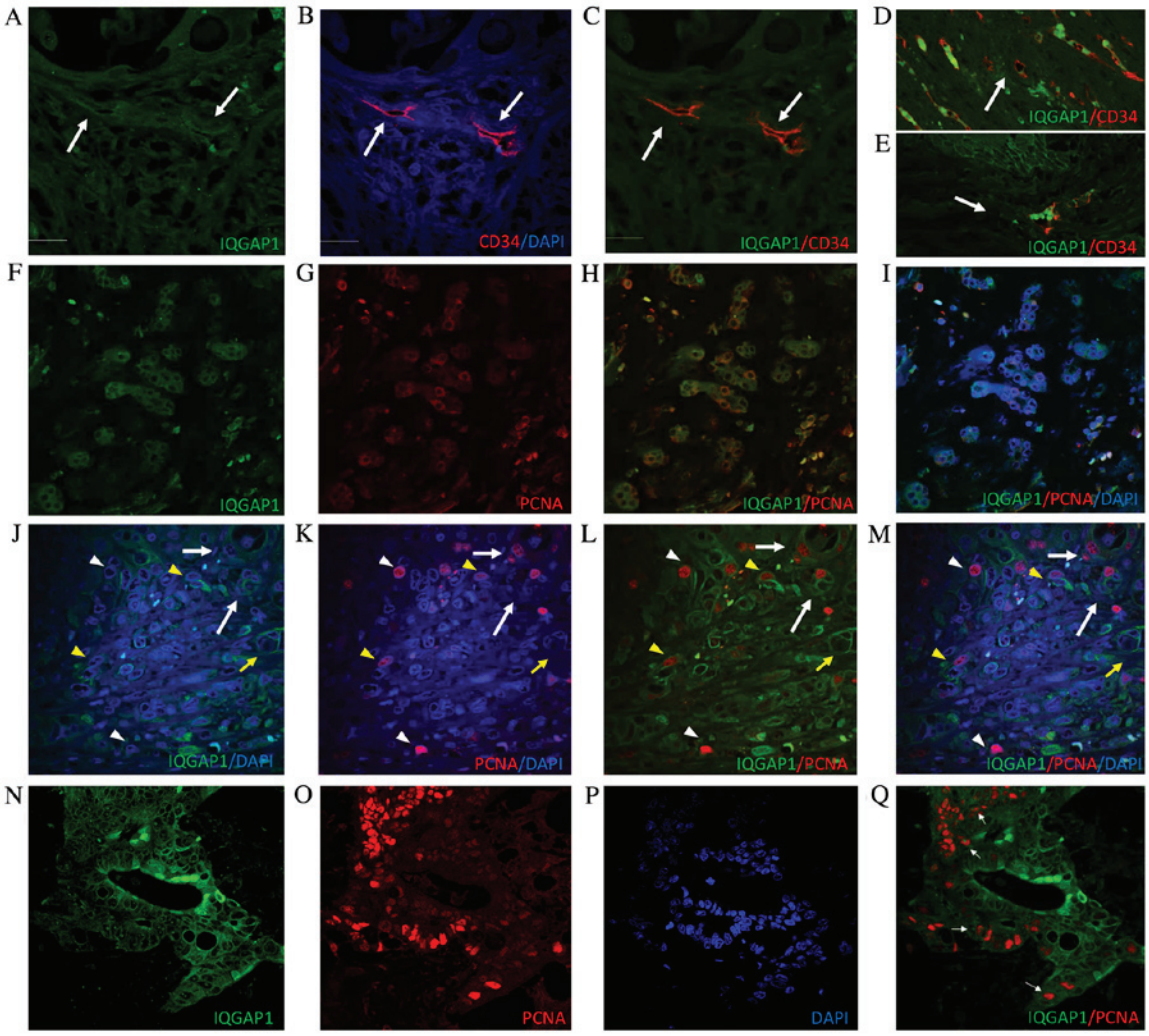

Figure 3. Confocal microscopic analysis of the protein expression by double immunostaining on paraffin-embedded tissue sections of CRC and metastasized liver for IQGAP1 (green) and CD34 (red) or PCNA (red) and DAPI. CRC tissue section; arrows point to tumor-associated vessels with positive staining for (A) IQGAP1 and (B) CD34 or (C) IQGAP1 and CD34 colocalization. Tumor-associated microvessels in (D) metastasized liver and in (E) CRC tissue sections. IQGAP1$^+$ CD34$^+$ microvessels are identified by arrows. (F-I) Metastasized liver double immunostaining for (F) IQGAP1 (green) and (G) PCNA (red). IQGAP1 and PCNA co-localized at the outer nuclear membrane in several cells of the tumor nests; (H) IQGAP1 and PCNA co-localization (I) in addition to DAPI. (J-M) Metastasized liver section double immunostaining for IQGAP1 (green) and PCNA (red). Thin arrow points to a tumor cell cluster where IQGAP1 was observed along the cell membrane; note the presence of a PCNA$^+$ cell in the cluster. Yellow arrow points to an IQGAP1$^+$ tumor-associated microvessel. Thick white arrow points to tumor-associated blood vessel with PCNA labeled endothelial cells. Yellow arrowhead points to an IQGAP1$^+$ PCNA$^+$ tumor cell. White arrowhead points to an IQGAP1$^-$ PCNA$^+$ tumor cell. (N-Q) CRC tissue section double immunostaining for (N) IQGAP1 (green) and (O) PCNA (red); (P) DAPI; (Q) IQGAP1 and PCNA colocalization. Note the positive IQGAP1 staining in the nucleoli of tumor cells (arrows). Scale bar, 50 μm. IQGAP1, IQ-motif containing GTPase activating protein 1; CD, cluster of differentiation; PCNA, proliferating cell nuclear antigen; CRC, colorectal adenocarcinoma.

stromal cells (Fig. 2H-L) and in microvessels present in areas adjacent to the metastasis (Fig. 2G and H). To assess the nature of these IQGAP1$^+$ vessels, the vascular endothelium marker CD34 was used. Confocal analyses of tissue sections double immune-labeled for CD34 and IQGAP1 revealed co-localization of each protein in several vessels (Fig. 3A-E).

Tables I and II specify the IQGAP1 expression signatures observed in the tissue specimens.

To evaluate the proliferative activity of tumor cells, the proliferation marker PCNA was used in double immunofluorescence experiments on formalin-fixed, paraffin-embedded tissue sections. In several malignant cells forming tumor nests, IQGAP1 and PCNA protein exhibited partial co-localization. The distribution of intranuclear PCNA and IQGAP1 surrounding the outer membrane of the nucleus suggests that these cells were in the early S phase (Fig. 3F-I).

In Fig. 3J-M, IQGAP1$^+$ staining was observed along the cell membrane of several tumor cells, and in tumor-associated blood and microvessels. Within the lesion, PCNA intensity and localization varied depending on the stage of the cell cycle in which the cells were. Notably, IQGAP1$^+$ staining was frequently observed in cells in G1/S phase when PCNA begins to translocate from the cytoplasm to the nucleus (Fig. 3F-I), or in cells in early S phase when PCNA expression in the nucleus is weaker (Fig. 3J-M, yellow arrowhead). High levels of PCNA in the nucleus helps to identify late S phase cells; within these cells, no IQGAP1$^+$ signal was observed (Fig. 3J-M, white arrowhead), except occasionally in the nucleolus (Fig. 3Q).

Given the key role of IQGAP1 in the regulation of the cytoskeleton, double immunofluorescence experiments were performed on CRC tissue sections to localize IQGAP1 and β-tubulin. As presented in Fig. 4, IQGAP1 co-localized with

Table I. IQGAP1 expression and localization in healthy colon and CRC tissues.

Cell type	Healthy colon	CRC
Epithelial cells (*Mucosae*)	+++ lm, am, n, c	+++/- pm, lm, c, n
Stromal cells (*Mucosae*)	-	++/-
Tumor cells	-	+++/- pm, c, n
Tumor associated stromal cells	-	++/-
Immune cells	?	+++
Endothelial cells	++ n	++ n, c
Smooth muscle cells	++ n	-
Neurons (*Myenteric plexus*)	++	-
Glial cells (*Myenteric plexus*)	++	-

-, negative; ++, moderate; +++, high; ++/-, variable from moderate to absent; +++/-, variable from high to absent; ?, indeterminate staining; lm, lateral membrane; am, apical membrane; pm, plasma membrane; c, cytoplasm; n, nucleus or nuclear envelope.

Table II. IQGAP1 expression and localization in healthy and colorectal adenocarcinoma metastasized liver.

Cell type	Healthy liver	Metastasized liver
Tumor cells	-	++/- pm, c
Hepatocytes	+++/- n, c	+++/- n, c
Epithelial cells (bile ducts)	+ am	++ pm
Tumor associated stromal cells	-	++

-, negative; +, weak; ++, moderate; +++, high; ++/-, variable from moderate to absent; +++/-, variable from high to absent; am, apical membrane; pm, plasma membrane; c, cytoplasm; n, nucleus or nuclear envelope.

microtubules at the cytoplasmic face of the nuclear envelope in certain cells (arrows). However, in other cells, the pole of the cell was stained for IQGAP1 with no label for β-tubulin. Nucleolar staining was often observed throughout the fields of observation (Figs. 1-4).

Discussion

The present study aimed to study the expression of IQGAP1 in CRC and liver metastases following the administration of adjuvant CT using immunohistochemistry. In contrast to normal cells, in which IQGAP1 was homogeneously distributed, cancer cells presented variable expression patterns, ranging from no expression to whole cell, high level of expression

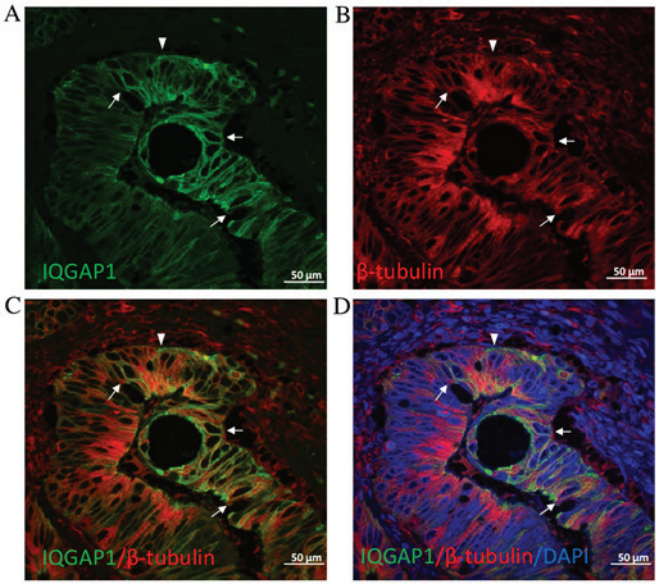

Figure 4. Confocal microscopic analysis of (A) IQGAP1 (green) and (B) β-tubulin (red) expression by double immunofluorescence staining on CRC tissue sections. (C) IQGAP1 and β-tubulin colocalization and with (D) the addition of the nuclear stain DAPI. In the majority of cells, IQGAP1 co-located with microtubules at the cytoplasmic face of the nuclear envelope (arrows). Note that several cells exhibited increased IQGAP1 expression at the plasma membrane (arrowhead) at areas with no (or extremely low) tubulin expression. IQGAP1, IQ-motif containing GTPase activating protein 1.

(Fig. 1A-C). As shown in Fig. 1C, maximum expression was observed at the growing front of the tumor gland indicating the expanding direction, which corresponded to the apical region of the expanding cell in which nuclei were in the opposite pole. Furthermore, double labeling by IQGAP1 and β-tubulin demonstrated that in certain tumor cells the association of each protein disappeared (Fig. 4), indicating clear points where epithelial to mesenchymal cell transition (EMT) occurs. This supports the role of IQGAP scaffold proteins in the regulation of membrane dynamics by coupling the cortical actin meshwork to microtubules via plus-end binding proteins and other proteins involved in intracellular signaling that, ultimately, results in modulation of more complex functions, including cytokinesis, cell migration, cell growth or survival. Specifically, IQGAP1 is observed in actin-dependent membrane structures (membrane ruffles implicated in cell locomotion and lamellipodia) interacting with the plus-end binding proteins cytoplasmic linker protein-170 and adenomatous polyposis coli (APC), tethering microtubules to the actin network (13,14). Furthermore, in the nuclear envelope of certain tumor cells, co-expression of IQGAP1 protein and β-tubulin was observed (Fig. 4). This co-localization of IQGAP1 with the microtubule network at the cytoplasmic face of the nuclear envelope has previously been described by Johnson and Henderson (15) in MCF-7 (breast cancer epithelial cells), HT29 (colon cancer epithelial cells) and NIH3T3 (non-tumor embryonic fibroblasts) cell lines, and was also correlated with a possible role for IQGAP1 in cell polarization and migration events, in addition to cell cycle-associated nuclear envelope assembly/disassembly. Johnson and Henderson (15) suggested that interactions between IQGAP1 and microtubules may tether these cytoskeletal networks to perinuclear actin via the

plus-end protein APC and/or interaction with other nuclear envelope proteins to regulate the microtubule organizing center and nuclear positioning for cell polarization during cell migration, a key process in tumorigenesis and carcinogenesis.

In the current study, increased expression and altered localization of IQGAP1 from the cytoplasm to the plasma membrane was observed in several tumor cells compared with healthy tissue (Figs. 1D, F and H, 2E and 4) may serve to decrease AJ stability, favoring dissociation of the tumor cells (12). IQGAP1 at the plasma membrane regulates the stability of the AJ complex, which is necessary for proper apical-basal polarity of epithelial cells that disappears during the EMT process (16).

In the present study, the co-localization of CD34 and IQGAP1 in several vessels (Fig. 3A-E) is indicative of a role for IQGAP1 in tumor vasculogenesis and/or in vascular invasion. Nakhaei-Nejad *et al* (17) studied the involvement of endothelial IQGAP1 in leukocyte transendothelial migration, and demonstrated, by RNAi silencing of IQGAP1 in human umbilical vein endothelial cells, that IQGAP1 and interendothelial junction-associated microtubules were involved in remodeling interendothelial junctions to facilitate lymphocyte diapedesis under physiological shear stress. Furthermore, Yamaoka-Tojo *et al* (18) reported that IQGAP1 is a novel vascular endothelial growth factor receptor 2 (VEGFR2) binding protein in quiescent endothelial cells and is important for the establishment of VE-cadherin-based cell-cell contacts, and suggested that IQGAP1 may function as a scaffold linking VEGFR2 to the β-catenin/VE-cadherin compound at the AJ (18).

PCNA is a DNA clamp that increases the processivity of DNA polymerase δ in eukaryotic cells, which is used as a marker of proliferating cells (19-21). The immunohistochemical experiments of the present study revealed that certain cells co-expressed IQGAP1 and PCNA in the cytoplasm, whereas others expressed IQGAP1 in the cytoplasm and PCNA in the nucleus, which is indicative of S phase (22). In addition, $CD34^+$ microvessels of CRC and metastatic sections co-express PCNA and IQGAP, while the majority of cancer cells do not contain intranuclear PCNA, though they may contain cytoplasmic, pointing to a quiescent phase while waiting for energy to be supplied in order for the carcinogenic process to progress (23).

As shown in Fig. 3F-M, during the synthesis of PCNA, PCNA and IQGAP1 are simultaneously expressed in the cytoplasm of cells within the liver. PCNA then enters into the nucleus and S phase of mitosis begins. A role for IQGAP1 in regulating early S phase replication events has been recently proposed. Johnson *et al* (23) identified nuclear localization of IQGAP1 in several mammalian cell lines. This nuclear localization was low in asynchronous cells, but was significantly increased in cells arrested in G1/S phase (23). The authors suggested that the protein enters the nucleus at G1/S phase and exits in late S phase. Furthermore, nuclear IQGAP1 was identified to function as part of a complex with replication protein A 32 kDa subunit and PCNA, suggesting a functional role for IQGAP1 in the reinitiation of S phase following DNA replication arrest (23).

As observed in the current study, nucleoli staining is often observed throughout the field of microscopic observation, which is consistent with Bielak-Zmijewska *et al* (24). The authors observed the presence of IQGAP1 in mouse oocyte nuclei, forming a ring around the nucleolus only in transcriptionally active oocytes, but not in transcriptionally silent ones or in growing oocytes treated with the transcription inhibitor α-amanitin, indicating an association between IQGAP1 expression in the nucleolus and RNA synthesis (24).

In conclusion, extremely few studies have analyzed IQGAP1 expression in colorectal tumors, and none have yet addressed IQGAP1 expression in CRC and its associated liver metastases. To the best of our knowledge, the present study is the first to provide a detailed analysis of IQGAP1 expression in CRC tissue sections and metastasized liver tissue samples, which were resected following oxaliplatin-based CT. Despite the homogeneous IQGAP1 staining pattern observed in healthy colon tissue sections, the CRC tissues exhibited heterogeneous expression (in terms of localization and intensity), which was more marked in the metastasized liver sections resected following CT treatment. However, more notable findings are the described effects over the cellular and subcellular distribution and its implications in the cancer biology. Therefore, IQGAP1 may be a novel cancer antigen, a surrogate biomarker of responses to CT, a candidate for the development of new clinical diagnostics and a new target for anti-cancer therapeutics.

Acknowledgements

The present study was supported by grants from the Health Institute of Charles III, Spain (no. FIS PI11/00114) and Microscopy was funded by a joint grant from the Insular Council of Tenerife, Spain; the Ministry of Science and Technology, Spain; and the European Regional Development Fund 2003/2004, Belgium (no. IMBRAIN-FP7-REGPOT-2012-31 637).

References

1. André T, Boni C, Mounedji-Boudiaf L, Navarro M, Tabernero J, Hickish T, Topham C, Zaninelli M, Clingan P, Bridgewater J, *et al*: Oxaliplatin, fluorouracil, and leucovorin as adjuvant treatment for colon cancer. N Engl J Med 350: 2343-2351, 2004.
2. Xu R, Zhou B, Fung PC and Li X: Recent advances in the treatment of colon cancer. Histol Histopathol 21: 867-872, 2006.
3. Morales M, Ávila J, González-Fernández R, Boronat L, Soriano ML and Martín-Vasallo P: Differential transcriptome profile of peripheral white cells to identify biomarkers involved in oxaliplatin induced neuropathy. J Pers Med 4: 282-296, 2014.
4. Rotoli D, Morales M, Del Carmen Maeso M, Del Pino García M, Morales A, Avila J and Martín-Vasallo P: Expression and localization of the immunophilin FKBP51 in colorectal carcinomas and primary metastases, and alterations following oxaliplatin-based chemotherapy. Oncol Lett 12: 1315-1322, 2016.
5. Johnson M, Sharma M and Henderson BR: IQGAP1 regulation and roles in cancer. Cell Signal 21: 1471-1478, 2009.
6. White CD, Brown MD and Sacks DB: IQGAPs in cancer: A family of scaffold proteins underlying tumorigenesis. FEBS Lett 583: 1817-1824, 2009.
7. Erickson JW, Cerione RA and Hart MJ: Identification of an actin cytoskeletal complex that includes IQGAP and the Cdc42 GTPase. J Biol Chem 272: 24443-24447, 1997.
8. Roy M, Li Z and Sacks DB: IQGAP1 is a scaffold for mitogen-activated protein kinase signaling. Mol Cell Biol 25: 7940-7952, 2005.
9. McDonald KL, O'Sullivan MG, Parkinson JF, Shaw JM, Payne CA, Brewer JM, Young L, Reader DJ, Wheeler HT, Cook RJ, *et al*: IQGAP1 and IGFBP2: Valuable biomarkers for determining prognosis in glioma patients. J Neuropathol Exp Neurol 66: 405-417, 2007.

10. Nabeshima K, Shimao Y, Inoue T and Koono M: Immunohistochemical analysis of IQGAP1 expression in human colorectal carcinomas: Its overexpression in carcinomas and association with invasion fronts. Cancer Lett 176: 101-109, 2002.
11. Holck S, Nielsen HJ, Hammer E, Christensen IJ and Larsson LI: IQGAP1 in rectal adenocarcinomas: Localization and protein expression before and after radiochemotherapy. Cancer Lett 356: 556-560, 2015.
12. Takemoto H, Doki Y, Shiozaki H, Imamura H, Utsunomiya T, Miyata H, Yano M, Inoue M, Fujiwara Y and Monden M: Localization of IQGAP1 is inversely correlated with intercellular adhesion mediated by e-cadherin in gastric cancers. Int J Cancer 91: 783-788, 2001.
13. Fukata M, Watanabe T, Noritake J, Nakagawa M, Yamaga M, Kuroda S, Matsuura Y, Iwamatsu A, Perez F and Kaibuchi K: Rac1 and Cdc42 capture microtubules through IQGAP1 and CLIP-170. Cell 109: 873-885, 2002.
14. Watanabe T, Wang S, Noritake J, Sato K, Fukata M, Takefuji M, Nakagawa M, Izumi N, Akiyama T and Kaibuchi K: Interaction with IQGAP1 links APC to Rac1, Cdc42, and actin filaments during cell polarization and migration. Dev Cell 7: 871-883, 2004.
15. Johnson MA and Henderson BR: The scaffolding protein IQGAP1 co-localizes with actin at the cytoplasmic face of the nuclear envelope: Implications for cytoskeletal regulation. Bioarchitecture 2: 138-142, 2012.
16. Noritake J, Watanabe T, Sato K, Wang S and Kaibuchi K: IQGAP1: A key regulator of adhesion and migration. J Cell Sci 118: 2085-2092, 2005.
17. Nakhaei-Nejad M, Zhang QX and Murray AG: Endothelial IQGAP1 regulates efficient lymphocyte transendothelial migration. Eur J Immunol 40: 204-213, 2010.
18. Yamaoka-Tojo M, Tojo T, Kim HW, Hilenski L, Patrushev NA, Zhang L, Fukai T and Ushio-Fukai M: IQGAP1 mediates VE-cadherin-based cell-cell contacts and VEGF signaling at adherence junctions linked to angiogenesis. Arterioscler Thromb Vasc Biol 26: 1991-1997, 2006.
19. Guzińska-Ustymowicz K, Pryczynicz A, Kemona A and Czyzewska J: Correlation between proliferation markers: PCNA, Ki-67, MCM-2 and antiapoptotic protein Bcl-2 in colorectal cancer. Anticancer Res 29: 3049-3052, 2009.
20. Bleau AM, Agliano A, Larzabal L, de Aberasturi AL and Calvo A: Metastatic dormancy: A complex network between cancer stem cells and their microenvironment. Histol Histopathol 29: 1499-1510, 2014.
21. Moldovan GL, Pfander B and Jentsch S: PCNA, the maestro of the replication fork. Cell 129: 665-679, 2007.
22. Connolly KM and Bogdanffy MS: Evaluation of proliferating cell nuclear antigen (PCNA) as an endogenous marker of cell proliferation in rat liver: A dual-stain comparison with 5-bromo-2'-deoxyuridine. J Histochem Cytochem 41: 1-6, 1993.
23. Johnson M, Sharma M, Brocardo MG and Henderson BR: IQGAP1 translocates to the nucleus in early S-phase and contributes to cell cycle progression after DNA replication arrest. Int J Biochem Cell Biol 43: 65-73, 2011.
24. Bielak-Zmijewska A, Kolano A, Szczepanska K, Maleszewski M and Borsuk E: Cdc42 protein acts upstream of IQGAP1 and regulates cytokinesis in mouse oocytes and embryos. Dev Biol 322: 21-32, 2008.

APPENDIX B
ARTICLE 2

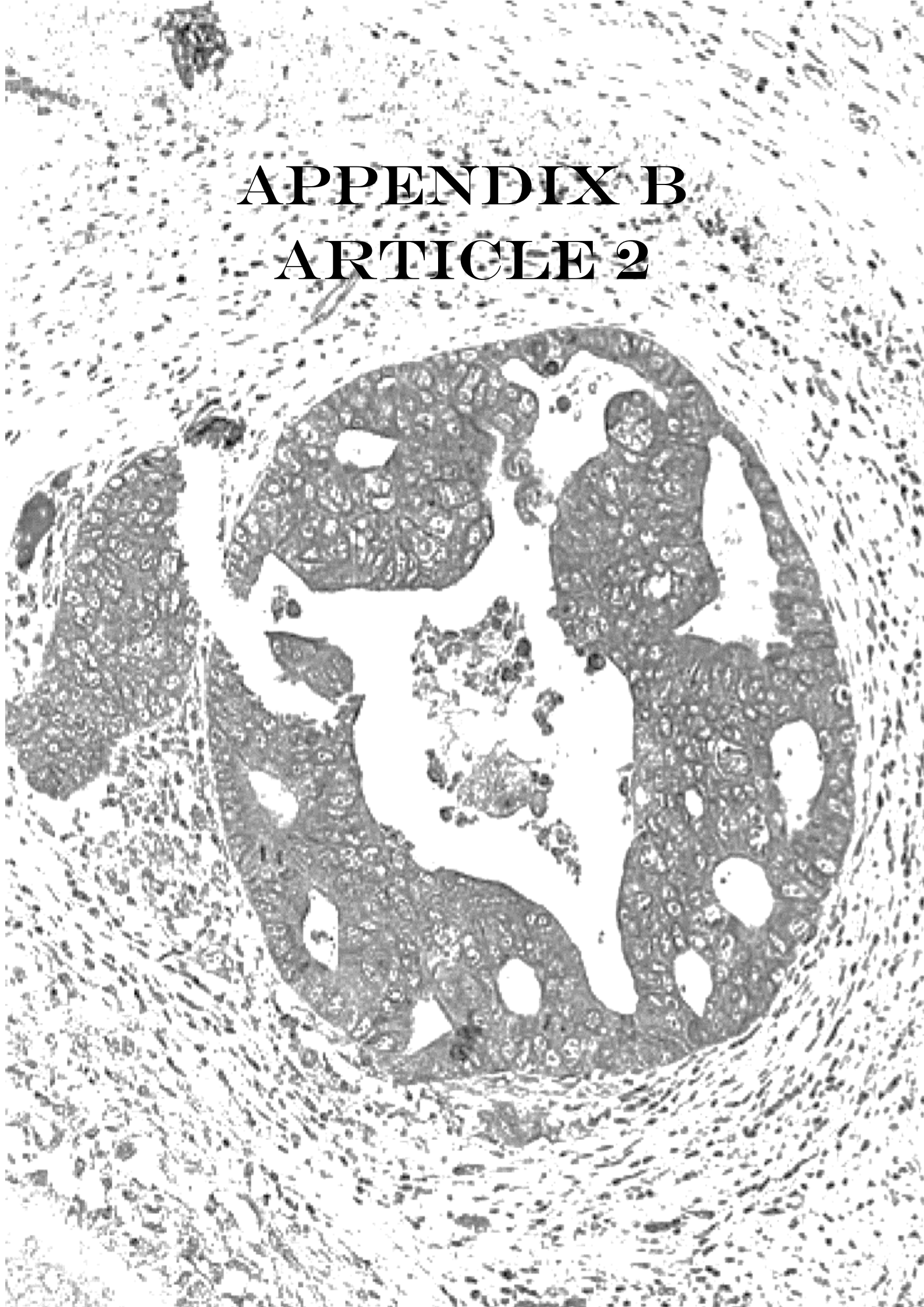

Expression and localization of the immunophilin FKBP51 in colorectal carcinomas and primary metastases, and alterations following oxaliplatin-based chemotherapy

DEBORAH ROTOLI[1,2*], MANUEL MORALES[3,4*], MARÍA DEL CARMEN MAESO[5], MARÍA DEL PINO GARCÍA[6], ARACELI MORALES[7], JULIO ÁVILA[1] and PABLO MARTÍN-VASALLO[1]

[1]Developmental Biology Laboratory, UD- Biochemistry and Molecular Biology and Centre for Biomedical Research of the Canary Islands, La Laguna University, La Laguna, 38206 Tenerife, Spain; [2]National Research Council, Institute of Endocrinology and Experimental Oncology, I-80131 Naples, Italy; [3]Service of Medical Oncology, University Hospital Nuestra Señora de Candelaria, 38010 Santa Cruz de Tenerife; [4]Unit of Medical Oncology, Hospiten® Hospitals, Santa Cruz de Tenerife, 38001 Tenerife; [5]Service of Pathology, University Hospital Nuestra Señora de Candelaria, 38010 Santa Cruz de Tenerife; [6]Laboratory of Biopathology, Hospiten® Hospitals, 38010 Tenerife; [7]Department of Physiology, Institute of Biomedical Technologies, School of Medicine and Centre for Biomedical Research of The Canary Islands, University of La Laguna, La Laguna, 38071 Santa Cruz de Tenerife, Spain

Received September 28, 2015; Accepted April 29, 2016

DOI: 10.3892/ol.2016.4772

Abstract. The immunophilin FK506-binding protein 5 (FKBP51) is a scaffold protein that serves a pivotal role in the regulation of multiple signaling pathways, integrating external and internal stimuli into distinct signal outputs. In a previous study, we identified several genes that are significantly up- or downregulated in the peripheral white cells (PWCs) of colorectal adenocarcinoma (CRC) patients undergoing oxaliplatin-based chemotherapy. In our screening, FKBP51 gene expression was downregulated following chemotherapy. In order to determine whether this alteration in gene expression observed in PWCs may be detected at the protein level in tumors and metastases following the administration of adjuvant chemotherapy, an immunohistochemical analysis of FKBP51 in CRC and primary metastasis tissues was performed. The present study confirmed the downregulation of FKBP51 gene expression elicited by chemotherapy with folinic acid (leucovorin), fluorouracil and oxaliplatin in metastasized liver tissue that had been resected after the oxaliplatin-based chemotherapy, compared with tissue section samples of CRC from patients (prior to antineoplastic treatment). Furthermore, the results indicated that, in CRC tissue sections, the expression of FKBP51 protein is associated with an immature phenotype of stromal fibroblasts and with the epithelial-to-mesenchymal transition (EMT) phenotype, suggesting a role for this protein in the EMT process in CRC. Finally, the observation that only certain cells of the stroma express FKBP51 protein suggests a potential role for this immunophilin as a stroma cell subtype marker.

Correspondence to: Professor Pablo Martín-Vasallo, Developmental Biology Laboratory, UD- Biochemistry and Molecular Biology and Centre for Biomedical Research of the Canary Islands, La Laguna University, Av. Astrofísico Sánchez, La Laguna, 38206 Tenerife, Spain
E-mail: pmartin@ull.es

*Contributed equally

Key words: colorectal cancer, oxaliplatin, FK506-binding protein 5, immunophilin

Introduction

In the Western world, colorectal cancer (CRC) is the fourth leading cause of cancer-associated mortality (1), and >95% of colorectal cancers are adenocarcinomas. The main risk factors are genetic factors (family history), a low fiber and high fat diet, and smoking (2). Following curative surgery alone, the percentage of patients that subsequently relapse and succumb to metastatic disease ranges from 40 to 50%. This percentage falls to 33% when patients receive postoperative adjuvant treatment with 5-fluorouracil (5-FU) and leucovorin, and to 23% when the platinum-containing compound oxaliplatin is added to this treatment [FOLFOX: folinic acid (leucovorin), 5-FU and oxaliplatin] (2,3).

Unfortunately, despite the positive results obtained by the combination protocols of oxaliplatin with fluoropyrimidines (e.g. 5-FU) and folinic acid (leucovorin) in disease-free survival of stage II or III colon cancer (3), unwanted side effects develop that can affect, to various degrees, the quality of life of the patients. Several side effects have been reported for oxaliplatin, which include gastrointestinal toxicity, moderate hematological toxicity, hypersensitivity and neurological toxicity. This unpredictable neural toxicity has quite unique features and determines the dose-limiting toxicity of oxaliplatin (4).

The identification of biomarkers that could predict the onset of these secondary effects would be of great value in preventing long-term toxicity or permanent damage in patients at risk. Recent research from our laboratory has led to the identification of several genes that are significantly up- or downregulated in peripheral white cells (PWCs) of CRC patients following oxaliplatin-based chemotherapy treatment (5). In our screening, the expression levels of the gene encoding for the immunophilin FK506-binding protein 5 (FKBP51) were 2.76-times lower [3,812 (pre) vs. 1,383 (post)] in PWCs after 3 cycles of oxaliplatin-based chemotherapy (5).

FKBP51 protein plays multiple roles in the regulation of a variety of signaling pathways, and has altered expression levels in many different tumor types. By regulating steroid receptor maturation, as well as the Akt and nuclear factor κB signaling pathways, FKBP51 is important in tumorigenesis and in the response to chemotherapy (6-13). FKBP51 belongs to a superfamily of peptidyl-prolyl isomerases (PPIs), which also includes FKBP52 and the cyclosporine A-binding protein cyclophilin-40. FKBP51 is a 51 kD FK506-binding protein with a C-terminal tetratricopeptide repeat (TPR) domain, and an N-terminal FK1 domain responsible for PPIase activity, which catalyzes the cis-trans conversion of prolyl peptide bonds within target proteins (14). Through the TPR domain, FKBP51 binds to heat shock protein 90 (HSP90) complexes, such as those associated with steroid hormone receptors. The mechanisms underlying the regulation of steroid hormone receptor signaling by this immunophilin and its physiological roles in endocrine-related processes are very well studied and will be further discussed in the discussion section.

Research in this field has led to the identification of FKBP51 as a potential therapeutic target for several endocrine-related diseases, such as metabolic and stress-related diseases, prostate cancer and breast cancer (13). Diseases associated with this protein include major depressive disorder and glucocorticoid resistance (Gene Ontology annotations). FKBP51 is a ubiquitous protein expressed in the cytoplasm, nucleus and mitochondria (14). Nuclear-mitochondrial shuttling is triggered by oxidative stress: The protein translocates to the nucleus upon the onset of oxidative stress to protect the cells from stress damage (7).

Recently, a role for the immunophilins FKBP51 and FKBP52 in regulating microtubules has been suggested, acting via their interaction with τ proteins (15). Regulation of microtubule dynamics by FKBPs has been associated with neurite outgrowth (16). Furthermore, FKBP51 has been identified as a regulator of cell death in response to gemcitabine and cytarabine treatment: High levels of FKBP51 expression were associated with sensitivity, while low levels of expression were associated with resistance to these drugs (17).

Several studies also link FKBP51 to cell proliferation and cancer. It has been demonstrated, for example, that it plays a role in negatively regulating the Akt pathway. Acting as a scaffold protein, FKBP51 promotes the interaction of Akt and PHLPP, a phosphatase that specifically dephosphorylates Akt at Ser473 and inhibits its activity (9). Recently it has been demonstrated that FKBP51 is key in promoting the activation of genes involved in melanoma progression (11), and modulates the transforming growth factor β (TGF-β) signal in malignant melanocytes, increasing the tumor-promoter potential of TGF-β (12). FKBP51 expression is also decreased in pancreatic cancer tissues and in numerous cancer cell lines.

In the current study, an immunohistochemical (IHC) analysis of FKBP51 in CRC tissue sections (namely before antineoplastic therapy) and primary metastases (resected after oxaliplatin-based chemotherapy) was performed in order to determine whether the alteration in FKBP51 gene expression observed in PWCs can be detected at the protein level, the nature of their role in tumoral physiopathology, and whether these alterations have any prognostic implications.

Materials and methods

Patients. The study was approved by the Ethics Committee of La Laguna University (La Laguna, Spain) and the Ethics Committee of Nuestra Señora de Candelaria University Hospital (HUNSC; Santa Cruz de Tenerife, Spain). All patients signed informed consent for diagnosis and research on tissue specimens, prior to entering the study. All subjects were treated with FOLFOX chemotherapy as follows: Day 1, oxaliplatin [100 mg/m^2 intravenous (i.v.) over 2 h], leucovorin calcium (400 mg/m^2 i.v. over 2 h); followed by 5-FU (400 mg/m^2 i.v. bolus) and by 5-FU (2,400 mg/m^2 i.v. over 46 h), every 14 days, days, and no patient underwent previous CT scans or received radiation therapy. The patients were treated between October 2010 and July 2015.

Several (between 10 and 15) mounted slides of paraffin-embedded tissue samples (5 μm thick; colon adenocarcinoma and metastasized liver and lung from selected patients) obtained during resection and clinical data were collected from 33 patients (16 males and 17 females), aged between 38 and 76 years, from the reference medical areas of HUNSC.

Antibodies. The following antibodies were used: Rabbit polyclonal antibody (pAb) against FKBP51 (#ab46002; Abcam, Cambridge, UK; dilution, 1.25:100); mouse monoclonal antibody against proliferating cell nuclear antigen (PCNA; clone PC10; #1486 772, Roche Diagnostics Deutschland GmbH, Mannheim, Germany; dilution, 1:100); fluorescein isothiocyanate (FITC)-conjugated goat pAb against rabbit IgG (#F9887; Sigma-Aldrich, St. Louis, MO, USA; dilution, 1:200); goat pAb against mouse IgG (DyLight® 650; #ab97018; Abcam, dilution, 1:100); biotin-conjugated goat pAb against rabbit IgG (H+L) (#31820; Thermo Fisher Scientific, Inc., Waltham, MA, USA; dilution, 1:300).

IHC. Immunoperoxidase staining of formalin-fixed, paraffin-embedded tissue sections was performed using an ordinary avidin-biotin method. Briefly, 5 μm-thick tissue sections were deparaffinized in xylene and hydrated in graded alcohol. Heat-induced epitope retrieval was achieved by heating samples in sodium citrate buffer pH 6.0 at 120˚C for 10 min in an autoclave. After non-specific sites were blocked with 5% non-fat dry milk in Tris-buffered saline (TBS) for 1 h at room temperature, endogenous biotin was blocked using an Avidin/Biotin Blocking Kit (Vector Laboratories, Inc., Burlingame, CA, USA). Primary antibody against FKBP51 (1.25:100) was applied to slides overnight at 4˚C. Biotin-conjugated anti-rabbit secondary antibody was incubated for 2 h at 37˚C at a dilution of 1:300. To block endogenous peroxidase activity, slides were incubated with 3% hydrogen peroxidase in methanol

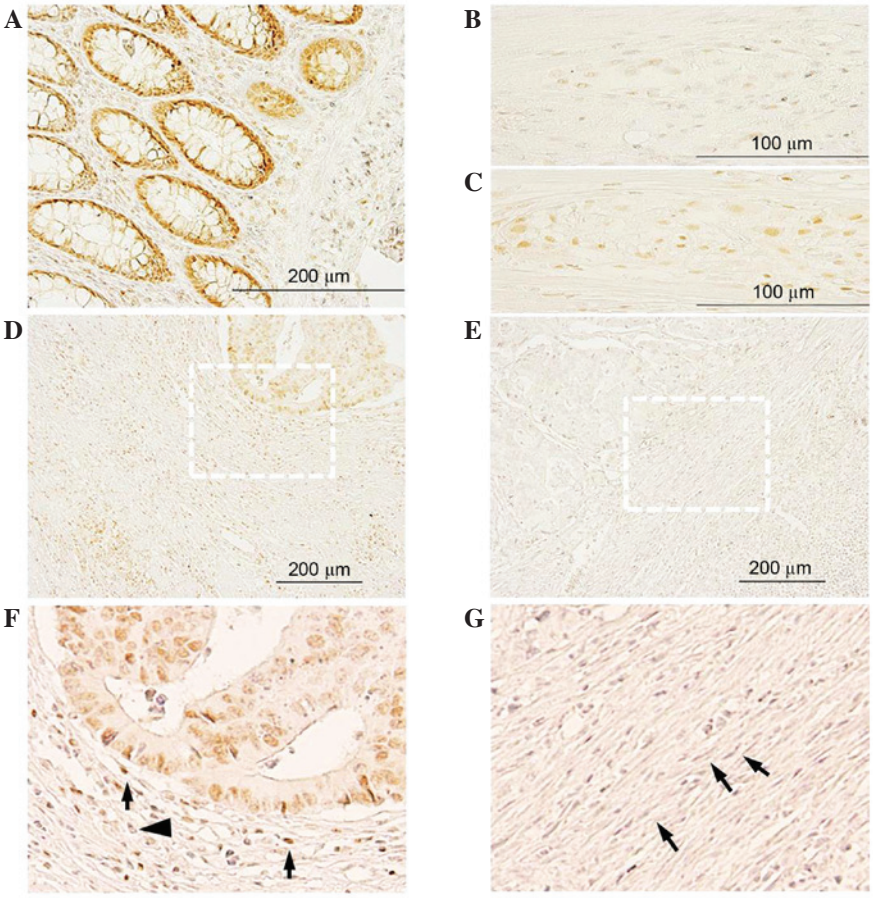

Figure 1. (A and B) FKBP51 expression in healthy colon: (A) Positive staining in enterocytes and cells of the lamina propria; (B) in healthy colon, few cells in Auerbach's plexus exhibit a weak signal. (C) By contrast, in colorectal cancer tissue sections, positive staining is observed in several cells of the plexus. (D-G) FKBP51 expression in colon adenocarcinoma: Tumor cells and inflammatory and fibrous stromal cells exhibit variable signals, from (D) strongly positive to (E) absent. (F) Magnification of (D), showing immature phenotype of stromal fibroblasts surrounding a lesion with positive FKBP51 cells. (G) Magnification of (E), showing mature phenotype of stromal fibroblasts surrounding a lesion with cells completely negatively expressing FKBP51. FKBP51, FK506-binding protein 5.

for 15 min. A Pierce ABC Peroxidase Staining Kit (Thermo Fisher Scientific, Inc.) was used to amplify the specific antibody staining. Concentrated 3,3'-diaminobenzidine Substrate (#IHC-101F; Bethyl Laboratories, Inc., Montgomery, TX, USA) was used to visualize IHC reactions. Samples incubated without primary antibodies were used as negative controls. Slides were counterstained with Harris Hematoxylin Solution DC (Panreac Quimica SLU, Barcelona, Spain) to visualize cell nuclei. Slides were mounted with Eukitt (Panreac Quimica SLU). An optical light microscope (BX50, Olympus Corporation, Tokyo, Japan) was used to visualize immunostaining results.

Image analysis and statistics. For semi-quantitative image analysis, the open resource digital image analysis software ImageJ was used, implemented with the IHC Profiler plug-in developed by Varghese *et al* (18), which creates a pixel-by-pixel analysis profile of a digital IHC image, and further assigns a score in a four tier system: High positive (pixel intensity range, 0-60), positive (pixel intensity range, 61-120), low positive (pixel intensity range, 121-180), negative (pixel intensity range, 181-235). All images were captured at the same magnification (40x) and with the same levels of contrast and brightness. Pearson's Correlation Coefficient and Student's *t*-test were performed using SPSS version 20 software (IBM SPSS, Madrid, Spain) in order to estimate the reliability of the study.

Double immunofluorescence simultaneous staining. Following the deparaffinization, hydration and heat-induced epitope retrieval procedures (as described), slides were incubated with 5% bovine serum albumin (catalog no. A9647; Sigma-Aldrich, St. Louis, MO, USA) and 1% Triton X-100 in TBS to block non-specific sites. Tissue sections were then incubated simultaneously with a mixture of two distinct primary antibodies (rabbit anti-FKBP51 and mouse anti-PCNA) overnight at 4°C, at concentrations of 1:50 and 1:100, respectively. Slides were then incubated for 1 h at room temperature with a mixture of two secondary antibodies (FITC-conjugated anti-rabbit and DyLight® 650-conjugated anti-mouse). Slides were mounted with ProLong® Diamond Anti-fade Mountant with DAPI (Molecular Probes; Thermo Fisher Scientific, Inc., Eugene, Oregon, USA) to visualize cell nuclei. Slides were analyzed using a confocal microscope (FV1000, Olympus Corporation).

Results

IHC analysis of FKBP51 expression in colon tissue samples from CRC patients. In healthy colon and in the apparently healthy region of the CRC tissue sections (Fig. 1), intestinal glands exhibited intense positive FKBP51 nuclear staining in enterocytes and in cells of the lamina propria (Fig. 1A). In healthy colon, few cells in the myenteric plexus exhibited a

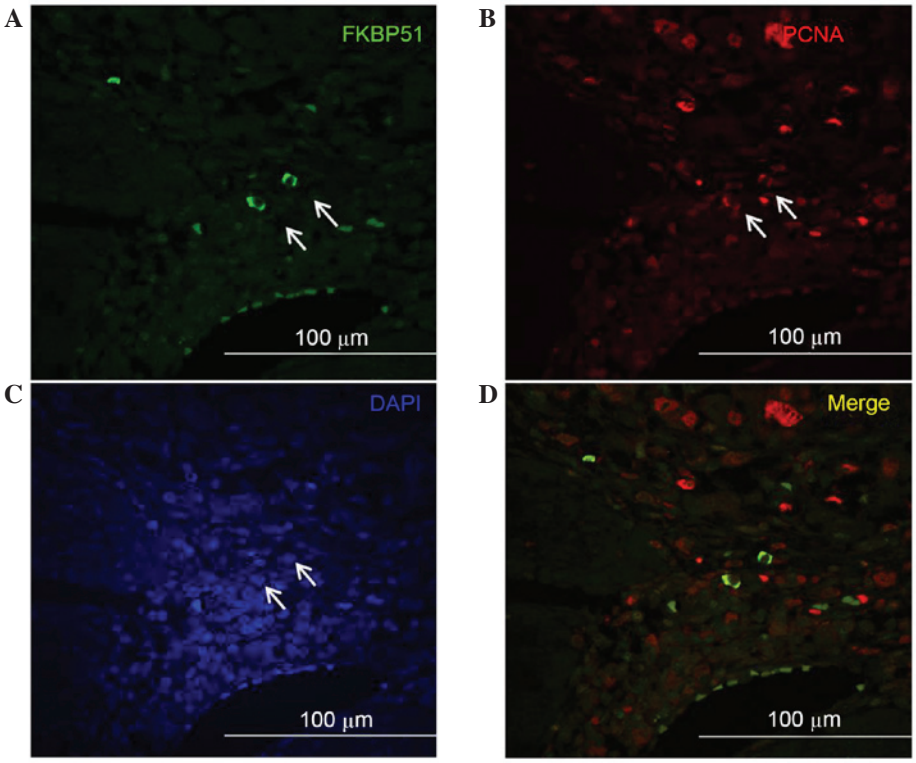

Figure 2. Double immunofluorescence imaging on colorectal cancer tissue sections. Confocal images of (A) FKBP51 (green) and (B) PCNA (red) expression in stromal cells; only certain cells in the stroma co-express FKBP51 and PCNA (arrows). (C) Nuclei were visualized by DAPI. (D) Merged image of (A) and (B). FKBP51, FK506-binding protein 5; PCNA, proliferating cell nuclear antigen.

weak signal (Fig. 1B), while in CRC tissue sections, several cells in the plexus were strongly positive (Fig. 1C).

In colon adenocarcinoma tissue sections, FKBP51 protein was localized in the cytoplasm and/or nucleus of tumor cells, as well as in inflammatory and fibrous stromal cells surrounding the lesions (Fig. 1D-G). In certain areas of the section, a variable positive signal could be observed in tumor cells, while in other areas, no staining was detected. Notably, the phenotype of the connective tissue surrounding the lesions appeared variable: In those areas where no immunophilin expression was observed in tumor and stromal cells, stromal fibroblasts exhibited a mature phenotype, with thin, wavy and small spindle cell morphology (Fig. 1E and G, arrows); by contrast, in those areas where positive FKBP51 immunostaining could be observed in tumor and stromal cells, fibroblasts exhibited an immature phenotype, with large, puffy, spindle-shaped morphology (Fig. 1F). An increased microvessel density and enhanced infiltration of tumor-associated macrophages was also observed in the connective tissue surrounding FKBP51-positive lesions (Fig. 1F).

In the stroma surrounding tumor nests, the expression of FKBP51 was variable, with cells exhibiting a strong positive signal (Fig. 1F, arrow) and others completely negative (Fig. 1F, arrowhead).

Double immunofluorescence experiments to detect FKBP51 and PCNA, the clamp subunit of DNA polymerase and marker of S phase of cell cycle (19), revealed that, among the stromal cells expressing PCNA, only a few coexpressed FKBP51 (Fig. 2). This suggests a potential role for this immunophilin protein as a marker of specific subtypes of stromal cells; however, further studies are needed to assess this hypothesis.

IHC analysis of FKBP51 expression in metastasized liver tissue samples from CRC patients. In the overall sections of healthy liver (Fig. 3C) and in the apparently healthy part of metastasized liver (Fig. 3D), there were areas with a more intense signal and well-delimited areas in which FKBP51 protein expression was weak or absent. Intense staining could be observed in the nuclei of hepatocytes lining the edge of the connective tissue capsule (Glisson's capsule) (Fig. 3A, arrows). By contrast, in metastasized liver, this nuclear signal was fainter (Fig. 3B, arrow). In metastases, the signal appeared faint or absent, while several of the inflammatory fibrous stroma cells exhibited a strong signal (Fig. 3E).

IHC analysis of FKBP51 expression in metastasized lung tissue samples from CRC patients. In healthy lung tissue, positive FKBP51 staining was observed in macrophages and endothelial cells. In the respiratory mucosa, a strong signal was present in the nuclei and cytoplasm of ciliated cells (data not shown). In metastasized lung, strong positive staining could be observed in macrophages (Fig. 4A, black arrow), in cells of the *lamina propria*, in endothelial cells and, to a lesser extent, in the nuclei of bronchial gland cells (Fig. 4C, arrowhead, thick arrow and thin arrow, respectively). In the bronchial epithelial cells, FKBP51 protein was localized to the nuclei and/or cytoplasm of ciliated cells; strong staining in the basal bodies of these cells was present (Fig. 4B, arrow). In the malignant area of the section, weakly positive or no staining was observed in tumor cells, while the signal appeared stronger in inflammatory and fibrous stromal cells surrounding the lesions (Fig. 4E and F). Fig. 4F shows the positive protein staining in several stromal cells between two metastases; the intracellular distribution

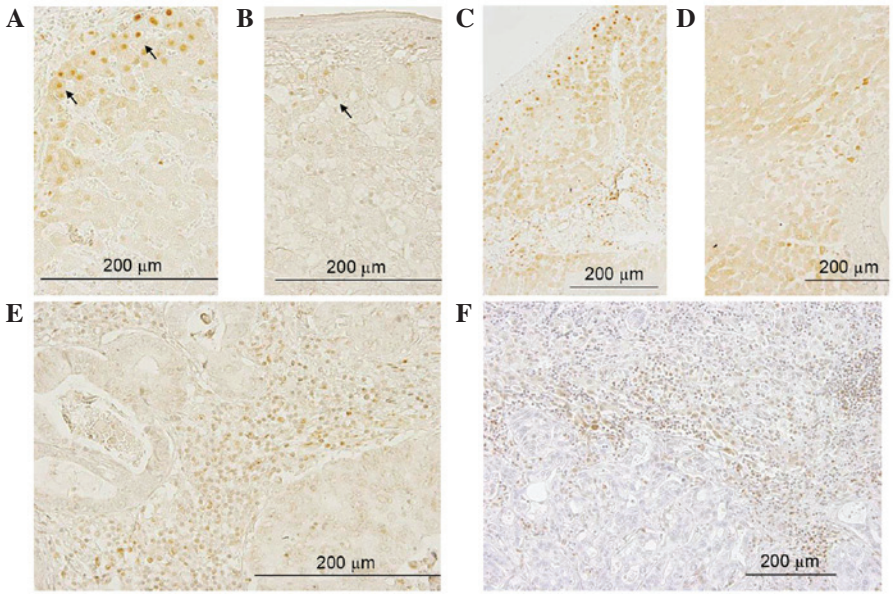

Figure 3. FKBP51 expression in healthy liver and in metastasized liver. Positive nuclear staining in hepatocytes lining the edge of Glisson's capsule (black arrows) was observed in (A) healthy and (B) metastasized liver tissue. Variable FKBP51 protein expression was present in (C) healthy liver and (D) apparently healthy parts of metastasized liver. (E and F) Inflammatory fibrous stroma exhibited positive staining in several cells, while in metastasis, the signal is (E) faint or (F) absent. FKBP51, FK506-binding protein 5.

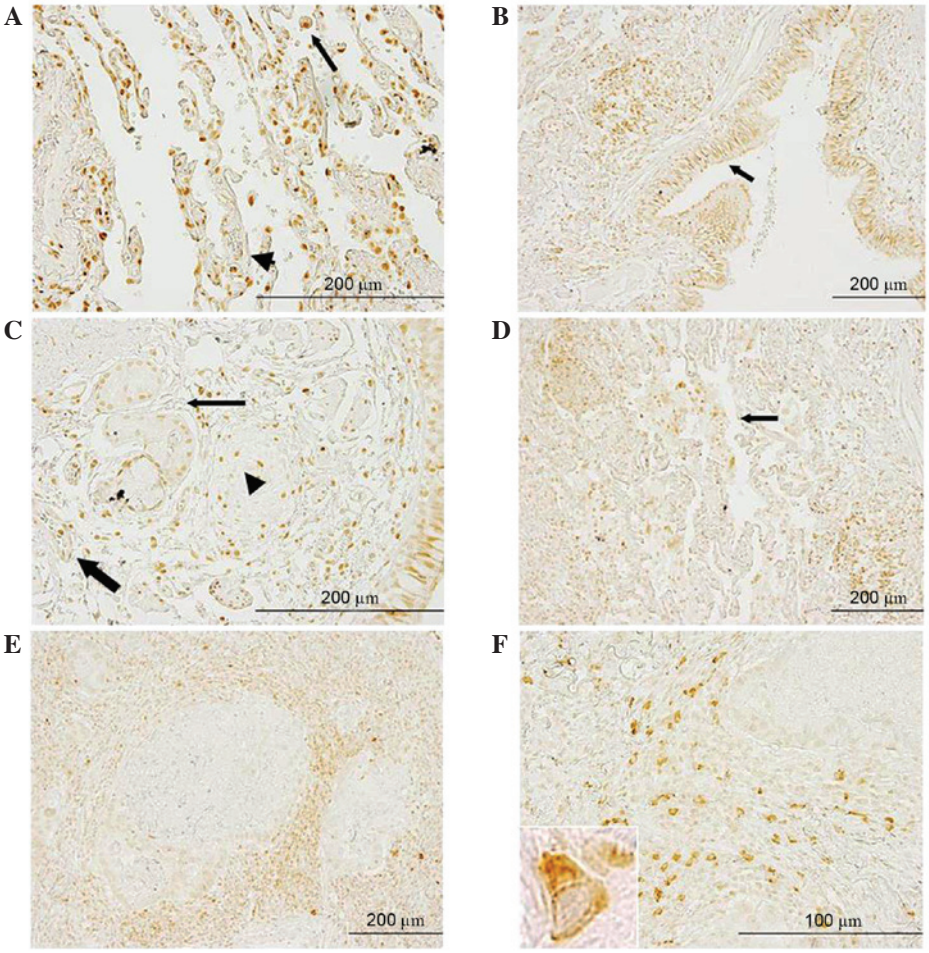

Figure 4. Anti-FK506-binding protein 5 immunostaining in metastasized lung tissue section. (A) Macrophages (arrow) and endothelial cells (arrowhead) exhibited strong positive signals. (B) Respiratory mucosa showed intense positive staining in the nuclei and cytoplasm of ciliated cells; intense staining in basal bodies of ciliated cells could be observed (arrow). (C) Strong positive staining was observed in cells of the lamina propria (arrowhead) and in endothelial cells (thick arrow); nuclei of bronchial gland cells exhibited a positive signal (thin arrow). (D) Clustered macrophages were visible (arrow). (E and F) Tumor cells exhibited weak positive staining, while a strong positive signal was observed in inflammatory and fibrous stromal cells surrounding the lesions. (F) The inset image (lower left) shows x100 magnification of a cell to illustrate further distribution detail.

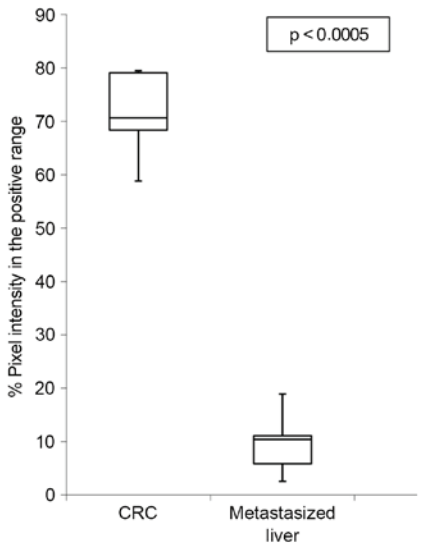

Figure 5. Box-and-whisker plot illustrating FKBP51 downregulation in metastasized liver tissue sections compared to FKBP51 expression in CRC tissue sections. Boxes indicate interquartile ranges, whiskers indicate ranges of maximal and minimal values. FKBP51, FK506-binding protein 5; CRC colorectal cancer.

pattern suggested mitochondrial localization of the protein in these cells.

FKBP51 protein is downregulated in metastasized liver tissue samples. Specimens were evaluated by two independent observers (a biologist and a pathologist) who were blinded to the conditions. In addition, ImageJ software and the open source plug-in IHC Profiler developed by Varghese *et al* (18) were used to compare the visual human interpretation to that of the computer-aided vision. Fig. 5 shows a box-and-whisker plot illustrating the results obtained using IHC Profiler to compare the percentage of positive pixels (pixel intensity range, 61-120) in the tissue samples. This clearly demonstrates the downregulation of FKBP51 protein in malignant liver specimens vs. CRC tissue samples (7.5±4.3% in liver vs. 71.3±7.6% in CRC; $P<0.003$).

No differences in distribution or in staining intensity were detected between samples from male or female patients, or among patients of different ages (data not shown).

Discussion

In a previous screening for biomarkers involved in oxaliplatin toxicity, FKBP5 was the gene whose transcriptional expression level was most downregulated quantitatively (5). In the current study, IHC analysis of FKBP51 protein expression and localization allowed observation of strong staining in the nuclei of enterocytes in healthy colon, whereas in colonic adenocarcinoma cells, the staining was localized in nuclei and cytoplasm. However, lesions exhibited variable staining, ranging from tumor nests with malignant cells strongly expressing FKBP51, to the surrounding stroma cells and lesions where no positive signal could be detected (Fig. 1E and F).

The observation that the expression of FKBP51 in tumor and stromal cells is associated with an immature phenotype of the surrounding stromal fibroblasts and with an increased microvessel density, as well as augmented tumor-associated macrophage infiltration, suggests a role for this protein in the epithelial-to-mesenchymal transition (EMT) process in CRC (20).

Patients in the current study received oxaliplatin-based chemotherapy prior to resection of the metastases. IHC analyses allowed the observation of changes in FKBP51 expression levels and localization in malignant liver compared with CRC. While in healthy liver FKBP51 protein exhibited strong staining in the nuclei of hepatocytes, in healthy regions of metastatic liver, the nuclear signal was fainter. The observed alterations in the liver tissue surrounding the metastases could be related to hepatic sinusoidal injury elicited by oxaliplatin therapy (21).

In liver metastases, the signal appeared faint or absent, while in the inflammatory fibrous stroma, several cells exhibited a strong signal (Fig. 3E). These structural changes could be associated with the effect of chemotherapy on tumor cells rather than with intrinsic changes of transformation of cells. This phenomenon is further supported by the fact that a patient with a predominantly negative immunostaining signal had a tumor (metastasis) that was completely resistant to chemotherapy. Lung metastases exhibited a similar expression pattern to liver metastases, with weak staining in tumor cells and a strong signal in inflammatory and fibrous stromal cells surrounding the metastases. Whether this weaker level of expression in the metastatic cells is related to chemotherapy or to their cell biology is to be determined by further studies.

FKBP51 and its related protein FKBP52 are HSP90 co-chaperones that influence steroid hormone receptor activity. These two immunophilins share a similar structure but act divergently due to differences in the FK1 domain and the proline-rich loop (13). Fig. 6 illustrates their coordinated functions. Due to differences in the FK1 domain, repression of hormone binding occurs in the presence of FKBP51, and potentiation in the presence of FKBP52. In the absence of a ligand, certain steroid hormone receptors reside primarily in the cytoplasm, whereas others are nuclear. Regardless of their primary localization, these receptors are not confined to any particular cell compartment, and instead shuttle continuously between the cytoplasm and nucleus (13). It is assumed that these signaling molecules move across the cell by simple diffusion. However, the fact that proteins of the HSP90-FKBP52 complex co-immunoprecipitate with the glucocorticoid and mineralocorticoid receptors, and with the dynein-dynactin complex (22-24), suggests that these motor proteins could power the retrograde movement of these steroid receptors. FKBP51 is generally considered to be a negative regulator of receptor function. Evidence suggests that it displays tissue- and/or cell-type-specific effects on receptor signaling (13). Furthermore, it has been reported that colorectal tumors produce glucocorticoids; these glucocorticoids would have immunosuppressive functions, leading to an increase in tumor survival and growth (25).

In transformed cells, the current results indicated a decrease in the expression levels of FKBP51, as observed in leukocytes. FKBP52 was not selected for analysis as no change in this gene was detected in the transcriptome analysis (5) or in the preliminary immunolocalization experiments. Fig. 6, which is based on the model of Storer *et al* (13), illustrates how a decrease in FKBP51 expression brings about the predominance or easier driving of the steroid receptor-hormone-HSP90-p23 complex to

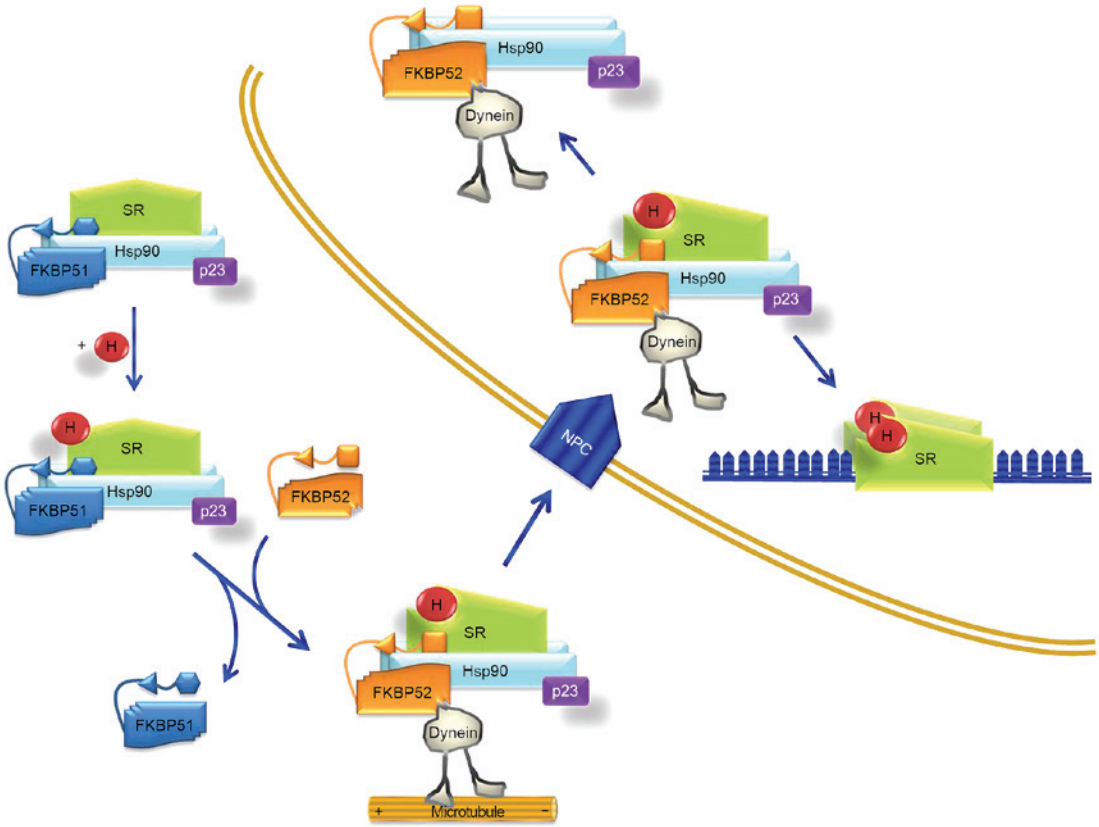

Figure 6. Model for FKBP51 interaction with steroid hormone receptor during translocation. Upon H binding, the SR heterocomplex exchanges FKBP51 for FKBP52, which is able to interact with dynein. The chaperone complex serves as a traction chain for the receptor through cytoskeletal tracts. The whole SR-chaperone complex translocates through the NPC. Receptor transformation is nucleoplasmic and facilitates binding of the steroid-activated receptor to promoter sites. Partially adapted from Storer *et al* (13). FKBP, FK506-binding protein; SR, steroid hormone receptor; H, steroid hormone; NPC, nuclear pore complex; Hsp90, heat shock protein 90.

the nucleus, making the transformed cell (at least after FOLFOX chemotherapy), somehow, more sensitive to steroid hormones. This fact needs to be further confirmed experimentally.

Baughman *et al* (26) reported in 1997 that FKBP51 is expressed in various tissues, but not in the colon, lung and spleen. In that study, the expression of FKBP51 was only analyzed by western blotting of protein lysate. However, in another study, in which different techniques were used (western blot, reverse transcription-polymerase chain reaction and IHC analyses), Mukaide *et al* (27) demonstrated that FKBP51 is expressed in normal epithelial cells and in adenocarcinoma cells in the human colon, and that there are no significant differences in the expression of FKBP51 between these cell types. Furthermore, the authors suggested that FKBP51 may suppress the proliferation of colorectal adenocarcinoma, possibly due to the suppression of function of the glucocorticoid receptors (27). The current findings only agree partially with these facts.

Previously, the RNA interference technique has been used to knock down the expression of FKBP5 in the A174 glioma cell line, revealing that FKBP5 expression aids in the regulation of glioma cell growth. By contrast, overexpression of FKBP5 markedly enhanced growth in this cell line (28). This fact agrees with the current results and explains a complementary effect of chemotherapy through FKBP pathways.

In summary, the present study supports the fundamental role of cell-by-cell IHC analysis in molecular data interpretation. The findings have demonstrated that the changes in FKBP51 gene expression elicited by FOLFOX chemotherapy in PWCs of CRC patients can be confirmed at the protein level in tissue samples of colon adenocarcinoma prior to chemotherapy, compared with tissue sections of metastasized liver resected after oxaliplatin-based chemotherapy. Furthermore, the results indicated that, in CRC tissue sections, the expression of FKBP51 in tumor and stroma cells is associated with the immature phenotype of stromal fibroblasts and with the EMT phenotype, suggesting a role for this protein in the EMT process in CRC. The expression of FKBP51 in neural cells of the Auerbach's and Meissner's plexus could explain the development of oxaliplatin-induced autonomic neuropathy (29).

Finally, the observation that only certain cells in the tumor-associated stroma express FKBP51 must be further investigated to assess the hypothesis of a potential role for this immunophilin as a stromal cell subtype marker (30-32).

Acknowledgements

The authors would like to thank Dr Sonja Kennington for English language supervision and critical reading of the manuscript. This study was supported by Health Research Fund (FIS) PI11/00114 and FIS PI12/00729 grants, Spain. The study was also supported partially by the Insular Council of Tenerife and MCT-FEDER 2003/2004 (Olympus FV1000), and by an Improving Biomedical Research in the

Canary Islands-7th Framework Program Research Potential (IMBRAIN-FP7-REGPOT)-2012-31637 grant.

References

1. Ferlay J, Shin HR, Bray F, Forman D, Mathers C and Parkin DM: Estimates of worldwide burden of cancer in 2008: GLOBOCAN 2008. Int J Cancer 127: 2893-2917, 2010.
2. Xu R, Zhou B, Fung PC and Li X: Recent advances in the treatment of colon cancer. Histol Histopathol 21: 867-872, 2006.
3. André T, Boni C, Mounedji-Boudiaf L, Navarro M, Tabernero J, Hickish T, Topham C, Zaninelli M, Clingan P, Bridgewater J, *et al*: Oxaliplatin, fluorouracil, and leucovorin as adjuvant treatment for colon cancer. N Engl J Med 350: 2343-2351, 2004.
4. Raymond E, Chaney SG, Taamma A and Cvitkovic E: Oxaliplatin: A review of preclinical and clinical studies. Ann Oncol 9: 1053-1071, 1998.
5. Morales M, Ávila J, González-Fernández R, Boronat L, Soriano ML and Martín-Vasallo P: Differential transcriptome profile of peripheral white cells to identify biomarkers involved in oxaliplatin induced neuropathy. J Pers Med 4: 282-296, 2014.
6. Erlejman AG, De Leo SA, Mazaira GI, Molinari AM, Camisay MF, Fontana V, Cox MB, Piwien-Pilipuk G and Galigniana MD: NF-kB transcriptional activity is modulated by FK506-binding proteins FKBP51 and FKBP52: A role for peptidyl-prolyl isomerase activity. J Biol Chem 289: 26263-26276, 2014.
7. Gallo LI, Lagadari M, Piwien-Pilipuk G and Galigniana MD: The 90-kDa heat-shock protein (Hsp90)-binding immunophilin FKBP51 is a mitochondrial protein that translocates to the nucleus to protect cells against oxidative stress. J Biol Chem 286: 30152-30160, 2011.
8. Li L, Lou Z and Wang L: The role of FKBP5 in cancer aetiology and chemoresistance. Br J Cancer 104: 19-23, 2011.
9. Pei H, Li L, Fridley BL, Jenkins GD, Kalari KR, Lingle W, Petersen G, Lou Z and Wang L: FKBP51 affects cancer cell response to chemotherapy by negatively regulating Akt. Cancer Cell 16: 259-266, 2009.
10. Romano S, D'Angelillo A, Pacelli R, Staibano S, De Luna E, Bisogni R, Eskelinen EL, Mascolo M, Cali G, Arra C and Romano MF: Role of FK506-binding protein 51 in the control of apoptosis of irradiated melanoma cells. Cell Death Differ 17: 145-157, 2010.
11. Romano S, Staibano S, Greco A, Brunetti A, Nappo G, Ilardi G, Martinelli R, Sorrentino A, Di Pace A, Mascolo M, *et al*: FK506 binding protein 51 positively regulates melanoma stemness and metastatic potential. Cell Death Dis 4: e578, 2013.
12. Romano S, D'Angelillo A, D'Arrigo P, Staibano S, Greco A, Brunetti A, Scalvenzi M, Bisogni R, Scala I and Romano MF: FKBP51 increases the tumour-promoter potential of TGF-beta. Clin Transl Med 3: 1, 2014.
13. Storer CL, Dickey CA, Galigniana MD, Rein T and Cox MB: FKBP51 and FKBP52 in signaling and disease. Trends Endocrinol Metab 22: 481-490, 2011.
14. Hubler TR, Denny WB, Valentine DL, Cheung-Flynn J, Smith DF and Scammell JG: The FK506-binding immunophilin FKBP51 is transcriptionally regulated by progestin and attenuates progestin responsiveness. Endocrinology 144: 2380-2387, 2003.
15. Jinwal UK, Koren J III, Borysov SI, Schmid AB, Abisambra JF, Blair LJ, Johnson AG, Jones JR, Shults CL, O'Leary JC III, *et al*: The Hsp90 cochaperone, FKBP51, increases Tau stability and polymerizes microtubules. J Neurosci 30: 591-599, 2010.
16. Chambraud B, Sardin E, Giustiniani J, Dounane O, Schumacher M, Goedert M and Baulieu EE: A role for FKBP52 in Tau protein function. Proc Natl Acad Sci USA 107: 2658-2663, 2010.
17. Li L, Fridley B, Kalari K, Jenkins G, Batzler A, Safgren S, Hildebrandt M, Ames M, Schaid D and Wang L: Gemcitabine and cytosine arabinoside cytotoxicity: Association with lymphoblastoid cell expression. Cancer Res 68: 7050-7058, 2008.
18. Varghese F, Bukhari AB, Malhotra R and De A: IHC Profiler: An open source plugin for the quantitative evaluation and automated scoring of immunohistochemistry images of human tissue samples. PLoS One 9: e96801, 2014.
19. Bleau AM, Agliano A, Larzabal L, de Aberasturi AL and Calvo A: Metastatic dormancy: A complex network between cancer stem cells and their microenvironment. Histol Histopathol 29: 1499-1510, 2014.
20. Ha SY, Yeo SY, Xuan Y and Kim SH: The prognostic significance of cancer-associated fibroblasts in esophageal squamous cell carcinoma. PLoS One 9: e99955, 2014.
21. Nalbantoglu IL, Tan BR Jr, Linehan DC, Gao F and Brunt EM: Histological features and severity of oxaliplatin-induced liver injury and clinical associations. J Dig Dis 15: 553-560, 2014.
22. Davies TH, Ning YM and Sánchez ER: A new first step in activation of steroid receptors: Hormone-induced switching of FKBP51 and FKBP52 immunophilins. J Biol Chem 277: 4597-4600, 2002.
23. Galigniana MD, Radanyi C, Renoir JM, Housley PR and Pratt WB: Evidence that the peptidylprolyl isomerase domain of the hsp90-binding immunophilin FKBP52 is involved in both dynein interaction and glucocorticoid receptor movement to the nucleus. J Biol Chem 276: 14884-14889, 2001.
24. Wochnik GM, Rüegg J, Abel GA, Schmidt U, Holsboer F and Rein T: FK506-binding proteins 51 and 52 differentially regulate dynein interaction and nuclear translocation of the glucocorticoid receptor in mammalian cells. J Biol Chem 280: 4609-4616, 2005.
25. Sidler D, Renzulli P, Schnoz C, Berger B, Schneider-Jakob S, Flück C, Inderbitzin D, Corazza N, Candinas D and Brunner T: Colon cancer cells produce immunoregulatory glucocorticoids. Oncogene 30: 2411-2419, 2011.
26. Baughman G, Wiederrecht GJ, Chang F, Martin MM and Bourgeois S: Tissue distribution and abundance of human FKBP51, and FK506-binding protein that can mediate calcineurin inhibition. Biochem Biophys Res Commun 232: 437-443, 1997.
27. Mukaide H, Adachi Y, Taketani S, Iwasaki M, Koike-Kiriyama N, Shigematsu A, Shi M, Yanai S, Yoshioka K, Kamiyama Y and Ikehara S: FKBP51 expressed by both normal epithelial cells and adenocarcinoma of colon suppresses proliferation of colorectal adenocarcinoma. Cancer Invest 26: 385-390, 2008.
28. Jiang W, Cazacu S, Xiang C, Zenklusen JC, Fine HA, Berens M, Armstrong B, Brodie C and Mikkelsen T: FK506 binding protein mediates glioma cell growth and sensitivity to rapamycin treatment by regulating NF-kappaB signaling pathway. Neoplasia 10: 235-243, 2008.
29. Vandamme M, Pauwels W and Bleecker JD: A case of delayed oxaliplatin-induced pseudo-obstruction: An atypical presentation of oxaliplatin neurotoxicity. Acta Clin Belg 70: 207-210, 2015.
30. Calon A, Lonardo E, Berenguer-Llergo A, Espinet E, Hernando-Momblona X, Iglesias M, Sevillano M, Palomo-Ponce S, Tauriello DV, Byrom D, *et al*: Stromal gene expression defines poor-prognosis subtypes in colorectal cancer. Nat Genet 10: 320-329, 2015.
31. Kuroda N, Nakayama H, Miyazaki E, Toi M, Hiroi M and Enzan H: The distribution of CD34-positive stromal cells and myofibroblasts in colorectal carcinoid tumors. Histol Histopathol 20: 27-33, 2005.
32. Sugimoto H, Mundel TM, Kieran MW and Kalluri R: Identification of fibroblast heterogeneity in the tumor microenvironment. Cancer Biol Ther 5: 1640-1646, 2006.

APPENDIX C
ARTICLE 3

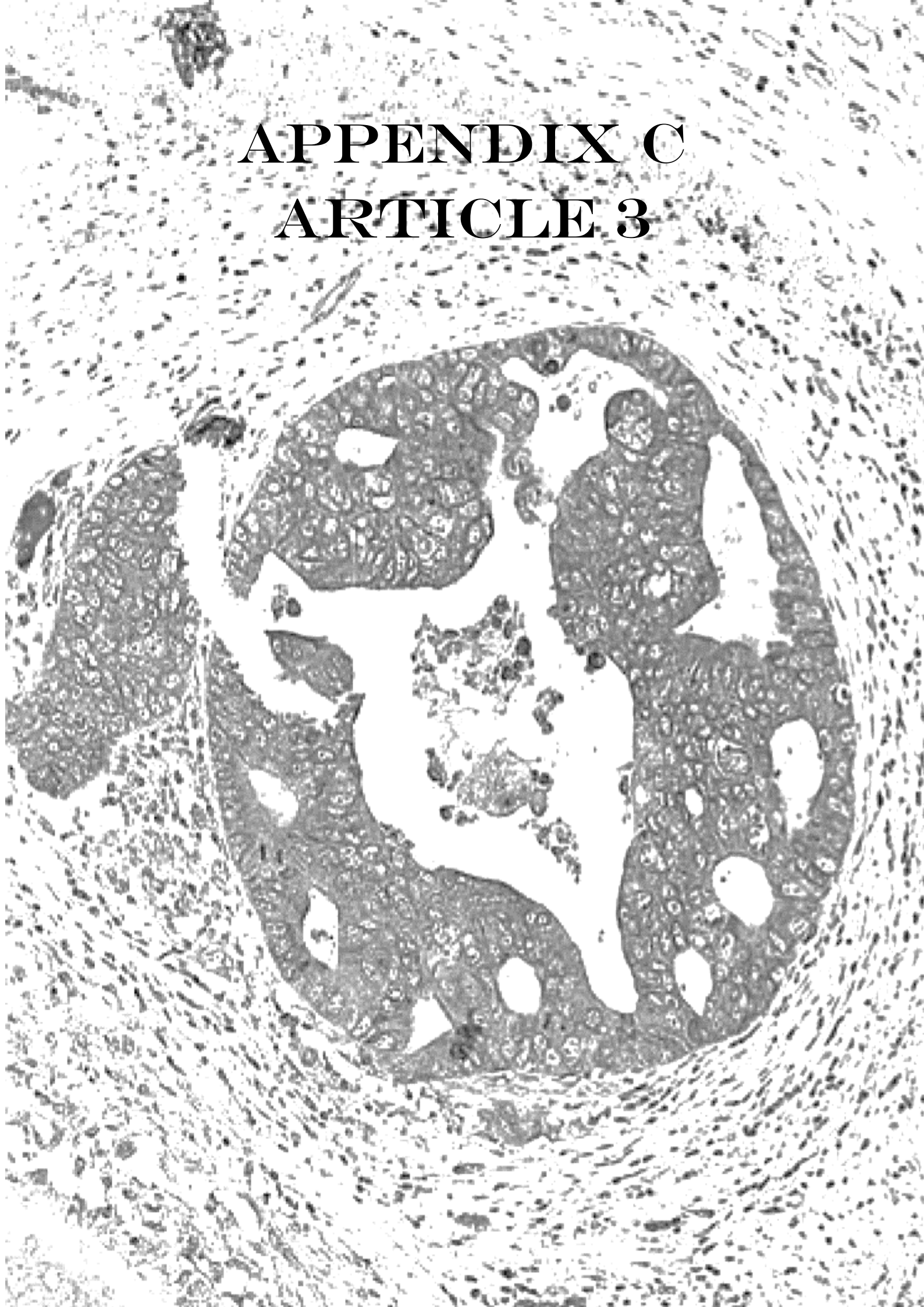

International Journal of
Molecular Sciences

MDPI

Article

Commitment of Scaffold Proteins in the Onco-Biology of Human Colorectal Cancer and Liver Metastases after Oxaliplatin-Based Chemotherapy

Deborah Rotoli [1,2], Manuel Morales [3,4], Julio Ávila [1], María del Carmen Maeso [5], María del Pino García [6], Ali Mobasheri [7,8] and Pablo Martín-Vasallo [1,*]

1 Laboratorio de Biología del Desarrollo, UD de Bioquímica y Biología Molecular and Centro de Investigaciones Biomédicas de Canarias (CIBICAN), Universidad de La Laguna, Av. Astrofísico Sánchez s/n., 38206 La Laguna, Spain; deborah_rotoli@yahoo.it (D.R.); javila@ull.es (J.Á.)
2 CNR—National Research Council, Institute of Endocrinology and Experimental Oncology (IEOS), Via Sergio Pansini 5, 80131 Naples, Italy
3 Service of Medical Oncology, University Hospital Nuestra Señora de Candelaria, 38010 Santa Cruz de Tenerife, Spain; mmoraleg@ull.es
4 Service of Medical Oncology, Hospiten®Hospitals, 38001 Santa Cruz de Tenerife, Spain
5 Service of Pathology, University Hospital Nuestra Señora de Candelaria, 38010 Santa Cruz de Tenerife, Spain; mmaefor@gmail.com
6 Department of Pathology, Hospiten®Hospitals, 38001 Santa Cruz de Tenerife, Spain; mariadelpino.garcia@hospiten.com
7 School of Veterinary Medicine, Faculty of Health and Medical Sciences, University of Surrey, GU2 7XH Guildford, UK; a.mobasheri@surrey.ac.uk
8 Center of Excellence in Genomic Medicine Research (CEGMR), King Fahd Medical Research Center (KFMRC), Faculty of Applied Medical Sciences, King AbdulAziz University, 21589 Jeddah, Saudi Arabia
* Correspondence: pmartin@ull.es; Tel.: +34-922-318-358; Fax: +34-922-318-354

Academic Editor: Peter J. K. Kuppen
Received: 22 February 2017; Accepted: 19 April 2017; Published: 22 April 2017

Abstract: Scaffold proteins play pivotal roles in the regulation of signaling pathways, integrating external and internal stimuli to various cellular outputs. We report the pattern of cellular and subcellular expression of scaffoldins angiomotin-like 2 (AmotL2), FK506 binding protein 5 (FKBP51) and IQ motif containing GTPase-activating protein 1 (IQGAP1) in colorectal cancer (CRC) and metastases in liver resected after oxaliplatin-based chemotherapy (CT). Positive immunostaining for the three scaffoldins was found in most cells in healthy colon, tumor, healthy liver and metastasized liver. The patterns of expression of AmotL2, FKBP51 and IQGAP1 show the greatest variability in immune system cells and neurons and glia cells and the least in blood vessel cells. The simultaneous subcellular localization in tumor cells and other cell types within the tumor suggest an involvement of these three scaffoldins in cancer biology, including a role in Epithelial Mesenchymal Transition. The display in differential localization and quantitative expression of AmotL2, FKBP51, and IQGAP1 could be used as biomarkers for more accurate tumor staging and as potential targets for anti-cancer therapeutics by blocking or slowing down their interconnecting functions. Tough further research needs to be done in order to improve these assessments.

Keywords: colorectal cancer; scaffold proteins; AmotL2; FKBP51; IQGAP1; metastasized liver; FOLFOX; oxaliplatin; pericytes; telocytes

1. Introduction

Scaffold proteins bring together and facilitate macromolecular interactions between multiple modular partners that are committed to a specific subcellular task, usually forming a stable complex in

a peculiar subcellular localization. These superstructures integrate functions such as enzymatic pathways, cell motility, protein sorting, signaling, stabilization, plasma membrane targeting of membrane proteins, recycling and cell polarity; in fact, they are involved in cell fate, tumorigenesis, migration, tumor progression and angiogenesis [1–3].

Colorectal cancer (CRC) is the fourth leading cause of cancer-associated mortality, and >95% of CRCs are adenocarcinomas [4,5]. FOLFOX (FOL—Folinic acid, leucovorin, F—Fluorouracil, 5-FU) or CAPOX (CA—capecitabine)-chemotherapy of CRC includes oxaliplatin (OX) [6] and is administered in the treatment of metastatic colorectal cancers in the neo-adjuvant, adjuvant and palliative setting, with an important percentage of unwanted side effects as peripheral neuropathy [7] and sinusoidal obstruction syndrome [8]. In the search for early markers of oxaliplatin-related toxicity, we studied the differential transcriptomics in peripheral white cells (PWCs) from patients receiving oxaliplatin-based chemotherapy (CT) and found 502 genes significantly up- or down-regulated as a result of CT [9]. Among those genes, some encoding scaffold proteins presented significant changes in their expression levels.

In our screening [9], after three cycles of oxaliplatin-based CT, the expression levels of the genes in PWCs varied as follows: *AmotL2* 3.5 times higher, *FKBP51* 2.76 times lower and *IQGAP1* with no detected pre-CT expression level to 229.5 relative to actin expression level [9].

AmotL2 (angiomotin-like 2) is a member of the angiomotin protein family responsible for maintaining cell-cell interactions to keep asymmetrical apical-basal polarity, avoiding endothelial detachment and promoting vascular tube formation. Human AmotL2 encodes two isoforms of a molecular mass of 100 and 60 kDa [10]. Most human cancers have an epithelial origin and the assessment of malignancy is based on the loss of apicalbasal polarity of the epithelial organization (epithelial mesenchymal transition (EMT)); however, whether this is a cause or consequence of tumor progression has yet to be established [11]. Loss of polarity, EMT and angiogenesis are crucial in CRC.

The immunophilin protein FKBP51 (FK506 binding protein 5) is a member of the peptidyl-prolyl isomerases (PPIs) superfamily [12]. This superfamily includes three distinct classes: the FK506-binding proteins (FKBPs) (e.g., FKBP12, FKBP51, and FKBP52), the CyclosporinA-binding proteins and the parvulin-like PPIs [13]. PPIs catalyze the *cis-trans* conversion of peptidylprolyl imide bonds in target proteins [14]. FKBP51 protein is localized in mitochondria, cytoplasm and nucleus [14–16]; is involved in the regulation of a variety of signaling pathways; and is considered as a molecular integrant of the adaptation process [17]. In many different tumors, altered expression levels have been described [18,19]. Through its influence on steroid receptor maturation, and the regulation of PKA [20], NF-κB [21], Akt [22] and transforming growth factor β (TGF β) [23] signaling pathways, FKBP51 plays an important role in tumorigenesis and response to anti-neoplastic therapy [24,25].

IQGAP1 (IQ motif containing GTPase-activating protein 1) is a multidomain protein ubiquitously expressed and the most versatile of the three here studied [26]. IQGAP1 modulates several cellular functions, i.e., cell cycle, cell morphology, motility, by linking elements of the cytoskeleton to cell adhesion and other signaling molecules [27,28], facilitating the space-time organization and the coordinated activation of structural and signaling molecules [29,30]. Because of this association with molecular partners, IQGAP1 accumulates in the plasma membrane at the invasive front in several cancer types [31–35].

In Figure 1, String analysis [36] shows experimental and databases evidences of known functional interactions among AmotL2, FKBP51 and IQGAP1 in several physiological and pathological situations through Yap1, Src and HSP90. The oncogene Src and the chaperone HSP90 are well-known genes and proteins. In zebrafish embryo, AmotL2 regulates the translocation of phosphorylated Src to peripheral cell–matrix adhesion sites [37], also required for proper architecture of actin filaments. Transcriptional coactivator YAP1 (Yes-associated protein 1) (Available online: http://www.uniprot.org/uniprot/P46937) can act both as a coactivator and a corepressor and is the downstream regulatory target in the Hippo signaling pathway responsible for organ size control and tumor suppression by restricting proliferation and promoting apoptosis [38,39]. It also controls cell proliferation in

response to cell contact, where the TEAD family are required for YAP-dependent gene expression [40]. The TEAD family of transcriptional enhancer factors, also known as TEA domain family, is also required for YAP-induced cell growth, oncogenic transformation, and epithelial-mesenchymal transition induction [41]. Some TEAD members are up-regulated in several types of cancer [42].

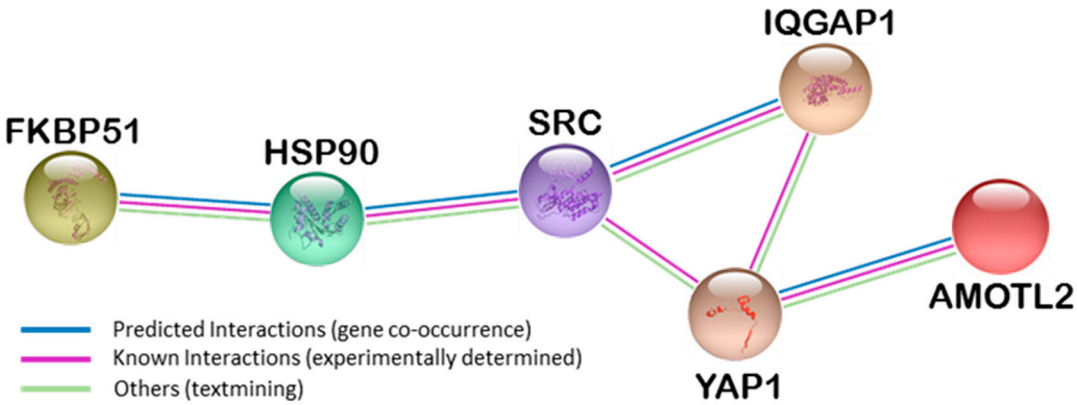

Figure 1. String analysis showing interactions among AmotL2, FKBP51 and IQGAP1 proteins. FKBP51 (FK506 binding protein 5); HSP90 (heat-shock protein 90); SRC (proto-oncogene tyrosine-protein kinase); IQGAP1 (IQ-motif containing GTPase-activating protein 1); YAP1 (yes associated protein); AmotL2 (angiomotin-like 2).

Here, we report on the cellular and sub-cellular localization and dynamics of three scaffold proteins, AmotL2, FKBP51 and IQGAP1 in colorectal primary tumors and their metastases and in apparently healthy areas of metastasized liver. The use of real human tumor samples, with its wide heterogeneity of cells, offers a more realistic and more dynamic insight into the onco-biology process and is superior to the use of primary cancer cells lines. Primary cancer cell lines studied in monolayer culture simply cannot replicate the tumor environment and the intricate complexities of the oncogenic process. Based on our findings, the published literature and information available in publicly accessible databases, we present a model of interactions between the proteins studied, a model that incorporates spatiotemporal interplay between the structural and signaling molecules involved in CRC tumorigenesis.

2. Results

2.1. AmotL2 in Healthy Colon and in CRC Tissue Samples

In healthy colon, AmotL2 specific staining of high intensity was observed in blood vessel cells (Figure 2A–C; v = vessels) and in stroma cells of the connective tissue surrounding Lieberkühn Crypts (LC) (Figure 2A). In the crypts, remarkable immunostaining for AmotL2 was present in epithelial cells (nucleus, cytoplasm, and tight junctions) with higher strength in the crypts facing the muscularis mucosae (mm) (Figure 2A). Positive AmotL2 labeling was also visible in nuclei of smooth muscle cells of the muscularis propria (mp) (Figure 2B) and in cells of submucosal glands (submg) (Figure 2C). Specific immunostaining for AmotL2 was also present in the cytoplasm of some nerve cell bodies of the myenteric plexus (MyP) as well as in some nerve fibers (Figure 2D,D').

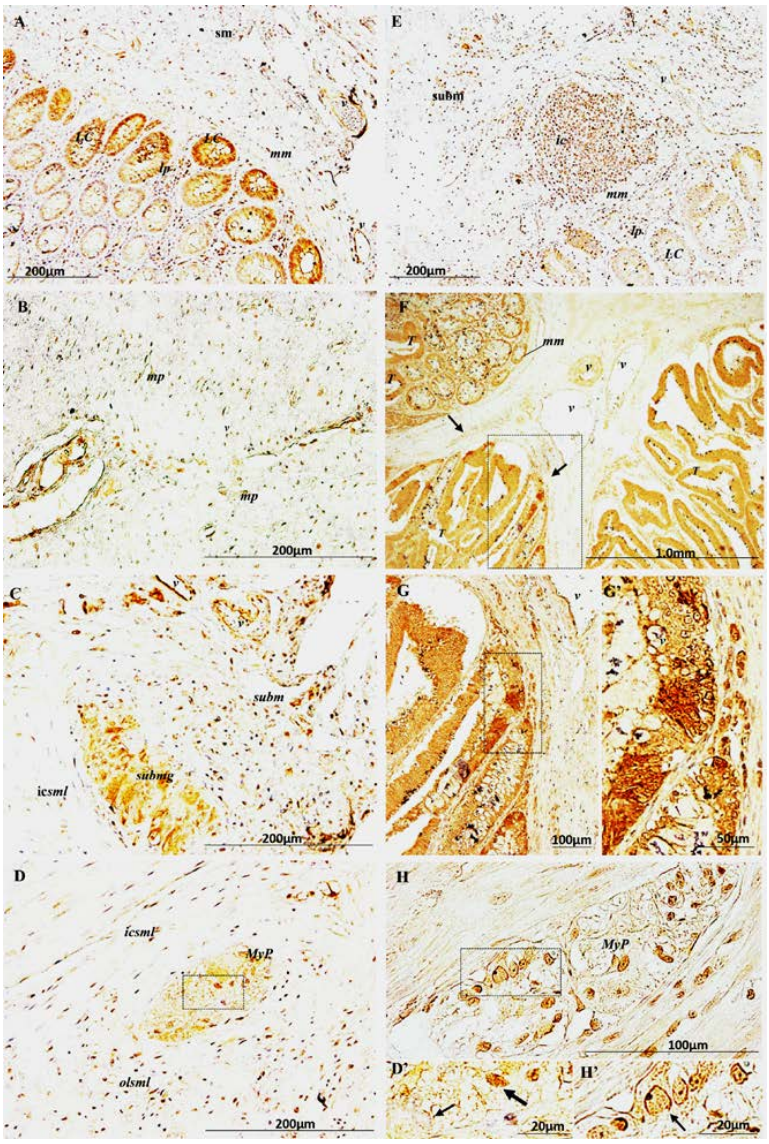

Figure 2. Immunolocalization of AmotL2 in: healthy colon (**A**–**D′**); and colorectal cancer (CRC) (**E**–**H′**); Healthy colon: (**A**) High intensity staining in nucleus, cytoplasm and tight junctions of epithelial cells of crypts facing the muscularis mucosae and stromal cells of lamina propria and submucosa; (**B**) Strong AmotL2^{+} labeling in nuclei of smooth muscle cells of the muscularis propria and in cells of the submucosal gland (**C**); (**D**,**D′**) AmotL2^{+} cytoplasmic expression in nerve cell bodies (thick arrow in **D′**) of myenteric plexus (**MyP**); some others are negative (thin arrow in **D′**); Immunopositive nerve fibers. CRC: (**E**) Faint immunostaining in colon epithelial cells and stronger in stromal and immune cells in the connective tissue surrounding epithelial crypts and in the submucosa; (**F**) Tumor tissue infiltrating intestinal epithelium; uniform AmotL2 staining in Lieberkühn Crypts. The intensity in the crypts facing the muscularis mucosae observed in healthy colon now is much weaker, while tumor cells exhibit a strong immunopositive staining in cytoplasm and nuclear membrane, becoming stronger at the invasive front and in budding cells (arrows); (**G**,**G′**) Magnifications of the boxed areas in (**F**,**G**), respectively; (**H**) Positive staining in neural cells of the myenteric plexus, faint in the cytoplasm and stronger in plasma membrane and nucleus (arrow in **H′**); (**D′**,**H′**) are magnifications of the boxed areas in (**D**,**H**) respectively. Strong AmotL2 immunostaining in blood vessel cells, both in healthy and tumor tissues (v). LC = Lieberkühn Crypts; lp = lamina propria; v = vessels; mm = muscularis mucosa; sbm = submucosal muscularis; sbmg = submucosal gland; ic = immune cells; mp = muscularis propria; icsml = inner circular smooth muscle layer; olsml = outer longitudinal smooth muscle layer; T = tumor lesion; MyP = myenteric plexus.

In unaffected areas of the intestinal epithelium surrounding CRC tissue samples, AmotL2 immunopositive staining was present in Lieberkühn Crypts at a lower intensity compared to healthy tissue (Figure 2E). Immune cells forming a large inflammation cluster in the submucosa showed strong labeling (Figure 2, ic = immune cells) as well as cells in the connective tissue surrounding the crypts and in endothelial cells (Figure 2, v). In tumor affected areas of the intestinal epithelium, Lieberkühn Crypts exhibited a stronger grade of AmotL2 specific staining (Figure 2F); however, the higher grade of expression in the crypts facing the muscularis mucosae observed in healthy colon was no longer visible. Immunostaining was present in tumor cells (cytoplasm and nuclear envelope) at a higher intensity in budding cells of the invasive front (Figure 2F–G′). Nerve fibers and the cytoplasm of all nerve cell bodies present in myenteric plexuses in CRC samples showed a fainter staining compared to what observed in healthy tissue, while plasma membrane and nucleus exhibited a stronger labeling (Figure 2H,H′).

2.2. AmotL2 in Healthy Liver and in CRC Metastasized Liver Tissue Samples

In healthy liver, the peri-portal hepatocytes, functionally identified as zone 1 where the oxygenated blood from hepatic arteries enters, exhibited a positive AmotL2 cytoplasmic staining that increased along the way to the central vein, functionally identified as zone 3, where blood flow is less oxygenated (Figure S1A–C). This grading of staining was not further observed in apparently healthy areas of metastasized liver samples (Figure S1E,G). Moreover, in the connective tissue surrounding portal tracts in healthy liver, except for a few lymphocytes, no significant population of any inflammatory cell was observed (Figure S1D), while the connective tissue of portal tracts of CRC metastasized liver tissue appeared highly infiltrated by AmotL2$^+$ immune cells, regardless of the presence or absence of malignant cells (Figure 3A,A_1 and Figure S1H). AmotL2$^+$ immune cells were also present in the connective tissue surrounding metastasis (Figure 3, asterisks). Metastasis showed high levels of AmotL2 staining in cytoplasm (Figure 3A–B_2); in addition, in malignant budding cells the nuclei were also positive (Figure 3B_2, arrows). In tumor associated blood vessels (v), high levels of AmotL2 specific labeling were observed in nucleus and cytoplasm of endothelial cells (Figure 3B_2,B_3).

2.3. AmotL2 in Blood Vessels

In blood vessels of healthy tissues and in tumor associated blood vessels (v), high levels of AmotL2 specific labeling was observed in nucleus and cytoplasm of endothelial cells (Figure 2, v; Figure 3C,D, v; Figure 4A–G, white arrows), pericytes (Figure S1D, arrow; Figure 4H–M, white arrows) and macrophages (Figure 4E–G, yellow arrows; Figure 4H–M, white arrowhead), identified for their morphology, localization and CD31$^+$ expression (Figure 4E–G, yellow arrows; Figure 4H–M, arrowhead). Figure 4N–Q shows images of double labeling of AmotL2 and CD31 (Figure 4N,O) or CD34 (Figure 4P,Q) in serial sections from the same tissue sample, where cells co-expressing the tree proteins can be observed in perivascular areas (arrows).

2.4. FKBP51

In healthy colon and in apparently healthy areas of CRC tissue sections, an intense positive FKBP51 nuclear staining in enterocytes of intestinal glands and in cells of the lamina propria was observed (Figure 5A). In CRC tissue sections, FKBP51 protein was localized in the cytoplasm and/or nucleus of tumor cells as well as in inflammatory and fibrous stromal cells surrounding the lesions (Figure 5B). Intensity of labeling varies with areas within the section, from a variable positive immunostaining in tumor cells to no staining detected in others.

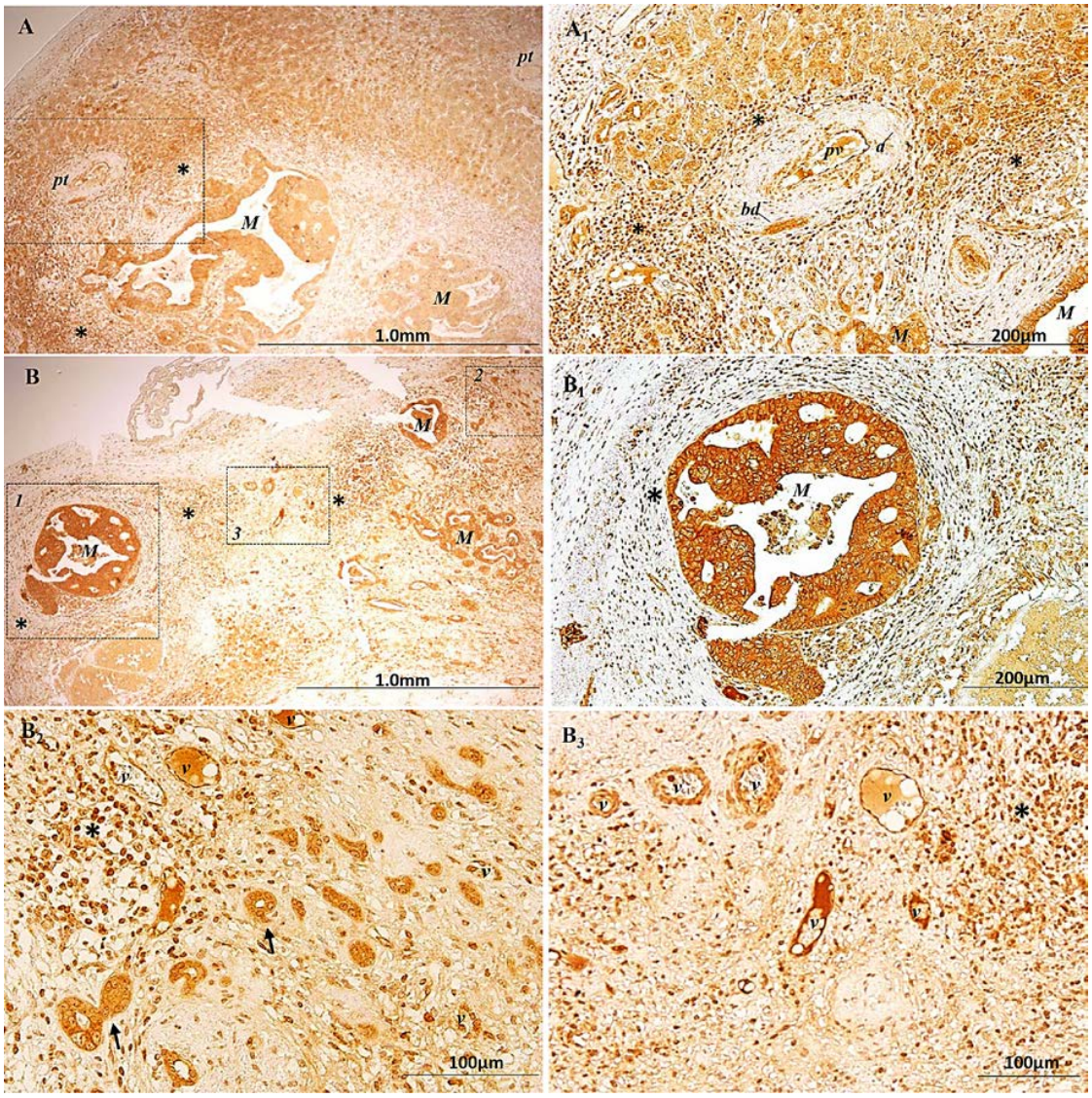

Figure 3. Immunolocalization of AmotL2 in CRC metastasized liver tissue samples. (**A**,**B**) Low magnification of AmotL2$^+$ staining in: hepatocytes surrounding portal tracts (**A**); and malignant cells (**A**,**B**). (**A$_1$**) Higher magnification of the inset in **A**; (**B$_1$**) Higher magnification of the inset 1 in **B**; Asterisks identify AmotL2$^+$ immune cells in the connective tissue surrounding metastasis and portal tracts. (**B$_2$**,**B$_3$**) Higher magnifications of the insets 2 and 3, respectively, showing the positive AmotL2 staining in nuclei of malignant budding cells (arrows in **B$_2$**) and in blood vessel cells (v in **B$_2$**,**B$_3$**). pt = portal tract; cv = central vein; a = artery; bd = bile duct; M = metastasis; * = clusters of Amotl2$^+$ immune cells.

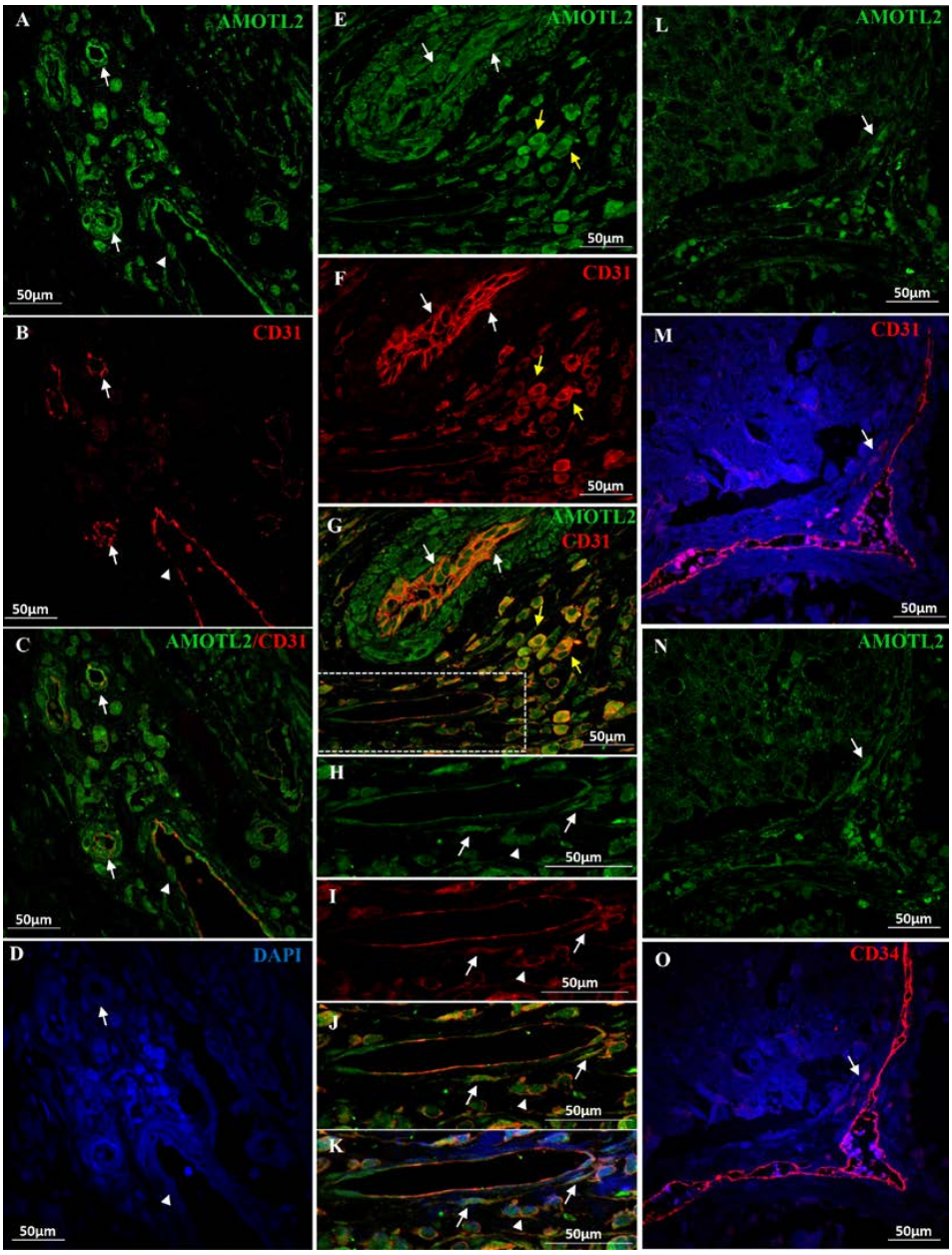

Figure 4. Double immunofluorescent staining of AmotL2 protein (green), the pan-macrophage and endothelial/pericyte marker CD31 (red) and the endothelial/telocyte marker CD34 in human CRC tissue sections. Cellularity is assessed with DAPI. (**A**–**D**) Blood cells of tumor associated vessels and micro-vessels (arrows) exhibit intense: AmotL2 (**A**); and CD31 (**B**) positive staining; both proteins co-localize along the vessel walls occasionally exhibiting a complementary pattern (**C**, merge). Arrowhead points to a AmotL2^{+} cell crossing the fenestrated endothelium; (**E**–**G**) Positive AmotL2/CD31staining is observed in endothelial cells (white arrows) and in macrophage-like cells surrounding the vessels (yellow arrows); (**H**–**M**) Higher magnifications of the boxed area in G showing the presence of AmotL2/CD31 positive pericytes (arrows) surrounding the blood vessel endothelium. Arrowheads point to AmotL2^{+}/CD31^{+} macrophages; (**H**) AmotL2 (green); (**I**) CD31 (red); (**L**) AmotL2/CD31 merged images; and (**M**) AmotL2/CD31/DAPI merged images; (**N**–**Q**) Representative images of double labeling of: AmotL2 (green) and CD31 (red) (**N**,**O**); or AmotL2 (green) and CD34 (red) (**P**,**Q**) in serial sections from the same tissue sample, where cells co-expressing the AmotL2/CD31/CD34 proteins can be observed in perivascular areas (arrows).

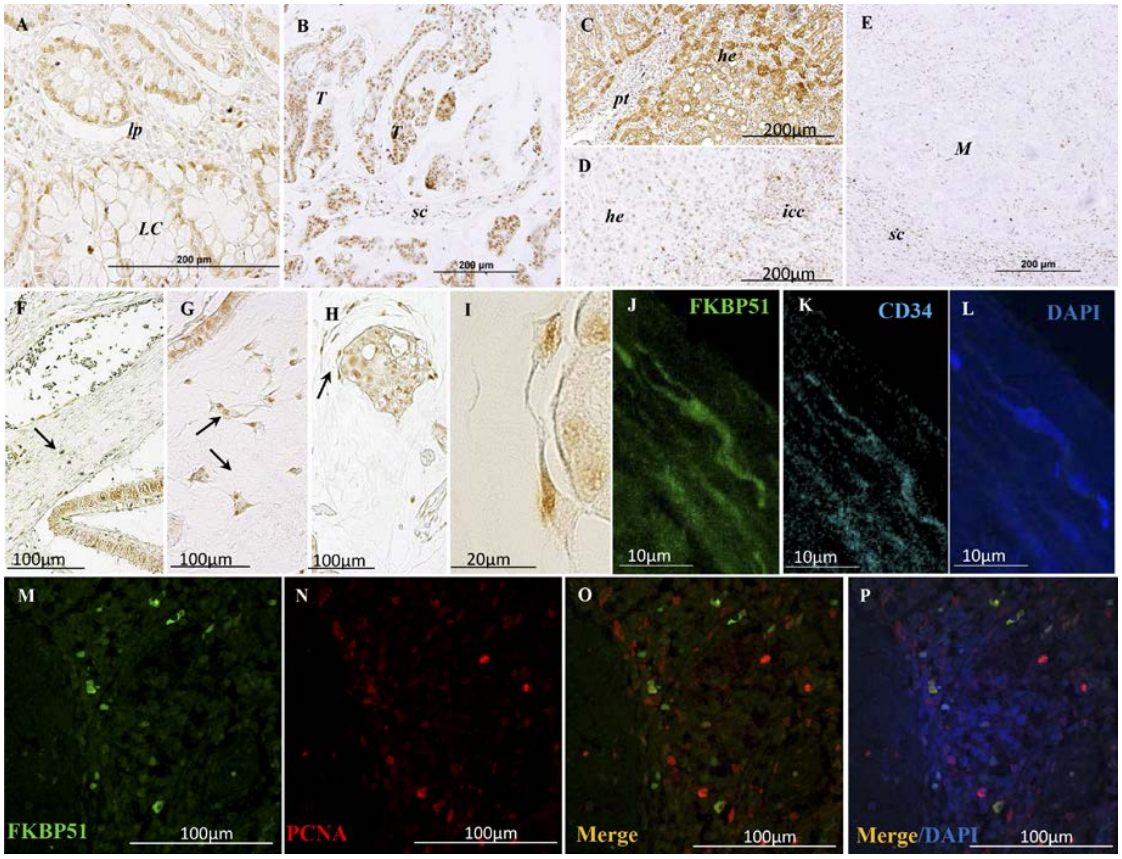

Figure 5. FKBP51 immunolocalization in paraffin-embedded tissue sections. (**A**) Staining is present in enterocytes (nucleus and cytoplasm) and in cells of the lamina propria in healthy colon and in unaffected areas of CRC tissue samples; (**B**) Variable positive immunostaining in nucleus and cytoplasm of CRC. Positive staining in stroma cells surrounding the lesions (sc); (**C**) Healthy liver; and (**D**) metastasized liver. Variable immunostaining in hepatocytes of both healthy liver and pathological tissue, ranging from high (**C**) to absent. In metastasized liver (**D**); in areas with high level of infiltrating immune cells (iic), cytoplasmic staining of hepatocytes is not detected, while immunostaining is localized in the nucleus; (**E**) In liver metastases, the immunostaining is faint or absent. Several stromal and inflammatory cells are FKBP51$^+$. Arrow in (**F**) points to a FKBP51$^+$ fibroblast showing an immature phenotype. Arrows in (**G**) point to FKBP51$^+$ telocyte-like cells with typical triangular cell bodies and 2 to 5 telopodes, interconnected forming a network; (**H**) CRC tumor nest enveloped by several telocyte-like FKBP51$^+$ cells (arrow); (**I**) Higher magnification of the cells pointed in (**H**); note the connection between telocyte-like cell and tumor nest; (**J**–**L**) Immunofluorescent colocalization of: FKBP51 (**J**, green); and CD34 (**K**, cyan), used as a telocyte marker. (**M**–**P**) CRC tissue section double immunostained with: FKBP51 (**M**, green); and PCNA (**N**, red); (**O**) FKBP51/CD34 merge; and (**P**) FKBP51/CD34/DAPI.

In healthy liver and in unaffected areas of metastasized liver, some areas showed intense immunostaining (Figure 5C) and other well delimited a weak or absent immunostaining for FKBP51. Interestingly in high inflammatory infiltration areas of metastasized tissue sections, the cytoplasmic staining of hepatocytes was no further observed, while the protein was localized in the nucleus (Figure 5D). In metastases, the immunostaining was faint or absent, while in the inflammatory fibrous stroma several cells displayed a strong immunostaining (Figure 5E).

The presence of FKBP51 in tumor and stroma cells has been associated with the immature phenotype of stromal fibroblasts and with the EMT phenotype, suggesting a role for this protein in the EMT process [16]. Further observations allowed us to identify telocyte-like FKBP51$^+$ cells

located in close proximity to tumor lesions and often forming networks (Figure 5G–I), characterized by triangular or spindle body and 2–5 long, slender cytoplasmic telopodes (Figure 5G–L). Double immunofluorescent experiments using CD34 as a telocyte marker and anti-FKBP51 antibodies showed co-staining images (Figure 4J–L).

To evaluate a possible role of FKBP51 over the proliferative activity of tumor cells, the proliferation marker PCNA [43] was used in double immunofluorescence experiments on formalin-fixed, paraffin-embedded CRC samples. In several malignant cells forming tumor nests, FKBP51 and PCNA protein exhibited partial colocalization, also a few stromal cells co-expressed both. The distribution of intranuclear PCNA and FKBP51 surrounding the outer membrane of the nucleus suggests that these cells were in the early S phase (Figure 5M–P).

2.5. IQGAP1

IQGAP1$^+$ immunostaining was observed in cytoplasm, nuclear envelope, and apical and lateral membrane of normal epithelial cells (Figure 6A). In tumor lesions, CRC cells exhibited a heterogeneous staining, with clusters of IQGAP1 negative cells (arrows in Figure 5B) mixed with IQGAP1$^+$ cells where the protein was localized in cytoplasm, lateral membrane, nuclear envelope and/or nucleus. High levels of labeling were also observed at the invasive front of the lesion (Figure 6C′). In many lesions, a strong apical IQGAP1$^+$ immunostaining was present (Figure 6C, arrow). Hepatocytes in healthy liver and in apparently healthy areas of CRC metastasized liver (Figure 6D,E, respectively) exhibited a heterogeneous positive IQGAP1 staining in cytoplasm, nuclear envelope and/or nucleus. Assuming the role of IQGAP1 protein in the regulation of the cytoskeleton functions; double immunofluorescent experiments were performed to co-localize IQGAP1 and β-tubulin proteins in tissue specimens of CRC-affected patients (Figure 6F–M). As can be observed in Figure 6F–M, in certain areas of tumor lesions and metastasis, the co-localization of IQGAP1 and β-tubulin was lost (Figure 6J–M, arrows; Figure S2A–H).

To further characterize the localization and expression of IQGAP1 protein, we performed double immunofluorescent staining of IQGAP1 protein and the endothelial/telocyte marker CD34 or the endothelial/pericyte/macrophage marker CD31. We identified CD34$^+$ telocytes (Figure 6N–Q and Figure S2I–P) and CD31$^+$ stromal cells co-expressing IQGAP1 (Figure 6R–U, arrows).

Table 1 summarizes expression levels of AmotL2, FKBP51 and IQGAP1 proteins in different cells of colon and liver from healthy individuals, CRC and metastasized liver after CT. Adjuvant treatment with FOLFOX-chemotherapy was as follows: Day 1, oxaliplatin 100 mg/m^2 intravenous (i.v.) over 2 h and leucovorin calcium 400 mg/m^2 i.v. over 2 h; followed by 5-fluorouracil 400 mg/m^2 i.v. bolus and by 5-fluorouracil 2400 mg/m^2 i.v. over 46 h, every 14 days. All patients received the chemotherapy after the resection of the primary tumor. Thus, the primaries were chemotherapy naïve, while the liver metastases were chemotherapy-treated. Fifteen (27.8%) patients presented liver metastasis after CT. Curative resections of liver metastasis were performed followed by adjuvant FOLFOX-CT. The average age of patients was 59 years old (range 35–78), with 29 (54%) males and 25 (46%) females. Eight patients (15%) were stage IV and underwent palliative surgery. The other patients, T3–T4, N1–N2 (85%) were stages partial response upon RECIST (Response Evaluation Criteria In Solid Tumors) criteria. The survival is 74% (40 patients), with a follow up of six years. Localization of tumors varied from cecum (4), ascending (13), transverse (8) colon, both flexures (7), sigmoid (16) colon and sigmo-rectal (3) area and rectum (3).

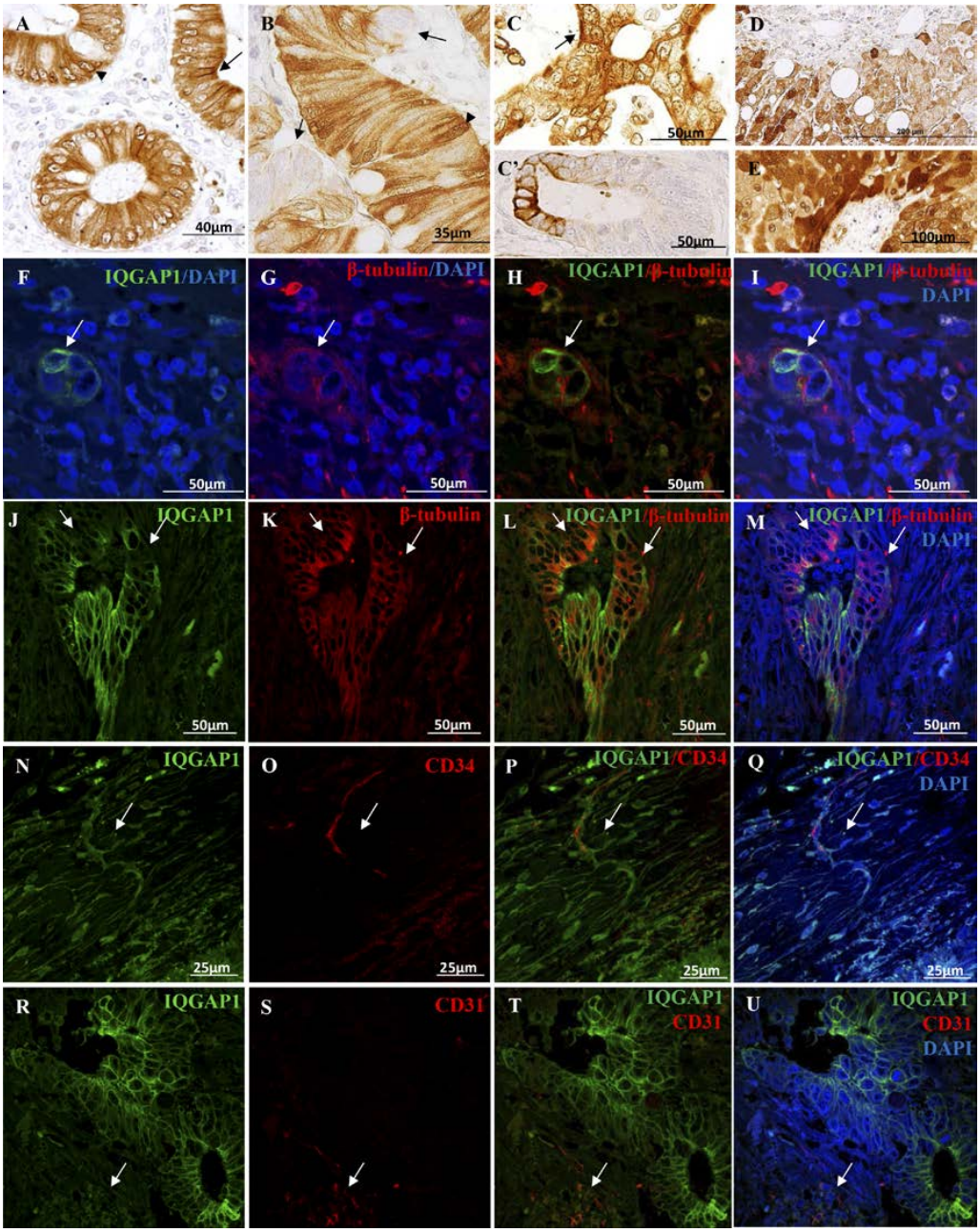

Figure 6. (**A**–**E**) Immunolocalization of IQGAP1 protein on paraffin-embedded tissue sections; (**A**) IQGAP1 staining in cytoplasm, apical and lateral membrane (arrow) and nuclear envelope (arrowhead) of normal epithelial cells; (**B**) Heterogeneous staining in tumor lesions, CRC IQGAP1^{+} cells (cytoplasm, lateral membrane, nuclear envelope and/or nucleus) and clusters of IQGAP1^{-} cells (arrows). Arrowhead: IQGAP1^{+} staining in nucleus; (**C**) CRC tumor lesion with strong apical staining (arrow in **C**). (**C'**) CRC tumor lesion with IQGAP1^{+} immunostaining at the invasive front.; (**D**,**E**) In healthy (**D**); and metastasized liver (**E**); heterogeneous IQGAP1^{+} staining in hepatocytes is observed (cytoplasm, nuclear envelope and/or nucleus); (**F**–**M**) IQGAP1 (green) and β-tubulin (red) double immunofluorescent staining in CRC. Variable expression/co-expression of both proteins in a budding tumor cell cluster (arrow in **F**–**I**) and in a tumor lesion (**J**–**M**). Arrows in J–M: IQGAP1^{-}/β-tubulin^{+} CRC tumor cell cluster. (**N**–**Q**) Double IQGAP1 (green) and CD34 (endothelial/telocyte marker-red) on CRC. Arrow points to a CD34^{+}/IQGAP1^{+} telocyte. (**R**–**U**) Co-expression of IQGAP1 (green) and CD31 (endothelial /macrophage marker-red) in several stromal cells of liver metastasis.

Table 1. Protein expression levels of AmotL2, FKBP51 and IQGAP1 in different cells of healthy colon and liver and in CRC and CRC-metastasized liver. − no expression, + faint, ++ medium, +++ high. Level/level variable level depending on area; ? indeterminate staining.

	AmotL2	IQGAP1	FKBP51
Healthy Colon			
Epithelial cells (*Mucosae*)	+/+++	+++	+++
Stromal cells (*Mucosae*)	+++	−	++
Immune system cells	+	?	++
Blood vessel cells	+++	++	−
Smooth muscle cells	+++	++	+
Neurous (*Myenteric plexus*)	+++	++	−/+
Glia cells (*Myenteric plexus*)	+++	++	−/+
Colorectal Cancer			
Tumor cells	+++	−/+++	−/++
Budding tumor cells	+++	−/+++	−/+
Tumor associated stromal cells	+++	−/++	−/+++
Epithelial cells (*Mucosae*)	++	−/+++	++
Immune system cells	+++	+++	+++
Smooth muscle cells	++	−	++
Blood vessel cells	+++	+++	−
Neurous (*Myenteric plexus*)	++	−	++
Glia cells (*Myenteric plexus*)	++	−	++
Healthy Liver			
Hepatocytes	+/+++	−/+++	−/++
Epithelial cells (Bile duct)	+	+	−
Blood vessel cells	+++	+++	−
Immune system cells	−	+	+
Metastasized Liver			
Tumor cells	+++	−/++	−/+
Budding tumor cells	+++	+++	−
Hepatocytes	++	−/+++	+/++
Epithelial cells (Bile duct)	++	++	−
Immune system cells	+++	+/++	++

3. Discussion

Cellularity of CRC consists of tumor cells, vascular endothelial cells and inflammatory immune cells infiltrating apparent normal colon tissue formed by mucosa, glandular, cryptal, submucosa and muscularis mucosa cells, interstitial cells, endothelial, pericytes and muscular cells of vessels and nerve cells of myenteric plexuses.

To give better information on CRC tumorigenesis and progression, instead of PCR and Western blotting methods in whole tumor pieces, for this study, we performed double immunolabeling for light and confocal microscopy in order to achieve a "cell by cell" analysis to obtain high quality subcellular localization data of AmotL2, FKBP51, and IQGAP1 proteins.

3.1. AmotL2 Expression in Healthy Colon and in CRC

AmotL2 localizes, virtually, in all kind of cells reported in this study but at different expression levels. Amot family includes Amot, AmotL1 and AmotL2. Amot is expressed as two different isoforms, AMOTp80 and AMOTp130 primarily localized to tight junctions [10,44]. As specified in Table 1, most cells express AmotL2 at variable levels. This fact agrees with the original report by Troyanovsky et al. [45] in several tissues and cell lines at the mRNA level, and also agrees with expression data by Microarray, RNAseq and Serial Analysis of Gene Expression (SAGE) reported by the GeneCards Human Gene Database (Available online: http://www.genecards.org/cgi-bin/carddisp.pl?gene=AMOTL2). However, little information is available on expression at the protein level. Summary in

GeneCards indicates the major line of AmotL2 expression at the protein level is blood white cells. Oxaliplatin-based CT increased AmotL2-mRNA levels in white cells [9].

The over population of pericytes in vascularized areas of CRC drives to think in the possibility that some of them could come from the EMT evolvement of CRC tumor cells [46]. Most EMT cancer cells seem to be located in perivascular space and closely associated with blood vessels, thereby simulating pericytes [46,47]. It has been suggested a reprogramming of carcinoma cells into pericyte-like cells during EMT essential for tumor vascular stabilization within a new promalignant effect of EMT [46]. From this point of view, AmotL2/CD31 co-expression in pericytes and CRC cell may be indicative of a common ancestry.

CD34 is selectively expressed on hematopoietic progenitor cells and the small vessel endothelium of a variety of tissues and telocytes [48,49]. Telocytes are generally defined based on a combination of peculiar morphology, typical interstitial location, mainly within muscle fibers [48], and expression of CD34 marker (although there are no strictly telocyte-specific markers). The increased population of pericytes and telocytes as well as certain population of cells coexpressing AmotL2/CD31/CD34 suggests a pre-commitment stage of cells from which they could take different decisions of final differentiation [50].

The participation of the angiomotin family isoforms AMOTp80 and AMOTp130 in cancer cell proliferation has been studied in liver and prostate cancer [51,52]. In liver, Amot-p130 acts as a tumorigenesis facilitator when associated to Yap cofactor, while, in prostate AMOTp80, not AMOT p130, functions as a tumor promoter by enhancing PCa cell proliferation. In lung adenocarcinoma, angiomotin p130 expression correlates with poor prognosis [53].

The variation levels and the subcellular redistribution of AmotL2 shown in this study in tumor cells, metastasis and blood vessels and adjacent cells are indicative of its involvement in the CRC tumorigenesis and progression processes.

3.2. AmotL2 Expression in Healthy Colon, Liver and in CRC-Metastasized Liver

Most liver cells types expressed AmotL2. Hepatocytes express AmotL2, apparently, in a gradient manner, with increasing intensity as a more oxygenated zone is closer (Figure S1A,B). Our images illustrate how hypoxic gradients may contribute to CRC metastasis implantation and development in liver and how the gradients of AmotL2 expression in hepatocytes become homogeneous after being metastasized. If the gradient expression pattern disappears because of FOLFOX-CT, or if the metastasizing process also affects it, remains to be studied.

The facts that AmotL2 was originally described as a protein responsible for maintaining polarized endothelial cells attached and involved in vessel formation in angiogenesis and with a role in tumorigenesis are indicative of the complexity of association as scaffold protein, probably depending on adaptors that commit AmotL2 to biologically apparently opposite functions. Deregulated AmotL2 expression in tumor and metastasized areas during tumor progression confirms what recently has been well established in colon cancer tumors, AmotL2 expression correlates with loss of polarity by means of hypoxia activated c-Fos, leading to loss of tissue architecture [11]. The complex c-Fos/hypoxia-induced p60 and AmotL2 interacting with the Crb3 and Par3 polarity complexes retain them in large vesicles, impeding them from reaching the apical membrane [11] and being involved, this way, in EMT.

3.3. FKBP51 Expression in Healthy Colon, Liver, CRC and Metastasized Liver

FKBP51 protein is localized in the nuclei of enterocytes in healthy tissue while in CRC is found in nuclei and cytoplasm, exhibiting a variable range, from strong to no detectable signal. Metastases in liver show a faint or absent FKBP51 immunostaining, while the inflammatory fibrous stroma depicts several cells with a strong immunostaining. This depiction could be related to the effect of chemotherapy on tumor cells rather than with intrinsic changes of transformation of cells.

The changes of FKBP51 expression in liver tissue surrounding the metastases reported in this study, could be related with hepatic sinusoidal injury elicited by oxaliplatin therapy [54].

A role for this protein in EMT has been suggested based on the expression of FKBP51 in tumor and stromal cells. Indeed, the expression of this immunophilin has been associated to immature phenotype of the surrounding stromal fibroblasts, increased micro vessel density and tumor associated macrophages infiltration, suggesting a role in CRC process [19].

FKBP51 and its co-isoform FKBP52 are HSP90 co-chaperones that modify steroid hormone receptor activity. Figures 6 and 7 illustrate their interaction with the glucocorticoid receptor. The HSP90-FKBP52 complex co-immunoprecipitate with the glucocorticoid (GR) and the mineralocorticoid receptors and with the dynein–dynactin complex [16,55,56], indicating a retrograde movement of steroid receptors. FKBP51 is considered a negative regulator of receptor function. The glucocorticoids secretion by some CRC could be related to this pathway and have immunosuppressive functions cooperating, this way, to tumor progression [57].

Cytoplasmic FKBP51 is involved in the pro-apoptotic effects of rapamycin: over cell survival and chemoresistance of cancer cell. Rapamycin inhibits FKBP51 and though hinders NF-κB activation [58]. Mitochondrial-nuclear redistribution of FKBP51 is regulated by the PKA pathway; PKA and FKBP51 mainly colocalize in the nuclear lamina. In the nucleus, FKBP51 is retained by its interaction with the nuclear matrix and chromatin, regulating expression of target genes [20] (Figure 7, pathway 3).

3.4. IQGAP1 Expression in Healthy Colon, Liver, CRC and Metastasized Liver

The homogeneous distribution of IQGAP1 in normal cells shifts to a broad expression pattern, ranging from no expression to high level of expression in the whole CRC tumor cell. IQGAP1 seems to be involved in tumor progression, since its maximum expression is at the growing front of tumor, just at the apical part of the expanding cells. The absence of IQGAP1 and β-tubulin co-immunostaining shows groups of tumor cells undergoing EMT.

The interaction of IQGAP1 with cytoplasmic plus-end binding proteins CLIP-170 and APC, tethering microtubules to the actin network promotes nuclear envelope membrane dynamics [59,60]. Co-localization of IQGAP1, F-actin and β-tubulin proteins at the nuclear envelope has been reported by Johnson et al. in MCF-7 (breast cancer epithelial cells), HT29 (colon cancer epithelial cells) and NIH3T3 (non-tumor embryonic fibroblasts) cell lines [61]. Those observations suggest a role for IQGAP1 in cell cycle-associated nuclear envelope assembly/disassembly and in survival, cell growth, cytokinesis, and cell migration: key processes in tumorigenesis and carcinogenesis [61].

The IQGAP1^{+} nucleoli, often found throughout the microscopy field, suggests a correlation between IQGAP1 expression and RNA synthesis in tumor cells, which agrees with the previous report [62] in mouse oocyte nucleus, forming a ring around the nucleolus only in transcriptionally active oocytes.

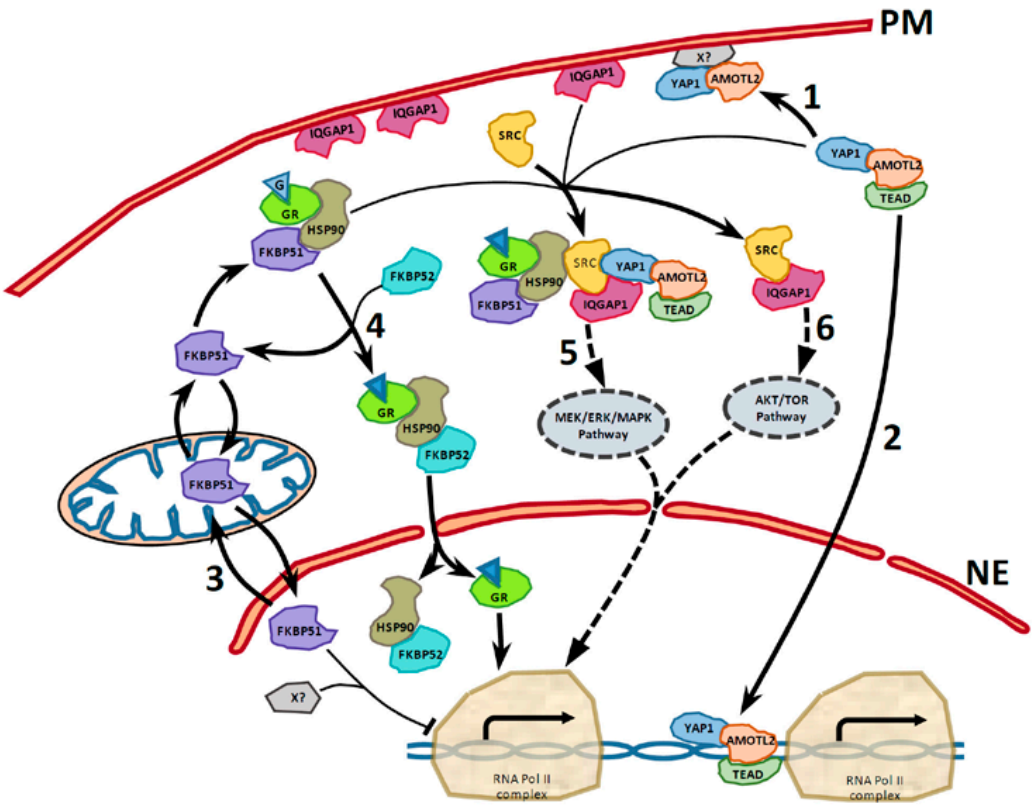

Figure 7. Model of direct or indirect protein-protein interaction of AmotL2, FKBP51, IQGAP2 and interacting partners. (PM) Plasma membrane. (NE) Nuclear envelope. AmotL2, as scaffold protein, may promote translocation and transcriptional activity of YAP. Upon YAP interaction with AmotL2, YAP shuttles between the cytoplasm and the nucleus. AmotL2 acts as a negative regulator of YAP by inducing its cytoplasmic retention or targeting it to cell junctions (**1**); Within the nucleus, YAP functions as a transcriptional coactivator of TEAD. The YAP-TEAD complex promotes the transcription of many genes that encode pro-proliferative and anti-apoptotic proteins. AmotL2 functions as a positive regulator of YAP by promoting its nuclear translocation (**2**), where AmotL2 may act as a cofactor for the transcription of a group of YAP-TEAD target genes (**2**); Both ways of translocation of FKBP51 between mitochondrial and nuclear pool. In the nucleus, FKBP51 regulates, presumably blocking, transcription of GR-target genes, and possibly other targets (**3**); Cytosolic FKBP51 interacts with glucocorticoid hormone receptor (GR) and HSP90. Upon binding, the GR heterocomplex exchanges FKBP51 for FKBP52. FKBP52-GR–chaperone complex is able to interact with dynein and walk by cytoskeletal tracts through cytosol and, through the nuclear pore, get into the nucleus, where dissociates and facilitates binding of the steroid-activated receptor to promoter sites (**4**); In its scaffolding function, IQGAP1 interacts with the MEK-ERK pathway hyperactivates ERK signaling and promotes tumor cell proliferation and survival (**5**). On the other hand, IQGAP1 interaction with the MEK-ERK pathway is dispensable in normal cell differentiation, growth, and survival [63]. IQGAP1 promotes cell division and proliferation through IQGAP1-TOR-Akt and suppresses differentiation and apoptosis driving to transformation [64].

3.5. Final Considerations and Future Research Directions

In this study, we confirm the fundamental role of the cell by cell immunohistochemical analysis in molecular oncology data interpretation, presenting data compatible with the involvement of AmotL2, FKBP51 and IQGAP1 proteins in the cellular EMT phenotype. We show evidence that the scaffoldins show variation in expression and localization at the protein level in tissue samples of pre-CT treated colorectal adenocarcinoma and in liver metastases from patients that underwent FOLFOX-CT. The co-localization of CD34 and AmotL2, FKBP51 and IQGAP1 in several vessels is

indicative of a role for these three scaffoldings in tumor angiogenesis and/or in vascular invasion. Indeed, Yamaoka-Tojo et al. have recently shown IQGAP1 as a VEGFR2 binding protein in quiescent endothelial cells, playing an important role in the establishment of VE-cadherin-based cell–cell contacts, and suggested that IQGAP1 may function as a scaffold linking VEGFR2 to the β-catenin/VE-cadherin compound at the adherens junctions (AJ) [65].

Several pieces of evidence point to a key role for these proteins in the dynamics of tumor cells and angiogenesis process, including expression in pericytes and/or telocytes. Variations in cellular expression here described renders scaffoldins AmotL2, FKBP51 and IQGAP1 an attractive group as biomarkers for diagnostic staging and as targets for therapy, although further research needs to be done to confirm and to precise these assessments.

Figure 7 shows a model of interactions of AmotL2, FKBP51, and IQGAP1 made upon integration of our data with the literature and other data from databanks. Scaffold proteins connect structural and signaling molecules in the spatiotemporal organization and activation in CRC tumorigenic cells [29,30]. The process takes place in different subcellular localizations and at variable expression levels depending on the status of the cell within the tumor. Further studies are needed to confirm the possible existence of the complex FKBP51-HSP90-SRC-YAP-AmotL2-IQGAP.

4. Materials and Methods

4.1. Patients, Tumor Tissue and Controls

The study was approved by the Ethics Committee of La Laguna University (La Laguna, Canary Islands, Spain) and the Ethical Committee of Nuestra Señora de Candelaria University Hospital (HUNSC); Santa Cruz de Tenerife, Canary Islands, Spain (No. 198/2008, approved on 16 September 2008). All patients signed an informed consent for diagnosis and research on tissue specimens before entering in the project. Paraffin-embedded tissue samples from 54 patients, ensuring patient anonymity, and the corresponding clinical data were obtained from the reference medical areas of HUNSC.

Following the same ethics and consent rules, colon and liver samples were obtained from surgery partial exeresis pieces after trauma of three control males.

4.2. Antibodies

The following primary antibodies were used: rabbit anti-human polyclonal antibody (PAb) against IQGAP1 (#ABT186 Millipore Corporation, Temecula, CA, USA) 1:500 for IHC-P, 1:250 for IF; rabbit pAb against FKBP51 (#ab46002; Abcam, Cambridge, UK) 1.25:100 for IHC-P, 1:50 for IF; rabbit pAb against AMOTL2 (#LS-C178611; LifeSpan BioSciences, Seattle, WA, USA) 1:100 for IHC-P, 1:50 for IF; mouse monoclonal antibody clone PC10 against anti-proliferating cell nuclear antigen (anti-PCNA, #1486 772, Roche Diagnostics GmbH, Mannheim, Germany) 1:100; mouse monoclonal anti-human cluster of differentiation (CD)31 (ready-to-use; #IR610 Dako, Glostrup, Denmark); mouse monoclonal anti-human CD34 Class II Clone QBEnd10 (ready-to-use; #IR632, Dako, Glostrup, Denmark A/S); mouse monoclonal anti-β tubulin (#sc-101527 Santa Cruz Biotechnology, Dallas, TX, USA) 1:150. Secondary antibodies: fluorescein isothiocyanate (FITC)-conjugated goat pAb against rabbit IgG (#F9887; Sigma-Aldrich, St. Louis, MO, USA; dilution, 1:200); goat pAb against mouse IgG (DyLight® 650; #ab97018; Abcam, dilution, 1:100); and biotin-conjugated goat pAb against rabbit IgG (H + L) (#31820; Thermo Fisher Scientific, Inc., Waltham, MA, USA; dilution, 1:300).

4.3. Immunohistochemistry

Samples were fixed in 10% formalin, for 48–72 h at 4 °C. Immunoperoxidase staining of paraffin-embedded tissue sections was performed using the avidin-biotin reaction. Briefly, 5-µm-thick tissue sections, deparaffinized in xylene and hydrated in graded alcohol baths, were autoclaved at 120 °C for 10 min in sodium citrate buffer (pH 6.0) to uncover hidden antigenic sites (antigen retrieval). Samples were then incubated for 1 h at room temperature with 5% non-fat dry milk

in Tris-buffered saline (TBS) to block non-specific sites. The Avidin/Biotin Blocking kit (Vector Laboratories Inc., Burlingame, CA, USA) was used to block endogenous biotin, according to the manufacturer's instructions. Primary antibodies were applied to slides overnight at 4 °C. Endogenous peroxidase activity was blocked by incubating the slides with 3% hydrogen peroxidase in methanol for 15 min. Biotin-conjugated anti-rabbit secondary antibody was incubated for 2 h at 37 °C, and the specific antibody staining was amplified with the ABC Peroxidase Staining kit (Thermo Fisher Scientific, Inc.). 3,3′-diaminobenzidine substrate concentrate (#IHC-101F; Bethyl Laboratories Inc., Montgomery, TX, USA) was used to visualize immunohistochemical reactions. Samples incubated without primary antibodies were used as a negative control. Slides were counterstained with Harris hematoxylin solution DC (#253949, Panreac Química SLU, Barcelona, Spain) to visualize cell nuclei and mounted with Eukitt mounting medium (#253681, Panreac Química SLU, Barcelona, Spain). An optical light microscope (BX50; Olympus Corporation, Tokyo, Japan) was used to visualize the results of the immunostaining.

4.4. Double Immunofluorescence Simultaneous Staining

Immunofluorescent staining of 10% formalin-fixed paraffin-embedded tissue sections was performed as previously described [47]. Briefly, 5-µm-thick tissue sections, deparaffinized in xylene and hydrated in a graded series of alcohol baths, were autoclaved at 120 °C for 10 min in sodium citrate buffer (pH 6.0) to uncover hidden antigenic sites (antigen retrieval). Samples were then incubated for 1 h at room temperature with 5% bovine serum albumin in Tris-buffered saline (TBS) to block non-specific sites. Tissue sections were then incubated simultaneously with a mixture of two distinct primary antibodies overnight at 4 °C. Slides were then incubated for 1 h at room temperature in the dark with a mixture of two secondary antibodies raised in different species and conjugated to different fluorochromes. Slides were mounted with ProLong® Diamond Anti-fade Mountant with DAPI (Molecular Probes®; Thermo Fisher Scientific, Inc.) to visualize cell nuclei. Slides were analyzed using Leica SP8 (Leica Microsystems, Wetzlar, Germany) confocal microscopes and Olympus FV1000 (Olympus Corporation, Tokyo, Japan).

4.5. Image Analysis and Statistical Analysis

To compile tables, two independent observers evaluated the specimens blindly. After an initial examination of the whole blind-coded material, cut-offs were established by consensus between each investigator. Staining intensities were graded as strong (+++), moderate (++), weak (+) or absent (−). When scorings differed by more than one unit, the observers re-evaluated the specimens to reach consensus, otherwise means of the scorings were calculated.

5. Conclusions

Positive immunostaining for scaffold AmotL2, FKBP51 and IQGAP1 proteins was found in most cells in healthy colon, tumor, healthy liver and metastasized liver. The expression patterns reveals the greatest variability in immune system and neural (neurons and glia) cells and the least in blood vessel cells. The simultaneous subcellular localization of these scaffoldines in tumor cells and other cell types within the tumor suggest a peculiar involvement in the onco-biology of CRC and metastasis, including a role in EMT.

Supplementary Materials: Supplementary materials can be found at www.mdpi.com/1422-0067/18/4/891/s1.

Acknowledgments: This work was supported by grant FIS PI11/00114 to Pablo Martín-Vasallo and grant FIS PI12/00729, Spain, to Julio Ávila. Supported partially by the Insular Council of Tenerife and grants MCT-FEDER 2003/2004 (Olympus FV-1000) and IMBRAIN-FP7-REGPOT-2012-31637 awarded to the Institute of Biomedical Technologies and the Center of Biomedical Research of the Canary Islands at Universidad de La Laguna.

Author Contributions: Deborah Rotoli, Manuel Morales and Pablo Martín-Vasallo conceived the study and its design. Manuel Morales, María del Carmen Maeso and María del Pino García selected the patients. Deborah Rotoli, Julio Ávila, Pablo Martín-Vasallo and Ali Mobasheri drafted and revised the manuscript. María del Carmen Maeso and María del Pino García selected and handled samples and supervised Histology. Deborah Rotoli carried out the immunohistochemistry assays, and took and organized the pictures. All authors analyzed and discussed results and draft versions of the manuscript. All authors read and approved the final manuscript.

Conflicts of Interest: The authors declare no conflict of interest.

Abbreviations

Amot	Angiomotin
APC	Adenomatous polyposis coli
CLIP-170	Cytoplasmic linker protein CLIP-170
CT	Chemotherapy
EMT	Epithelial mesenchymal transition
FKBP	FK506 binding protein
FOLFOX	FOL—Folinic acid, leucovorin, F—Fluorouracil, 5-FU, OX—Oxaliplatin
HSP90	Heat shock protein 90
IQGAP1	IQ-motif containing GTPase activating protein 1
MAPK	Mitogen-activated protein kinase
PCNA	Proliferating cell nuclear antigen
TEAD	Transcriptional enhancer factors
YAP	Yes-associated protein

References

1. Bendris, N.; Schmid, S.L. Endocytosis, metastasis and beyond: Multiple facets of SNX9. *Trends Cell Biol.* **2017**, *27*, 189–200. [CrossRef] [PubMed]
2. Herrero-Garcia, E.; O'Bryan, J.P. Intersectin scaffold proteins and their role in cell signaling and endocytosis. *Biochim. Biophys. Acta* **2017**, *1864*, 23–30. [CrossRef] [PubMed]
3. Garbett, D.; Bretscher, A. The surprising dynamics of scaffolding proteins. *Mol. Biol. Cell* **2014**, *25*, 2315–2319. [CrossRef] [PubMed]
4. Blanco-Calvo, M.; Concha, A.; Figueroa, A.; Garrido, F.; Valladares-Ayerbes, M. Colorectal Cancer Classification and Cell Heterogeneity: A Systems Oncology Approach. *Int. J. Mol. Sci.* **2015**, *16*, 13610–13632. [CrossRef] [PubMed]
5. Trinh, A.; Trumpi, K.; De Sousa, E.M.; Wang, X.; de Jong, J.H.; Fessler, E.; Kuppen, P.J.; Reimers, M.S.; Swets, M.; Koopman, M.; et al. Practical and Robust Identification of Molecular Subtypes in Colorectal Cancer by Immunohistochemistry. *Clin. Cancer Res.* **2017**, *23*, 387–398. [CrossRef] [PubMed]
6. Andre, T.; Boni, C.; Mounedji-Boudiaf, L.; Navarro, M.; Tabernero, J.; Hickish, T.; Topham, C.; Zaninelli, M.; Clingan, P.; Bridgewater, J.; et al. fluorouracil, and leucovorin as adjuvant treatment for colon cancer. *N. Engl. J. Med.* **2004**, *350*, 2343–2351. [CrossRef] [PubMed]
7. Pachman, D.R.; Loprinzi, C.L.; Grothey, A.; Ta, L.E. The search for treatments to reduce chemotherapy-induced peripheral neuropathy. *J. Clin. Investig.* **2014**, *124*, 72–74. [CrossRef] [PubMed]
8. Seo, A.N.; Kim, H. Sinusoidal obstruction syndrome after oxaliplatin-based chemotherapy. *Clin. Mol. Hepatol.* **2014**, *20*, 81–84. [CrossRef] [PubMed]
9. Morales, M.; Avila, J.; Gonzalez-Fernandez, R.; Boronat, L.; Soriano, M.L.; Martin-Vasallo, P. Differential transcriptome profile of peripheral white cells to identify biomarkers involved in oxaliplatin induced neuropathy. *J. Pers. Med.* **2014**, *4*, 282–296. [CrossRef] [PubMed]
10. Bratt, A.; Wilson, W.J.; Troyanovsky, B.; Aase, K.; Kessler, R.; Van Meir, E.G.; Holmgren, L. Angiomotin belongs to a novel protein family with conserved coiled-coil and PDZ binding domains. *Gene* **2002**, *298*, 69–77. [CrossRef]
11. Mojallal, M.; Zheng, Y.; Hultin, S.; Audebert, S.; van, H.T.; Johnsson, P.; Lenander, C.; Fritz, N.; Mieth, C.; Corcoran, M.; et al. AmotL2 disrupts apical-basal cell polarity and promotes tumour invasion. *Nat. Commun.* **2014**, *5*, 4557. [CrossRef] [PubMed]

12. Erlejman, A.G.; De Leo, S.A.; Mazaira, G.I.; Molinari, A.M.; Camisay, M.F.; Fontana, V.; Cox, M.B.; Piwien-Pilipuk, G.; Galigniana, M.D. NF-κB transcriptional activity is modulated by FK506-binding proteins FKBP51 and FKBP52: A role for peptidyl-prolyl isomerase activity. *J. Biol. Chem.* **2014**, *19*, 26263–26276. [CrossRef] [PubMed]
13. Shaw, P.E. Peptidyl-prolyl isomerases: A new twist to transcription. *EMBO Rep.* **2002**, *3*, 521–526. [CrossRef] [PubMed]
14. Hubler, T.R.; Denny, W.B.; Valentine, D.L.; Cheung-Flynn, J.; Smith, D.F.; Scammell, J.G. The FK506-binding immunophilin FKBP51 is transcriptionally regulated by progestin and attenuates progestin responsiveness. *Endocrinology* **2003**, *144*, 2380–2387. [CrossRef] [PubMed]
15. Barik, S. Immunophilins: For the love of proteins. *Cell. Mol. Life Sci.* **2006**, *63*, 2889–2900. [CrossRef] [PubMed]
16. Galigniana, M.D.; Radanyi, C.; Renoir, J.M.; Housley, P.R.; Pratt, W.B. Evidence that the peptidylprolyl isomerase domain of the hsp90-binding immunophilin FKBP52 is involved in both dynein interaction and glucocorticoid receptor movement to the nucleus. *J. Biol. Chem.* **2001**, *276*, 14884–14889. [CrossRef] [PubMed]
17. Rein, T. FK506 binding protein 51 integrates pathways of adaptation: FKBP51 shapes the reactivity to environmental change. *Bioessays* **2016**, *38*, 894–902. [CrossRef] [PubMed]
18. Mukaide, H.; Adachi, Y.; Taketani, S.; Iwasaki, M.; Koike-Kiriyama, N.; Shigematsu, A.; Shi, M.; Yanai, S.; Yoshioka, K.; Kamiyama, Y.; et al. FKBP51 expressed by both normal epithelial cells and adenocarcinoma of colon suppresses proliferation of colorectal adenocarcinoma. *Cancer Investig.* **2008**, *26*, 385–390. [CrossRef] [PubMed]
19. Rotoli, D.; Morales, M.; Del Carmen, M.M.; Del Pino, G.M.; Morales, A.; Avila, J.; Martin-Vasallo, P. Expression and localization of the immunophilin FKBP51 in colorectal carcinomas and primary metastases, and alterations following oxaliplatin-based chemotherapy. *Oncol. Lett.* **2016**, *12*, 1315–1322. [CrossRef] [PubMed]
20. Toneatto, J.; Guber, S.; Charo, N.L.; Susperreguy, S.; Schwartz, J.; Galigniana, M.D.; Piwien-Pilipuk, G. Dynamic mitochondrial-nuclear redistribution of the immunophilin FKBP51 is regulated by the PKA signaling pathway to control gene expression during adipocyte differentiation. *J. Cell Sci.* **2013**, *126*, 5357–5368. [CrossRef] [PubMed]
21. Storer, C.L.; Dickey, C.A.; Galigniana, M.D.; Rein, T.; Cox, M.B. FKBP51 and FKBP52 in signaling and disease. *Trends Endocrinol. Metab.* **2011**, *22*, 481–490. [CrossRef] [PubMed]
22. Pei, H.; Li, L.; Fridley, B.L.; Jenkins, G.D.; Kalari, K.R.; Lingle, W.; Petersen, G.; Lou, Z.; Wang, L. FKBP51 affects cancer cell response to chemotherapy by negatively regulating Akt. *Cancer Cell* **2009**, *16*, 259–266. [CrossRef] [PubMed]
23. Romano, S.; D'Angelillo, A.; D'Arrigo, P.; Staibano, S.; Greco, A.; Brunetti, A.; Scalvenzi, M.; Bisogni, R.; Scala, I.; Romano, M.F. FKBP51 increases the tumour-promoter potential of TGF-β. *Clin. Transl. Med.* **2014**, *3*, 1–3. [CrossRef] [PubMed]
24. Gallo, L.I.; Lagadari, M.; Piwien-Pilipuk, G.; Galigniana, M.D. The 90-kDa heat-shock protein (Hsp90)-binding immunophilin FKBP51 is a mitochondrial protein that translocates to the nucleus to protect cells against oxidative stress. *J. Biol. Chem.* **2011**, *286*, 30152–30160. [CrossRef] [PubMed]
25. Li, L.; Lou, Z.; Wang, L. The role of FKBP5 in cancer aetiology and chemoresistance. *Br. J. Cancer* **2011**, *104*, 19–23. [CrossRef] [PubMed]
26. Abel, A.M.; Schuldt, K.M.; Rajasekaran, K.; Hwang, D.; Riese, M.J.; Rao, S.; Thakar, M.S.; Malarkannan, S. IQGAP1: Insights into the function of a molecular puppeteer. *Mol. Immunol.* **2015**, *65*, 336–349. [CrossRef] [PubMed]
27. Erickson, J.W.; Cerione, R.A.; Hart, M.J. Identification of an actin cytoskeletal complex that includes IQGAP and the Cdc42 GTPase. *J. Biol. Chem.* **1997**, *272*, 24443–24447. [CrossRef] [PubMed]
28. Roy, M.; Li, Z.; Sacks, D.B. IQGAP1 is a scaffold for mitogen-activated protein kinase signaling. *Mol. Cell. Biol.* **2005**, *25*, 7940–7952. [CrossRef] [PubMed]
29. Malarkannan, S.; Awasthi, A.; Rajasekaran, K.; Kumar, P.; Schuldt, K.M.; Bartoszek, A.; Manoharan, N.; Goldner, N.K.; Umhoefer, C.M.; Thakar, M.S. IQGAP1: A regulator of intracellular spacetime relativity. *J. Immunol.* **2012**, *188*, 2057–2063. [CrossRef] [PubMed]
30. White, C.D.; Erdemir, H.H.; Sacks, D.B. IQGAP1 and its binding proteins control diverse biological functions. *Cell Signal.* **2012**, *24*, 826–834. [CrossRef] [PubMed]

31. Johnson, M.; Sharma, M.; Henderson, B.R. IQGAP1 regulation and roles in cancer. *Cell Signal.* **2009**, *21*, 1471–1478. [CrossRef] [PubMed]
32. Nabeshima, K.; Shimao, Y.; Inoue, T.; Koono, M. Immunohistochemical analysis of IQGAP1 expression in human colorectal carcinomas: Its overexpression in carcinomas and association with invasion fronts. *Cancer Lett.* **2002**, *176*, 101–109. [CrossRef]
33. Rotoli, D.; Perez-Rodriguez, N.D.; Morales, M.; Maeso, M.D.; Avila, J.; Mobasheri, A.; Martin-Vasallo, P. IQGAP1 in podosomes/invadosomes is involved in the progression of glioblastoma multiforme depending on the tumor status. *Int. J. Mol. Sci.* **2017**, *18*, E150. [CrossRef] [PubMed]
34. Rotoli, D.; Morales, M.; del Carmen, M.M.; del Pino, G.M.; Gutierrez, R.; Valladares, F.; Avila, J.; Díaz-Flores, L.; Mobasheri, A.; Martin-Vasallo, P. Alterations in IQGAP1 expression and localization in colorectal carcinomas and liver metastases following oxaliplatin based chemotherapy. *Oncol. Lett.* **2016**, *12*, 1315–1322. [PubMed]
35. White, C.D.; Brown, M.D.; Sacks, D.B. IQGAPs in cancer: A family of scaffold proteins underlying tumorigenesis. *FEBS Lett.* **2009**, *583*, 1817–1824. [CrossRef] [PubMed]
36. Szklarczyk, D.; Franceschini, A.; Wyder, S.; Forslund, K.; Heller, D.; Huerta-Cepas, J.; Simonovic, M.; Roth, A.; Santos, A.; Tsafou, K.P.; et al. STRING v10: Protein-protein interaction networks, integrated over the tree of life. *Nucleic Acids Res.* **2015**, *43*, D447–D452. [CrossRef] [PubMed]
37. Huang, H.; Lu, F.I.; Jia, S.; Meng, S.; Cao, Y.; Wang, Y.; Ma, W.; Yin, K.; Wen, Z.; Peng, J.; et al. AmotL2 is essential for cell movements in zebrafish embryo and regulates c-Src translocation. *Development* **2007**, *134*, 979–988. [CrossRef] [PubMed]
38. Hao, Y.; Chun, A.; Cheung, K.; Rashidi, B.; Yang, X. Tumor suppressor LATS1 is a negative regulator of oncogene YAP. *J. Biol. Chem.* **2008**, *283*, 5496–5509. [CrossRef] [PubMed]
39. Porazinski, S.; Wang, H.; Asaoka, Y.; Behrndt, M.; Miyamoto, T.; Morita, H.; Hata, S.; Sasaki, T.; Krens, S.F.; Osada, Y.; et al. YAP is essential for tissue tension to ensure vertebrate 3D body shape. *Nature* **2015**, *521*, 217–221. [CrossRef] [PubMed]
40. Hong, W. Angiomotin'g YAP into the nucleus for cell proliferation and cancer development. *Sci. Signal.* **2013**, *6*, e27. [CrossRef] [PubMed]
41. Zhao, B.; Ye, X.; Yu, J.; Li, L.; Li, W.; Li, S.; Yu, J.; Lin, J.D.; Wang, C.Y.; Chinnaiyan, A.M.; et al. TEAD mediates YAP-dependent gene induction and growth control. *Genes Dev.* **2008**, *22*, 1962–1971. [CrossRef] [PubMed]
42. Landin-Malt, A.; Benhaddou, A.; Zider, A.; Flagiello, D. An evolutionary, structural and functional overview of the mammalian TEAD1 and TEAD2 transcription factors. *Gene* **2016**, *591*, 292–303. [CrossRef] [PubMed]
43. Moldovan, G.L.; Pfander, B.; Jentsch, S. PCNA, the maestro of the replication fork. *Cell* **2007**, *129*, 665–679. [CrossRef] [PubMed]
44. Bratt, A.; Birot, O.; Sinha, I.; Veitonmaki, N.; Aase, K.; Ernkvist, M.; Holmgren, L. Angiomotin regulates endothelial cell-cell junctions and cell motility. *J. Biol. Chem.* **2005**, *280*, 34859–34869. [CrossRef] [PubMed]
45. Troyanovsky, B.; Levchenko, T.; Mansson, G.; Matvijenko, O.; Holmgren, L. Angiomotin: An angiostatin binding protein that regulates endothelial cell migration and tube formation. *J. Cell Biol.* **2001**, *19*, 1247–1254. [CrossRef]
46. Shenoy, A.K.; Jin, Y.; Luo, H.; Tang, M.; Pampo, C.; Shao, R.; Siemann, D.W.; Wu, L.; Heldermon, C.D.; Law, B.K.; et al. Epithelial-to-mesenchymal transition confers pericyte properties on cancer cells. *J. Clin. Investig.* **2016**, *126*, 4174–4186. [CrossRef] [PubMed]
47. Diaz-Flores, L.; Gutierrez, R.; Madrid, J.F.; Varela, H.; Valladares, F.; Acosta, E.; Martin-Vasallo, P.; Diaz-Flores, L., Jr. Pericytes. Morphofunction, interactions and pathology in a quiescent and activated mesenchymal cell niche. *Histol. Histopathol.* **2009**, *24*, 909–969. [PubMed]
48. Popescu, L.M.; Faussone-Pellegrini, M.S. TELOCYTES—A case of serendipity: The winding way from Interstitial Cells of Cajal (ICC), via Interstitial Cajal-Like Cells (ICLC) to TELOCYTES. *J. Cell. Mol. Med.* **2010**, *14*, 729–740. [CrossRef] [PubMed]
49. Diaz-Flores, L.; Gutierrez, R.; Garcia, M.P.; Saez, F.J.; Aparicio, F.; Diaz-Flores, L., Jr.; Madrid, J.F. Uptake and intracytoplasmic storage of pigmented particles by human $CD34^+$ stromal cells/telocytes: Endocytic property of telocytes. *J. Cell. Mol. Med.* **2014**, *18*, 2478–2487. [CrossRef] [PubMed]
50. Smythies, J. Intercellular signaling in cancer-the SMT and TOFT hypotheses, exosomes, telocytes and metastases: Is the messenger in the message? *J. Cancer* **2015**, *6*, 604–609. [CrossRef] [PubMed]

51. Yi, C.; Shen, Z.; Stemmer-Rachamimov, A.; Dawany, N.; Troutman, S.; Showe, L.C.; Liu, Q.; Shimono, A.; Sudol, M.; Holmgren, L.; et al. The p130 isoform of angiomotin is required for Yap-mediated hepatic epithelial cell proliferation and tumorigenesis. *Sci. Signal.* **2013**, *6*, ra77. [CrossRef] [PubMed]
52. Zeng, H.; Ortiz, A.; Shen, P.F.; Cheng, C.J.; Lee, Y.C.; Yu, G.; Lin, S.C.; Creighton, C.J.; Yu-Lee, L.Y.; Lin, S.H. Angiomotin regulates prostate cancer cell proliferation by signaling through the Hippo-YAP pathway. *Oncotarget* **2016**, *8*, 10145–10160. [CrossRef] [PubMed]
53. Jang, S.H.; Cho, H.D.; Lee, J.H.; Lee, H.J.; Hong, S.A.; Cho, J.; Kim, H.J.; Oh, M.H. Reduced angiomotin p130 expression correlates with poor prognosis in lung adenocarcinoma. *BMJ J.* **2016**. [CrossRef]
54. Nalbantoglu, I.L.; Tan, B.R., Jr.; Linehan, D.C.; Gao, F.; Brunt, E.M. Histological features and severity of oxaliplatin-induced liver injury and clinical associations. *J. Dig. Dis.* **2014**, *15*, 553–560. [CrossRef] [PubMed]
55. Davies, T.H.; Ning, Y.M.; Sanchez, E.R. A new first step in activation of steroid receptors: Hormone-induced switching of FKBP51 and FKBP52 immunophilins. *J. Biol. Chem.* **2002**, *277*, 4597–4600. [CrossRef] [PubMed]
56. Wochnik, G.M.; Ruegg, J.; Abel, G.A.; Schmidt, U.; Holsboer, F.; Rein, T. FK506-binding proteins 51 and 52 differentially regulate dynein interaction and nuclear translocation of the glucocorticoid receptor in mammalian cells. *J. Biol. Chem.* **2005**, *280*, 4609–4616. [CrossRef] [PubMed]
57. Sidler, D.; Renzulli, P.; Schnoz, C.; Berger, B.; Schneider-Jakob, S.; Fluck, C.; Inderbitzin, D.; Corazza, N.; Candinas, D.; Brunner, T. Colon cancer cells produce immunoregulatory glucocorticoids. *Oncogene* **2011**, *30*, 2411–2419. [CrossRef] [PubMed]
58. Romano, S.; Mallardo, M.; Romano, M.F. FKBP51 and the NF-κB regulatory pathway in cancer. *Curr. Opin. Pharmacol.* **2011**, *11*, 288–293. [CrossRef] [PubMed]
59. Fukata, M.; Watanabe, T.; Noritake, J.; Nakagawa, M.; Yamaga, M.; Kuroda, S.; Matsuura, Y.; Iwamatsu, A.; Perez, F.; Kaibuchi, K. Rac1 and Cdc42 capture microtubules through IQGAP1 and CLIP-170. *Cell* **2002**, *109*, 873–885. [CrossRef]
60. Watanabe, T.; Wang, S.; Noritake, J.; Sato, K.; Fukata, M.; Takefuji, M.; Nakagawa, M.; Izumi, N.; Akiyama, T.; Kaibuchi, K. Interaction with IQGAP1 links APC to Rac1, Cdc42, and actin filaments during cell polarization and migration. *Dev. Cell.* **2004**, *7*, 871–883. [CrossRef] [PubMed]
61. Johnson, M.A.; Henderson, B.R. The scaffolding protein IQGAP1 co-localizes with actin at the cytoplasmic face of the nuclear envelope: Implications for cytoskeletal regulation. *Bioarchitecture* **2012**, *2*, 138–142. [CrossRef] [PubMed]
62. Bielak-Zmijewska, A.; Kolano, A.; Szczepanska, K.; Maleszewski, M.; Borsuk, E. CDC42 protein acts upstream of IQGAP1 and regulates cytokinesis in mouse oocytes and embryos. *Dev. Biol.* **2008**, *322*, 21–32. [CrossRef] [PubMed]
63. Sanchez-Laorden, B.; Viros, A.; Marais, R. Mind the IQGAP. *Cancer Cell* **2013**, *23*, 715–717. [CrossRef] [PubMed]
64. Tekletsadik, Y.K.; Sonn, R.; Osman, M.A. A conserved role of IQGAP1 in regulating TOR complex 1. *J. Cell Sci.* **2012**, *125*, 2041–2052. [CrossRef] [PubMed]
65. Yamaoka-Tojo, M.; Tojo, T.; Kim, H.W.; Hilenski, L.; Patrushev, N.A.; Zhang, L.; Fukai, T.; Ushio-Fukai, M. IQGAP1 mediates VE-cadherin-based cell–cell contacts and VEGF signaling at adherence junctions linked to angiogenesis. *Arterioscler. Thromb. Vasc. Biol.* **2006**, *26*, 1991–1997. [CrossRef] [PubMed]

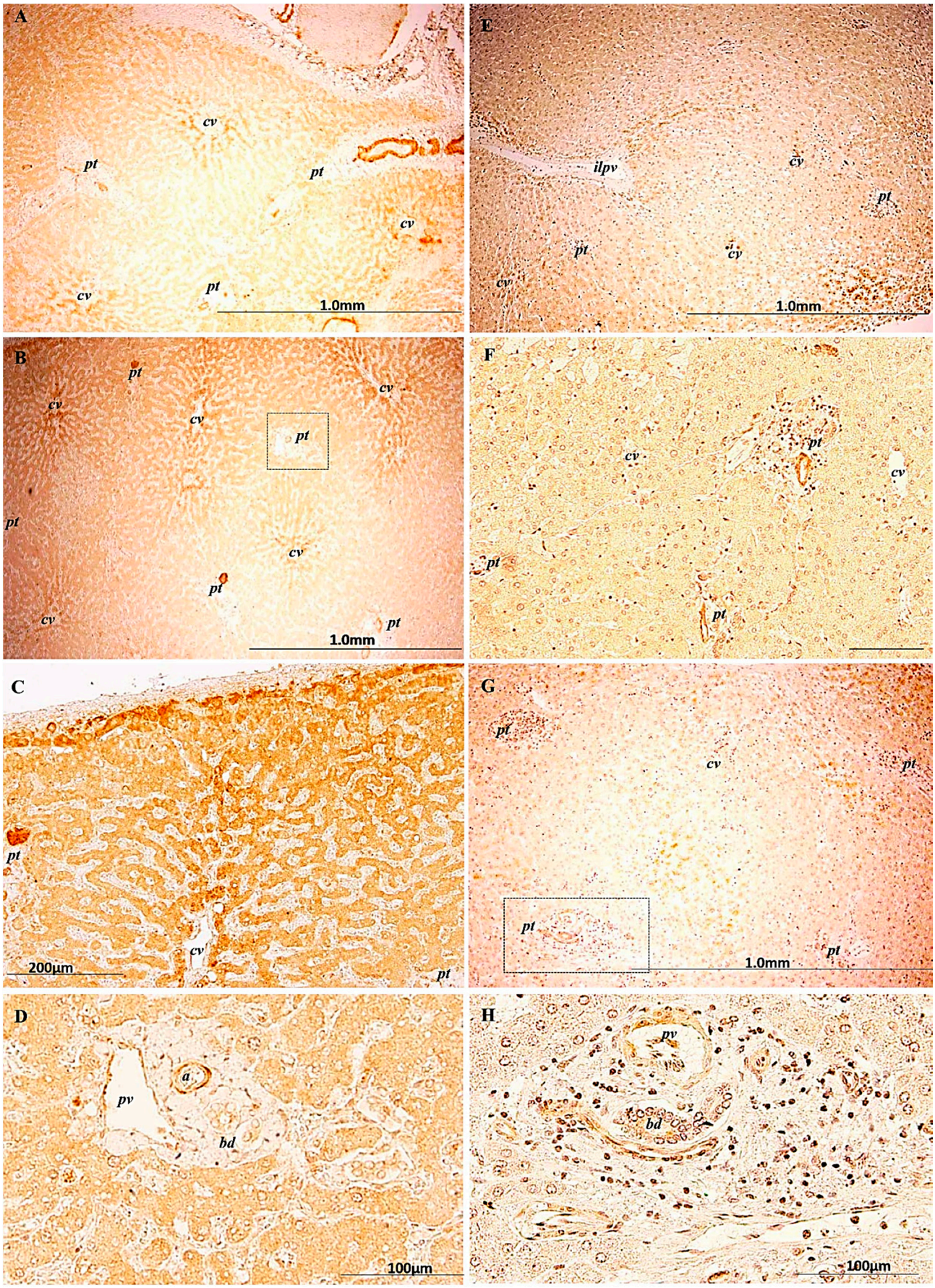

Figure S1. Immunohistochemical characterization of AmotL2 expression in healthy (A-D) and CRC metastasized liver (E-H). In healthy liver tissue sections a positive AMOTL2 cytoplasmic expression gradient is observed in hepatocytes, with

higher grades of expression in peri-venous hepatocytes (A-C). This grading of staining disappears in apparently healthy areas of metastasized liver samples (E-G). (D) and (H) are higher magnifications of the insets in B and G respectively, showing the presence of numerous inflammatory AmotL2^{+} cells in the connective tissue that surrounds portal tracts of metastasized CRC liver tissue samples (H), not observed in healthy liver (D). ***pt***=portal tract ***cv***=central vein ***ilpv***=inter lobular portal vein ***a***=artery ***bd***=bile duct ***M***=metastasis

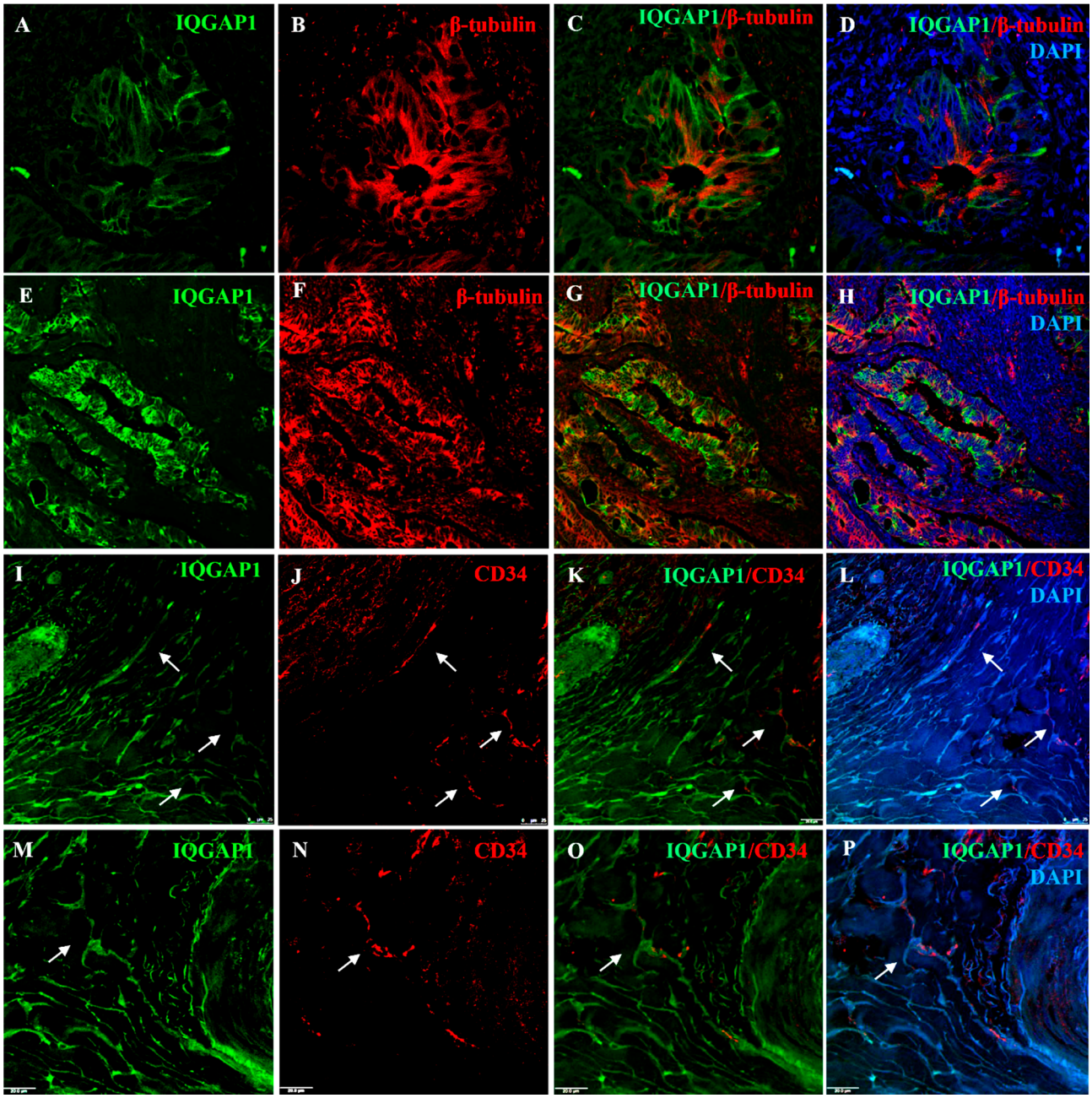

Figure S2. (**A–H**) Double immunolocalization of IQGAP1 (green) and β-tubulin (red) in CRC tissue samples. (**I–L)** Double immunolocalization of IQGAP1 (green) and CD34 (red) in CRC tissue samples. Arrows point to IQGAP1^{+}/CD34^{+} telocytes. (**M–N**) Higher magnification of panels I–L to appreciate the peculiar morphology of telocytes (arrow).

APPENDIX D
ARTICLE 4

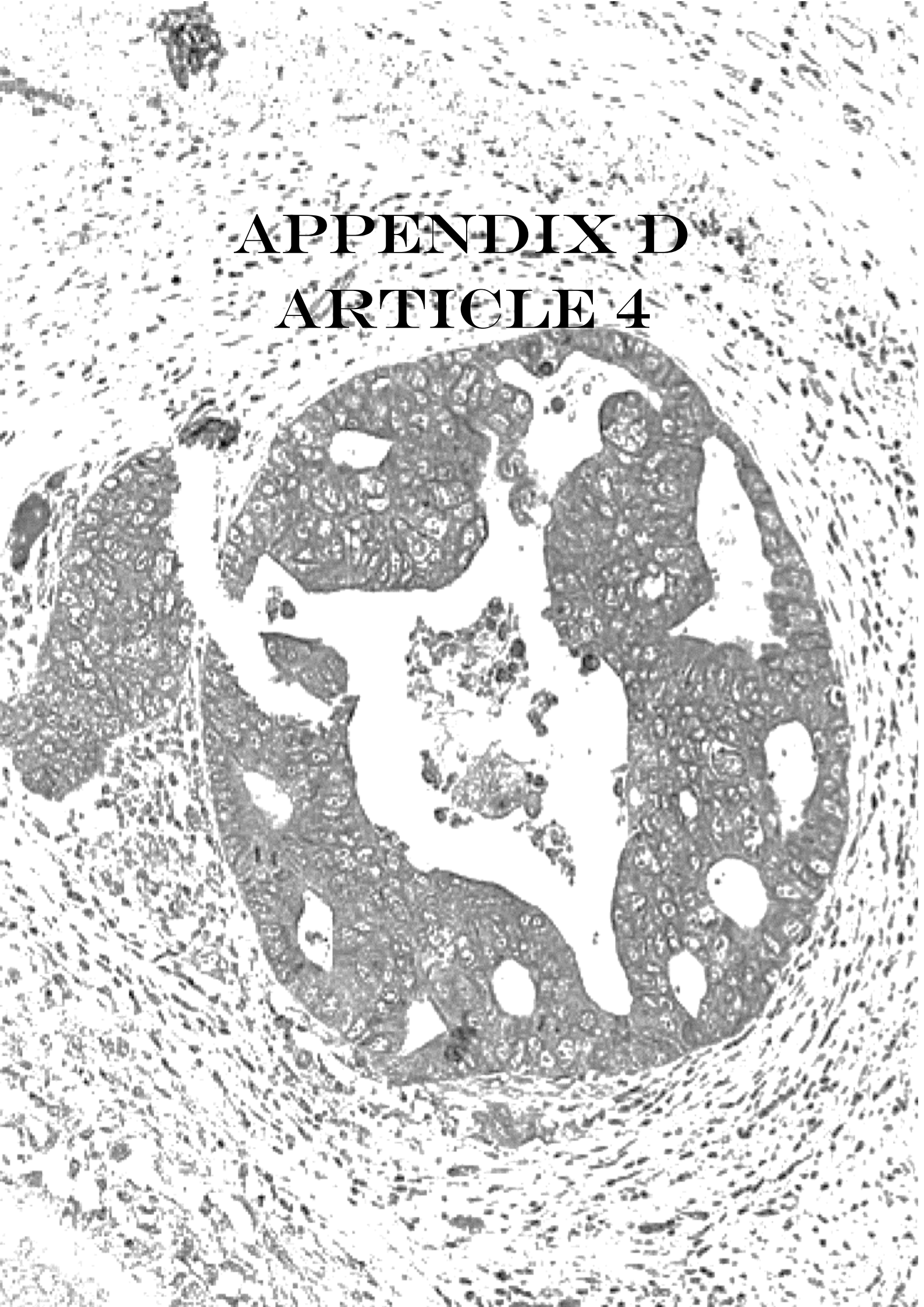

frontiers in Physiology

ORIGINAL RESEARCH
published: 29 January 2016
doi: 10.3389/fphys.2016.00009

Na,K-ATPase Isozymes in Colorectal Cancer and Liver Metastases

Marc Baker Bechmann[1†], Deborah Rotoli[1,2†], Manuel Morales[3,4], María del Carmen Maeso[5], María del Pino García[6], Julio Ávila[1], Ali Mobasheri[7,8] and Pablo Martín-Vasallo[1]*

[1] Laboratorio de Biología del Desarrollo, UD de Bioquímica y Biología Molecular and Centro de Investigaciones Biomédicas de Canarias, Universidad de La Laguna, Santa Cruz de Tenerife, Spain, [2] Institute of Endocrinology and Experimental Oncology, National Research Council, Naples, Italy, [3] Service of Medical Oncology, University Hospital Nuestra Señora de Candelaria, Santa Cruz de Tenerife, Spain, [4] Medical Oncology, Hospiten Hospitals, Santa Cruz de Tenerife, Spain, [5] Service of Pathology, University Hospital Nuestra Señora de Candelaria, Santa Cruz de Tenerife, Spain, [6] Department of Pathology, Hospiten Hospitals, Santa Cruz de Tenerife, Spain, [7] Department of Veterinary Preclinical Sciences, Faculty of Health and Medical Sciences, University of Surrey, Guildford, UK, [8] Faculty of Applied Medical Sciences, Center of Excellence in Genomic Medicine Research, King Fahd Medical Research Center, King AbdulAziz University, Jeddah, Saudi Arabia

The goal of this study was to define Na,K-ATPase α and β subunit isoform expression and isozyme composition in colorectal cancer cells and liver metastases. The α1, α3, and β1 isoforms were the most highly expressed in tumor cells and metastases; in the plasma membrane of non-neoplastic cells and mainly in a cytoplasmic location in tumor cells. α1β1 and α3β1 isozymes found in tumor and metastatic cells exhibit the highest and lowest Na^+ affinity respectively and the highest K^+ affinity. Mesenchymal cell isozymes possess an intermediate Na^+ affinity and a low K^+ affinity. In cancer, these ions are likely to favor optimal conditions for the function of nuclear enzymes involved in mitosis, especially a high intra-nuclear K^+ concentration. A major and striking finding of this study was that in liver, metastasized CRC cells express the α3β1 isozyme. Thus, the α3β1 isozyme could potentially serve as a novel exploratory biomarker of CRC metastatic cells in liver.

Keywords: Na/K-ATPase isozymes, sodium pump isozymes, colorectal cancer, colorectal cancer liver metastases, Na/K-ATPase isoforms colorectal cancer immunohistochemistry

OPEN ACCESS

Edited by:
Sigrid A. Langhans, AI duPont Hospital for Children, USA

Reviewed by:
Alessandro Sardini, Imperial College, UK
Alexi Alekov, Medizinische Hochschule Hannover, Germany

****Correspondence:***
Pablo Martín-Vasallo
pmartin@ull.es

† These authors have contributed equally to this work.

Specialty section:
This article was submitted to Membrane Physiology and Membrane Biophysics, a section of the journal Frontiers in Physiology

Received: *07 November 2015*
Accepted: *11 January 2016*
Published: *29 January 2016*

Citation:
Baker Bechmann M, Rotoli D, Morales M, Maeso MC, García MP, Ávila J, Mobasheri A and Martín-Vasallo P (2016) Na,K-ATPase Isozymes in Colorectal Cancer and Liver Metastases. Front. Physiol. 7:9. doi: 10.3389/fphys.2016.00009

INTRODUCTION

Colorectal cancer (CRC) is one of the major causes of neoplasia-related morbidity and mortality, representing the second major cause of disease incidence among females and the third among males (Jemal et al., 2011). In the western world, CRC is the 4th leading cause of death (Ferlay et al., 2010). Metastatic CRC cells can invade, populate and flourish in a new niche and ultimately cause organ dysfunction and death. CRC spawns metastases in liver, lungs, bone marrow and brain (Chiang and Massague, 2008). However, it is the liver where CRC cells metastasize most frequently (Hess et al., 2006). The first line treatment for CRC involves surgery and adjuvant oxaliplatin based chemotherapy. A common side effect of this treatment strategy is oxaliplatin-induced peripheral neuropathy (Pachman et al., 2014).

Previous research from our group has led to the identification of several genes, which were shown to be significantly up-, or down- regulated in peripheral white cells (PWCs) of CRC patients, due to oxaliplatin-based chemotherapy (Morales et al., 2014). Interestingly, one of the differentially expressed genes was the isoform α3 of the *Na,K-ATPase*; mRNA levels of *Na,K-ATPase* α3 subunit

were down-regulated 2.6-fold. Moreover, an alteration in the intracellular location of Na,K-ATPase α3 isoform has been reported in human CRC tumor cells vs. normal colon (Sakai et al., 2004). Additionally, other laboratories have shown differential expression in cells, altered subcellular localization and down regulation of the β subunit of the Na^+/K^+-ATPase in carcinoma cells (Rajasekaran et al., 1999, 2001a,b, 2010).

Na,K-ATPase is an integral protein in the plasma membrane of all animal cells that transports three sodium ions out and two potassium ions into the cell, against electrochemical gradient (Skou, 1957; Jorgensen et al., 2003). This activity is necessary for the regulation of the cellular ionic homeostasis and maintaining the electrochemical gradient required for ion channel function and secondary active transport (Mobasheri et al., 2000). Recently, additional functions for the Na,K-ATPase in the cell have been proposed, as a signal transducer and transcription activator (Aizman et al., 2001; Miyakawa-Naito et al., 2003; Harwood and Yaqoob, 2005; Yuan et al., 2005; Zhang et al., 2006) affecting cell proliferation (Abramowitz et al., 2003), cell motility (Barwe et al., 2005), and apoptosis (Wang and Yu, 2005). Besides this, the Na,K-ATPase is the receptor of cardiotonic glycosides. It is functionally composed of catalytic α (100–112 kDa) and regulatory β (45–55 kDa) subunit and an optional γ (6.5–10 kDa) subunit belonging to the FXYD family of proteins (Mercer et al., 1993).

Na,K-ATPase is expressed as several isozymes. Four different isoforms of the α subunit have been found in humans (Blanco, 2005). The α1 isoform (*ATP1A1* gene) is expressed almost in all tissues. Isoform α2 (*ATP1A2* gene) is the predominant isoform in skeletal muscle (Hundal et al., 1992), brain (astrocytes) (McGrail et al., 1991), heart (Zahler et al., 1992), and adipose tissue (Lytton et al., 1985). The α3 isoform (*ATP1A3* gene) is primarily found in the brain (neurons) (Hieber et al., 1991; McGrail et al., 1991) and isoform α4 (*ATP1A4* gene) is only expressed in testis (Woo et al., 2000). In reference to the β subunit, three different isoforms have been identified: β1 (*ATP1B1* gene), β2 (*ATP1B2* gene) and β3 (*ATP1B3* gene). While β1 has a generalized expression in almost all tissues and cells, the expression of the other β isoforms are more restricted to certain tissues and cells. The β2 isoform is found in skeletal muscle (Lavoie et al., 1997), pineal gland (Shyjan et al., 1990), and nervous tissues (Peng et al., 1997), whereas β3 is present in testis, retina, liver, and lung (Malik et al., 1996; Zahler et al., 1996; Arystarkhova and Sweadner, 1997; Martin-Vasallo et al., 2000). The expression pattern of the Na,K-ATPase subunit-isoforms is subjected to developmental and hormonal regulation and can be altered during disease (Book et al., 1994; Charlemagne et al., 1994; Charlemagne and Swynghedauw, 1995; Ewart and Klip, 1995; Zahler et al., 1996).

The purpose of this study was to determine the cellular and subcellular localization of the α and β subunit isoforms of Na,K-ATPase in CRC and its liver metastasis using a panel of well-characterized isoform-specific antibodies. The primary hypothesis of this study was that metastatic cancer cells possess a unique expression phenotype of Na,K-ATPase isozymes, similar to that of CRC cells.

MATERIALS AND METHODS

Tissue Samples

The Ethics Committee of the Universidad de La Laguna (ULL) and Ethical Committee of the Hospital Universitario Nuestra Señora de Candelaria (HUNSC) approved this study. All patients signed an informed-consent document for diagnosis and research on tissue specimen before being enrolled in the project. All the study subjects were treated with FOLFOX CT: day 1 oxaliplatin 100 mg/m^2 iv over 2 h; leucovorin calcium 400 mg/m^2 iv over 2 h; followed by 5-fluorouracil 400 mg/m^2 iv bolus and by 5-fluorouracil 2400 mg/m^2 iv over 46 h; every 14 days. Paraffin-embedded tissue samples and clinical data were obtained from 15 patients (7 males, 8 females) and 1 control male from the reference medical areas of HUNSC.

Antibodies

Table 1 shows antibodies and references used in this study. Secondary antibodies used were goat anti-rabbit IgG or goat anti-mouse IgG. Biotinylated secondary antibody was used for immunohistochemistry (IHC), whereas secondary antibodies targeted with specific fluorochromes were used for immunofluorescence (IF).

Immunohistochemistry

Five-micron thick paraffin embedded tissue sections were deparaffinized in xylene and hydrated in graded series of alcohol baths. Heat mediated antigen retrieval was performed in an autoclave at 120°C for 10 min in sodium citrate buffer pH 6.0 before commencing the IHC staining protocol. To remove endogenous peroxidase activity, sections were incubated with 3% H_2O_2 in methanol for 15 min at room temperature. Non-specific sites were blocked with 5% Fetal Bovine Serum (FBS), 0.3% Triton-X-100 in Tris-buffered saline (TBS) for 1 h at room temperature. Endogen biotin was blocked with the Avidin/Biotin Vector Blocking Kit (Vector Laboratories Inc., #SP-2001, Burlingame, CA 94010, USA) according to the manufacturer's instructions. Primary antibodies (see **Table 1**) were incubated O/N at 4°C. Slices were then incubated for 2 h at 37°C with biotin-conjugated secondary antibodies (see **Table 1**). Antibodies for IHC were diluted in TBS, 5% FBS, 0.1% Triton. To amplify the specific antibody staining, ABC complex (Pierce, Thermo Fisher Scientific Inc., #32020, Waltham, MA, USA) was applied to the sections, prepared according to manufacturer's instruction and incubated for 1 h at room temperature. 3,3′-diaminobenzidine (DAB) Substrate Concentrate (Bethyl Laboratories Inc., #.IHC-101F, Montgomery, Texas, USA) was used to visualize immunoperoxidase activity. Slides were counterstained with Harris Hematoxylin solution DC (Panreac, #256991.1610 Barcelona, Spain) to visualize cell nuclei. Samples were mounted with Eukitt (Panreac, #253681, Barcelona, Spain) and optical light microscope (Olympus BX50, Tokyo, Japan) was used to visualize IHC staining results. Images were acquired using the Olympus DP70 camera and the DP controller software 2.1.1.183 (Copyright 2001–2004 Olympus Corporation). Negative control experiments were carried out by

TABLE 1 | Antibodies used in this study. α1(620) (Sztul et al., 1987), α3 (Pietrini et al., 1992), α3 (XVIF9-G10) (Arystarkhova and Sweadner, 1996), SpETβ1 and SpETβ2 (Gonzalez-Martinez et al., 1994).

Antibody	Target	Host	Type	Dilution	Source
α1(620)	α1-isoform*	R	P	1:1000	M. J. Kashgarian
α3	α3-isoform*	R	P	1:600	M. Caplan
α3 (XVIF9-G10)	α3-isoform*	M	Mc	1:5	Arystarkhova and Sweadner
SpETβ1	β1-isoform*	R	P	1:600	P. Martin-Vasallo
SpETβ2	β2-isoform*	R	P	1:600	P. Martin-Vasallo
Anti-proliferating cell antigen (Anti-PCNA)	PCNA	M	Mc	1:100	Boehringer Mannheim
Anti-rabbit IgG (H+L), biotin conjugated (2°)	Rabbit-IgG	G	P	1:300	Pierce
Anti-rabbit IgG (whole molecule), FITC-conjugated (2°)	Rabbit-IgG	G	P	1:200	Sigma
Anti-mouse IgG, DyLight®650-conjugated (2°)	Mouse-IgG	G	P	1:100	Abcam

R, rabbit; G, goat; M, mouse; Mc, monoclonal; P, polyclonal.
**subunit-isoforms of the Na,K-ATPase, 2°: secondary antibody.*

following the procedure stated above but without incubating with primary antibody.

Double Immunofluorescence Simultaneous Staining

As with the IHC samples, tissue sections for IF staining were paraffin embedded. After deparaffinization, hydration and heat-induced epitope retrieval procedure (as described above for the IHC staining), slides were incubated with 5%BSA, 0.3%Triton-X-100 in TBS to block non-specific sites. Then tissue sections were incubated simultaneously with a mixture of two distinct primary antibodies (e.g., rabbit against human target 1 and mouse against human target 2) overnight at 4°C. Slices were then incubated for 1 h at room temperature in dark with a mixture of two secondary antibodies (see **Table 1**) conjugated to two different fluorochromes (i.e., FITC-conjugated against rabbit-Sigma and DyLight®650-conjugated against mouse-Abcam). Antibodies for IF were diluted in TBS, 1% bovine serum albumin (BSA), 0.1% Triton. Slides were mounted with ProLong®Diamond Anti-fade Mountant with DAPI (Molecular Probes by Life Technologies, #P36962, Eugene, Oregon, USA) to visualize cell nuclei. Slides were acquired and analyzed using Olympus confocal microscope (Olympus FV1000, Tokyo, Japan) and the software FV10-ASW1.3; Lasers: Diode 405 nm, Argon multiline 458/488/514, HeNe 633 nm. Images were acquired by sequential scan (first sequence Diode and HeNe, second sequence Argon) to avoid overlapping of channels. Image resolution 1024 × 1024. Objective lens: 60X/1.35 NA oil Plan-Apochromat. Negative control experiments were carried out by following the same immunohistochemical procedure but with the primary antibody omitted.

Image Analysis and Scoring

Samples were evaluated by two independent observers who were blinded to the clinical data. Scores were graded as absent (−), moderate (+) or strong (+ + +) for any specific kind of cell. These cut-offs were established by consensus of all investigators. For all tumors this grading was applied to three different patterns of Na,K-ATPase α and β subunit isoform staining in tumor cells: staining of the plasma membrane; staining of the nuclear envelope and staining of the cytoplasm.

Final results were computed as the product of staining intensities. In cases where scorings differed, the observers re-evaluated samples to consensus. All samples were analyzed and scored.

RESULTS

Na,K-ATPase α1 and α3 Isoform Expression in CRC

In healthy colon tissue (**Figures 1A,C**), the α1 isoform was detected at the basolateral side of the plasma membrane of epithelial cells lining the colonic *mucosae* of Lieberkühn Crypts and in discrete stromal cells in the connective tissue surrounding the crypts. In turn, α1 isoform was mainly detected in a peri-nuclear location in tumor cells (**Figures 1B,D**). Mesenchymal cells from the stromal tissue surrounding the tumor also exhibited positive immunostaining (**Figures 1B,D**).

The Na,K-ATPase α3 isoform was detected on epithelial cells lining the colonic crypts and on cells from the *lamina propria* in healthy colon (**Figure 1E**). The α3 isoform was mainly detected in or near the plasma membrane of epithelial cells and in the cytoplasm of positively stained cells in the stroma. In CRC tumor samples, the α3 isoform was mainly located in a peri-nuclear location in CRC tumor cells, while in the plasma membrane of these cells staining was negative (**Figure 1F**). Stromal cells surrounding the tumor were also α3-positive. Immunolabeling for the α3 isoform was also detected in microvascular endothelial cells (**Figure 1H**) and in cells from the inflammatory reaction associated with CRC within the stroma (**Figure 1G**), where the α3 isoform showed an intense and specific peri-nuclear labeling.

Na,K-ATPase β1 Isoform Expression in CRC

The β1 isoform of Na,K-ATPase was detected in epithelial cells from the normal colonic *mucosae* (**Figure 2A**). There was a high positive staining at the baso-lateral side of polarized epithelial cells that line the colonic Lieberkühn crypts (**Figure 2B**).

In CRC tumors, the β1 isoform presented a less defined expression pattern. This isoform was detected in some tumor cells, but the location was not well-defined, and was seen in

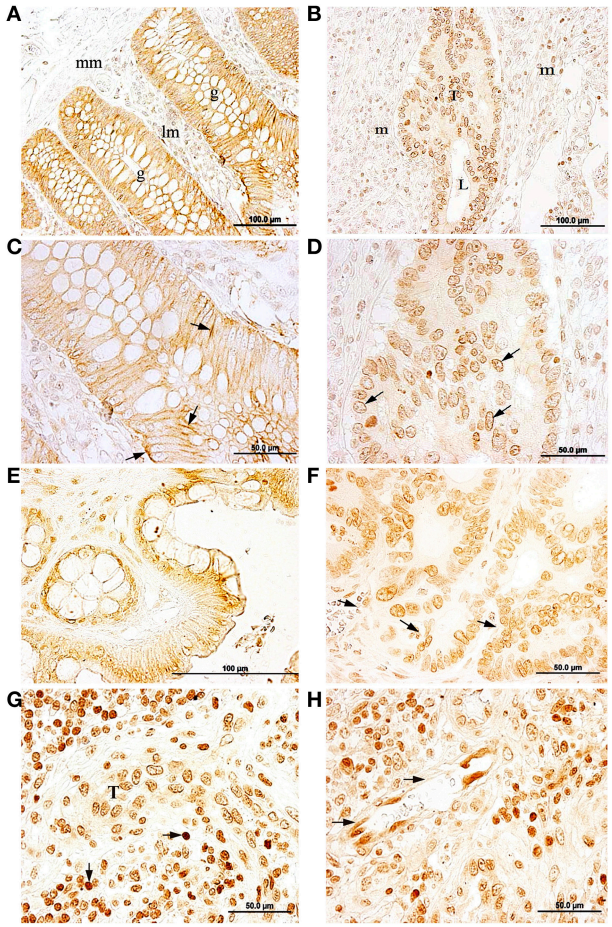

FIGURE 1 | Immunolocalization of the Na,K-ATPase α1 and α3 subunit isoforms in normal colon and colorectal cancer (CRC). (A,C) α1 immunostaining in baso-lateral side of polarized epithelial cells in healthy colonic *mucosae*, black arrow. g, colonic gland (Lieberkühn crypts); mm, *muscularis mucosae*; lm, *lamina propia mucosae*. (**B,D)** peri-nuclear labeling for the α1 isoform in tumor cells. T, tumor; L, lumina; m, mesenchymal tissue. **(E)** α3 immunostaining in plasma membrane of healthy colon epithelial tissue. **(F)** α3 expressed peri-nuclearly in CRC tumor (arrows). **(G)** α3 immunostaining in tumor cells (T) surrounded by immune cells (arrows). **(H)** Endothelial cells expressing the α3 isoform in a peri-nuclear location (arrows).

several subcellular locations within the tumor. In some tumor cells β1 staining was peri-nuclear (**Figure 2C**), while in others a peripheral location was observed (**Figure 2C**).

In addition, in healthy tissue, β1 was detected in cells of the myenteric plexus, also known as the Auerbach's plexus, within the muscular tissue of the *muscularis propia* (**Figure 2E**). In the cells from the plexus, Na,K-ATPase β1 isoform was detected in or near the cytoplasmic membrane of axons and dendrites of neurons and glial cells (**Figure 2F**).

Na,K-ATPase β2 Isoform Expression in CRC

The β2 isoform was detected at the baso-lateral side of polarized epithelial cells from the normal colonic *mucosae* and in

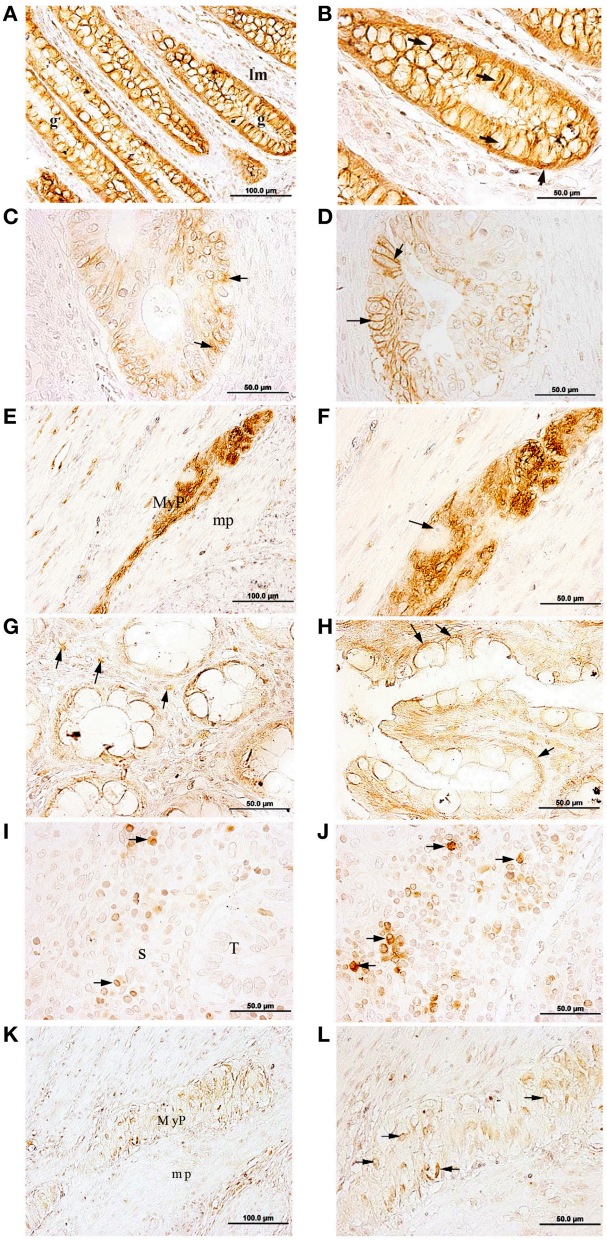

FIGURE 2 | Immunolocalization of the Na,K-ATPase β1 and β2 isoforms in normal colon and CRC. (A,B) β1 is mainly located at the baso-lateral side of polarized epithelial cells from the normal colonic *mucosae* (arrows in **B**). **(C)** β1 is located in the cytosol of tumor cells (arrows). **(D)** β1 is located at the cell membrane of tumor cells (arrows). **(E)** Cells from the myenteric plexus (MyP) at the *muscularis propia* (mp) express β1. **(F)** β1 isoform is mainly located in or near the cytoplasmic membrane of the neurons and/or glia; a neuron nucleus with visible nucleolus is indicated using an arrow. g, colonic gland (Lieberkühn crypts); lm: *lamina propia mucosae*. **(G)** Selected cells from the connective tissue of the *mucosae* express the β2 isoform (arrows). **(H)** β2 is mainly located at the baso-lateral side of polarized epithelial cells from the normal colon *mucosae* (arrows). **(I)** β2 was not detected in tumor cells from adenocarcinomatous glands (T); however, some stroma (S) cells express β2 (arrows). **(J)** Possible leukocytes of the stroma expressing β2 (arrows). **(K)** Cells from the myenteric plexus (MyP) at the *muscularis propia* (mp) express β2. **(L)** β2 isoform is mainly located at the soma of glia cells (arrows).

selected fibroblastic and immune cells from the *lamina propria* (**Figure 2G**) and (**Figure 2H**). In colon adenocarcinoma cells, the β2 isoform was not detected (**Figures 2I,J**). However, some immune cells located in the stromal tissue surrounding the tumor, were β2 positive while others remained negative (**Figures 2I,J**). In immunopositive cells, β2 staining was detected peri-nuclearly and also throughout the cytoplasm. Immunostaining intensity for the β2 isoform varied from strong to weak across cells in this region. In myenteric plexus (**Figure 2K**) the β2 isoform was detected in the soma of neural cells (**Figure 2L**).

Co-Expression of Na,K-ATpase α3 and β1 Isoforms and PCNA

In CRC, some cells from adenocarcinomatous glands showed positive staining to both PCNA (nuclei) and Na,K-ATPase α3 isoform (cytoplasm) (**Figure 3**), and PCNA and β1 isoform (plasma membrane) (**Figure 3**).

Na,K-ATPase α1 and α3 Isoform Expression in CRC Metastases in Liver

In healthy liver tissue, hepatocytes were immunopositive for α1, in the plasma membrane (**Figure 4A**). Bile ducts cells were also α1 positive (**Figure 4B**), and the staining was detected mainly at the baso-lateral side of the plasma membrane. In metastases, the Na,K-ATPase α1 isoform was detected in cytoplasm and in the cytoplasmic membrane of cells of metastatic tumor niches (**Figures 4C,D**).

In normal healthy liver, Na,K-ATPase α3 isoform was not detected in any cell types (**Figure 4E**). However, in metastatic tumor cells within the liver, the α3 isoform was detected (**Figure 4F**; Supplementary Figure S1D) in a peri-nuclear location and spread across the cytoplasm. Staining intensity varied among cells, from strong to weak labeling. In addition to tumor cells, this isoform was also detected in immune cells located at the outermost part of the liver (**Figure 4G**). In apparently healthy liver tissue surrounding metastases, Na,K-ATPase α3 isoform was detected peri-nuclearly and also throughout the cytoplasm of hepatocytes (**Figure 4H**).

Na,K-ATPase β1 and β2 Isoforms Expression in Metastasis

In metastasized liver, the β1 isoform was detected at the plasma membrane of hepatocytes (**Figure 5A**), bile ducts epithelial cells (**Figure 5B**) and peri-nuclearly and/or in the cytoplasm of cells in disorganized and necrotic tissue (**Figures 5C,D**; Supplementary Figure S1C).

In healthy liver tissue, the β2 isoform was detected in the cytoplasm of some cells and in peri-nuclear locations in others (**Figures 5E,F**), with variable staining intensities among cells ranging from strong to weak. A weak but specific signal for the β2 isoform was also detected in bile ducts cells at the portal triads (**Figure 5G**). However, the β2 isoform was not detected in metastatic tumor cell niches (**Figure 5H**).

We were unable to detect the α2 and β3 subunit isoforms as their expression levels were probably below the threshold of the ABC amplified immunohistochemical detection technique employed in this study.

Na,K-ATPase α3 and β1 Isoforms Coexpression in Metastasis

In order to further confirm the co-expression of the α3 and β1 subunits isoforms in the same metastatic cells in the liver, using a different and monoclonal antibody, we performed confocal microscopy co-localization experiments. Image analysis and scoring was done using same procedure as in all other cases

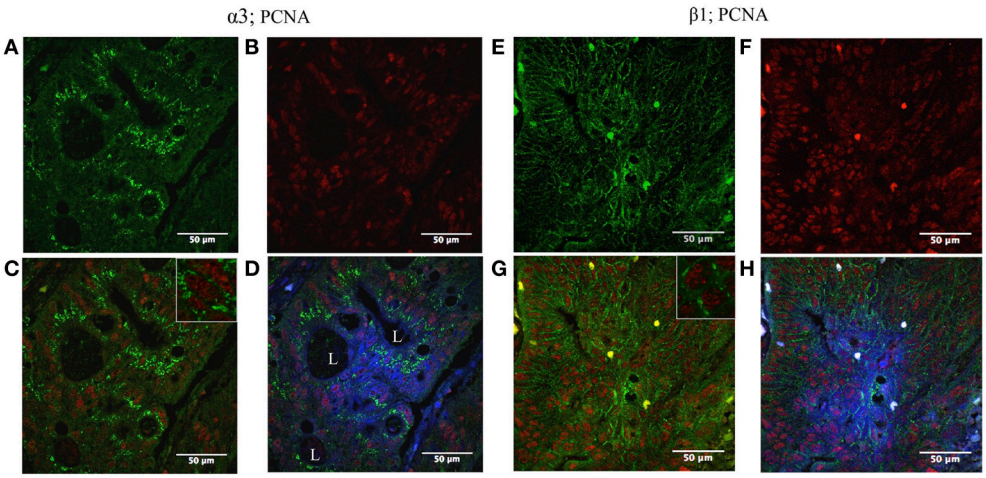

FIGURE 3 | Double immunofluorescence localization of Na,K-ATPase α3 and β1 isoform and proliferating cell nuclear antigen (PCNA) in CRC. Left panel: **(A)** α3 isoform is expressed in colon tumor cells (green). **(B)** High numbers of tumor cells express PCNA (red). **(C)** The tumor cells express both PCNA and the α3 isoform (blue and green merged). **(D)** α3 isoform is mainly located internally at the cytoplasm; blue (DAPI), red (PCNA), and green (α3 isoform) merged image. L, lumina. Right panel: **(E)** β1 isoform is expressed in colonic tumor cells (green). **(F)** High number of tumor cells expresses PCNA (red). **(G)** The tumor cells express both PCNA and β1 isoform (red and green merged). **(H)** Blue (DAPI), red (PCNA), and green (β1 isoform) merged image.

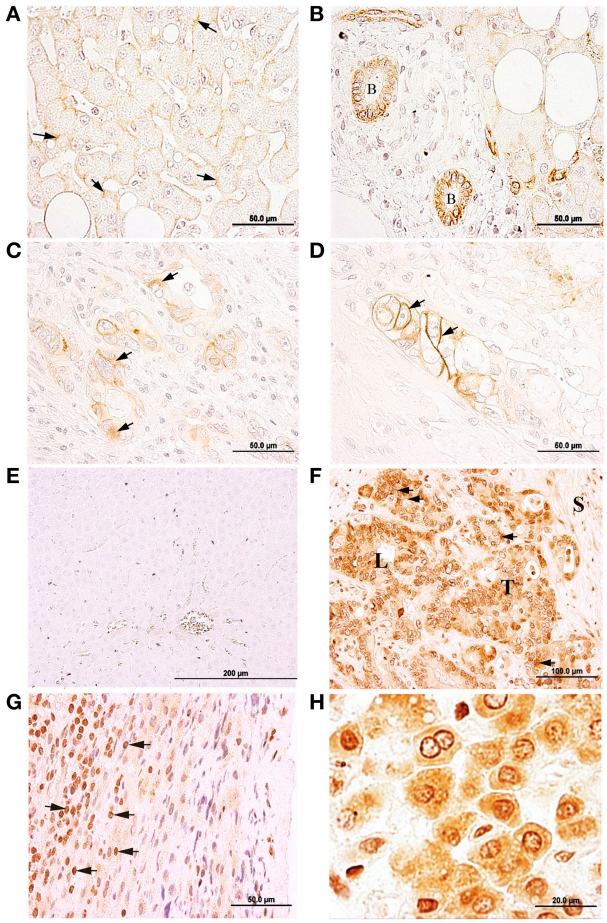

FIGURE 4 | Immunolocalization of the Na,K-ATPase α1 and α3 isoforms in normal liver and liver metastasis. (A) α1 isoform is located at the plasma membrane of the hepatocytes (arrows). **(B)** Bile duct epithelial cells (B) express α1 isoform, mainly at the baso-lateral side of cell membrane. **(C)** α1 isoform is located at the cytosol of metastatic tumor cells (arrows). **(D)** α1 is present at a peripheral position in metastatic tumor cells (arrows). **(E)** Negative immunolocalization of the α3 isoform in normal liver tissue. **(F)** α3 isoform is mainly located at a peri-nuclear position but also detected all-over the cytoplasm. **(G)** Inflammatory reaction established at the outermost part of the liver; α3 IHC-positive cells may correspond to cells from the immune system (arrows), such as leukocytes. **(H)** In normal liver tissue from a metastasized liver, hepatocytes express α3 in peri-nuclear and cytoplasmic locations.

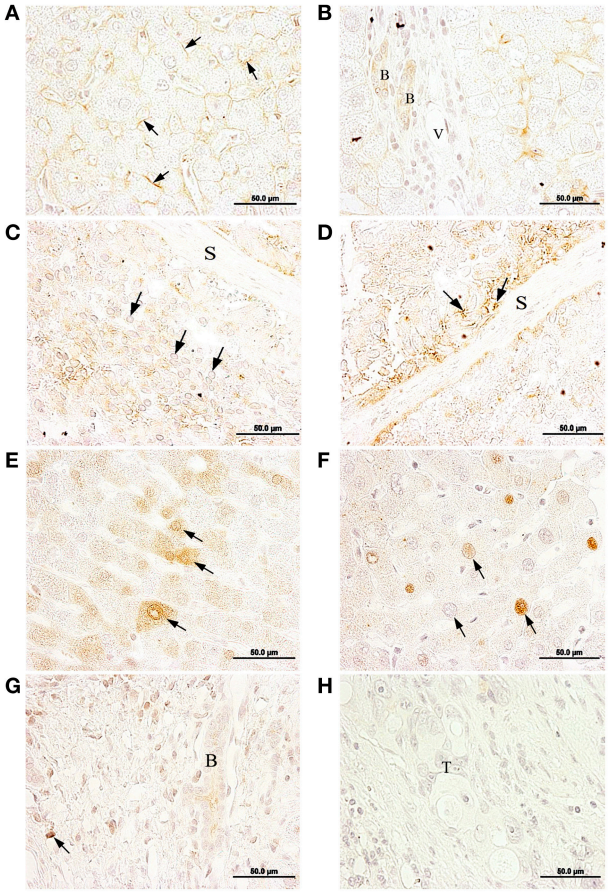

FIGURE 5 | Immunolocalization of the Na,K-ATPase β1 and β2 isoforms in normal liver tissue and liver metastasis. (A) β1 isoform is mainly located at the cytoplasmic membrane of hepatocytes (arrows) from normal liver. **(B)** Bile duct epithelial cells (B) express β1, V, venule. **(C)** Nuclei of metastatic tumor cells (arrows). **(D)** β1 IHC-positive staining at necrotic tissue is signaled with arrows; S, septum. **(E)** β2 is differentially expressed at the cytoplasm of neighboring hepatocytes (arrows) of normal liver. **(F)** Hepatocytes with different degrees of β2 immunostaining at a peri-nuclear position in neighboring hepatocytes (arrows) of normal liver. **(G)** In normal liver, a bile duct (B) and cells from the lining connective tissue (arrow) express β2. **(H)** Metastatic tumor cells (T) do not express β2.

and stated in the Materials and Methods section. As shown in **Figure 6** and in Supplementary Figure S1, both of them co-localize in a number of metastatic cells in percentages ranging from + to +++, depending on the sample and on the area within the same sample. Most of them showed further more than 2/3 of total metastatic cells.

DISCUSSION

In this study we explored the cellular and subcellular localization of the α and β subunit isoforms of Na,K-ATPase in CRC and its liver metastases. The aim of this work was to test the hypothesis that metastatic cancer cells possess a unique expression phenotype of Na,K-ATPase isozymes, which may be similar to that of CRC cells. **Table 2** summarizes the cell-specific Na,K-ATPase subunit-isoforms expression and **Table 3** highlights the possible cell-specific Na,K-ATPase isozymes present in healthy colon, colorectal cancer, healthy liver and metastasized liver.

Based on the results presented we propose that the predominating isozymes in tumor cells from the colon and metastases in the liver are α1β1 and α3β1. The α3β1 isozyme of Na,K-ATPase is only present in liver metastases but not in healthy liver, thus, the α3β1 isozyme could serve as a novel exploratory biomarker of CRC metastatic cells in liver. Further studies should be carried out to test the utility of this observation.

Subunits of Na,K-ATPase have the ability to form functional isoenzymes by a promiscuous association of α and β isoforms

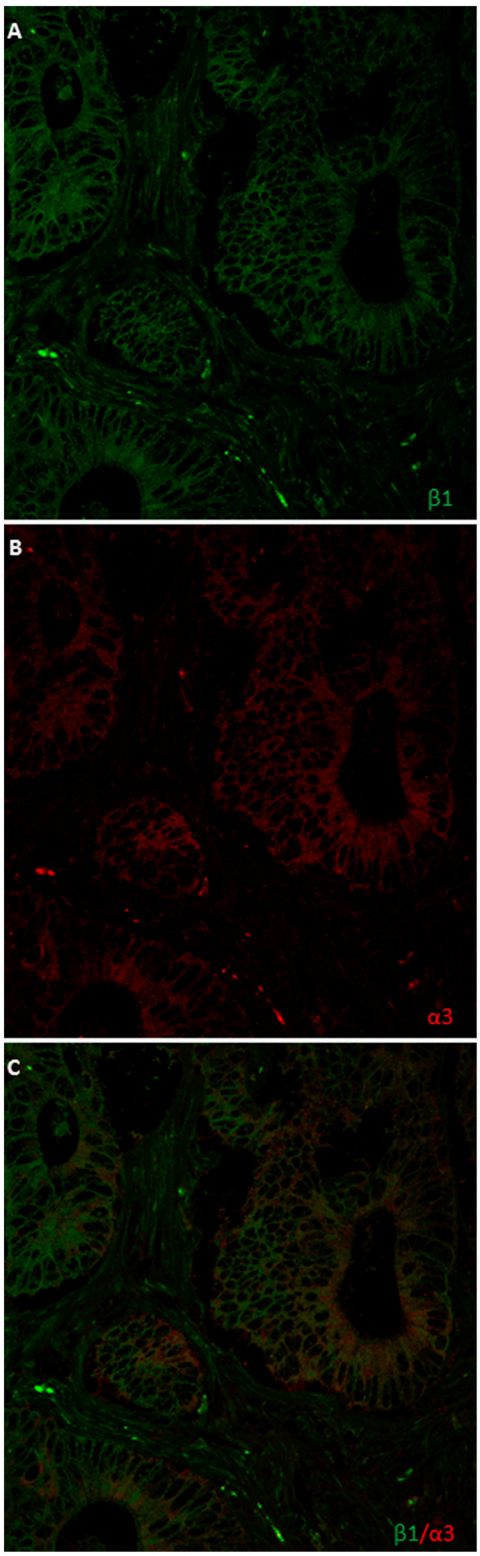

FIGURE 6 | Double immunofluorescence localization of Na,K-ATPase α3 and β1 isoform in liver metastasis. (A) α3 isoform is located at a peri-nuclear position and all-over the cytoplasm. **(B)** β1 isoform is mainly located at the plasma membrane of metastases cells and in nuclear envelope. **(C)** Merge.

TABLE 2 | Cell-specific Na,K-ATPase subunit-isoform expression in normal colon, colorectal cancer, normal liver, and metastasized liver.

	α1	α3	β1	β2
Normal colon				
Epithelial cells (*Mucosae*)	+++	+++	+++	+
Mesenchymal cells (*Submucosae*)	+	+	+	+
Smooth muscle cells (*Muscularis mucosae*)	?	?	?	?
Neurons (Myenteric plexus)	?	+	+++	?
Glia cells (Myenteric plexus)	?	?	+++	+++
Smooth muscle cells (*Muscularis propia*)	?	+	–	+
Colorectal cancer				
Tumor cells	+++	+++	+++	–
Mesenchymal cells (not immune system cells)	+	+++	–	+
Immune system cells	?	+++	?	?
Endothelial cells	?	+++	–	?
Epithelial cells (*Mucosae*)	+++*	+++	+++	–
Normal liver				
Hepatocytes	+++	–	+++	+
Ephitelial cells (bile duct)	+++	–	+	+
Endothelial cells	–	–	–	–
Mesenchymal cells (connective tissue)	–	–	–	+
Metastasized liver				
Tumor cells	+++	+++	+	–
Hepatocytes	?	+	?	–*
Epithelial cells (Bile duct)	+++	?	?	?
Mesenchymal cells (connective tissue)	–	+	–	–
Immune system cells	–	+++	?	?

*+ + +, indicates a high staining level; +, indicates low staining level; –, indicates no staining detected; and ?, indicates indeterminate staining, according to our observations. *Data not shown.*

to confer significantly different kinetic and biological properties. The apparent affinities for cations and ouabain have been determined by expressing recombinant enzymes in heterologous systems. Affinities of human isozymes expressed in *Xenopus laevis* oocytes are α1β1>α2β1>α3β1 for Na^+ and α3β1=α1β1>α1β3>α1β2>α2β1>α3β3>α3β2>α2β3>α2β2 for K^+ (Blanco and Mercer, 1998; Crambert et al., 2000). Tumor cells and metastatic cells have isozymes with highest and lowest Na^+ affinity and surrounding mesenchymal cells possess isozymes with medium range affinity. Regarding K^+ affinity, tumor and metastasis cells possess Na,K-ATPase isozymes of high K^+ affinity and mesenchymal cells low K^+ affinity. These are the isozyme combinations that permit an optimal performance of the enzymes involved in protein synthesis and transfer of phosphor groups (Glynn, 1985) processes both involved in carcinogenesis.

Another objective of this study was to correlate the mitotic index related to the expression of isoforms by co-localization of those along with PCNA, the clamp subunit of DNA polymerase δ marker of cell proliferation (Kubben et al., 1994; Bleau et al., 2014) and carried out further analysis by confocal microscopy. **Figure 3** shows cells expressing the α3 and β1 isoforms in CRC tumor cells, in which no correlation was seen between sodium pump isoforms and PCNA protein expression, that is, high

TABLE 3 | Possible cell-specific Na, K-ATPase isozymes present in normal colon, colorectal cancer, normal liver, and metastasized liver.

	α1β1	α1β2	α3β1	α3β2
NORMAL COLON				
Epithelial cells (*Mucosae*)	+++	+	+++	+
Mesenchymal cells (*Submucosae*)	+	+	+	+
Smooth muscle cells (*Muscularis mucosae*)	?	?	?	?
Neurons (Myenteric plexus)	?	?	+++	?
Glia cells (Myenteric plexus)	?	?	?	?
Smooth muscle cells (*Muscularis propia*)	–	?	–	+++
COLORECTAL CANCER				
Tumor cells	+++	–	+++	–
Mesenchymal cells (Not immune system cells)	–	+	–	+++
Immune system cells	?	?	?	?
Endothelial cells	–	?	–	?
Epithelial cells (*Mucosae*)	+++	–	+++	–
NORMAL LIVER				
Hepatocytes	+++	+	–	–
Ephitelial cells (Bile duct)	+++	+++	–	–
Endothelial cells	–	–	–	–
Mesenchymal cells (Connective tissue)	–	–	–	–
METASTIZED LIVER				
Tumor cells	+++	–	+++	–
Hepatocytes	?	–	?	–
Epithelial cells (Bile duct)	?	?	?	?
Mesenchymal cells (Connective tissue)	–	–	–	–
Immune system cells	–	–	?	?

+ + +, Indicates a possible high level of the isozyme; +, indicates a possible low presence of the isozyme; –, indicates no possibility; and ?, indicates indeterminate staining, according to our observations.

expression of PCNA can be found in cells with either, high or low, expression level of α3 or β1 and vice versa.

Hideki Sakai and co-workers (Sakai et al., 2004) used western blotting to demonstrate a decrease in α1 isoform expression in CRC and, inversely, an increase in the α3 isoform compared to the accompanying healthy *mucosae*. In addition they did not observe a significant expression level of Na,K-ATPase α2 isoform either in the CRC or in the accompanying healthy *mucosae*. Our study, confirms their observations. In addition, in recent studies of hepatocellular carcinoma, a significantly higher α3 level expression was shown in western blots compared to the accompanying non-tumor tissues, whereas no significant increases in expression of α1 and α2 proteins was observed (Shibuya et al., 2010).

Recently, it has been suggested that the cellular distribution and expression of Na,K-ATPase α3 isoform affects the anti-proliferative effects of oleandrin, a cardiac glycoside that inhibits the Na,K-ATPase (Yang et al., 2014). These authors demonstrated that healthy, as opposed to neoplastic colonic and lung tissues, exhibit different distributions of the α3 isoform. While the α3 isoform was predominantly located in the cytoplasmic membrane in healthy colon and lung, the distribution of this isoform was shifted to a predominantly peri-nuclear location in tumors. These observations have been corroborated by our laboratory. Furthermore, our results showed a subcellular location shift for the α1 isoform, which was mainly located at the basolateral side of the plasma membrane of healthy colonic epithelial cells, shifting to a peri-nuclear position in CRC tumor cells.

The α1 and α3 subunit isoforms were detected in all cells lining the colonic crypts. These isoforms were not only expressed in epithelial cells in healthy colon *mucosae*, but they were also detected in mesenchymal cells from the *lamina propria*. The α3 isoform presents a high expression level in neurons of the central nervous system (Hieber et al., 1991; McGrail et al., 1991). The present study shows specific staining for α3 in neurons from myenteric plexus.

Regarding the β subunit, it has been reported that expression of both the β1 and β2 mRNAs were decreased in renal, lung and hepatocellular carcinomas (Akopyanz et al., 1991), and that expression levels of the corresponding proteins was decreased in human clear cell renal cell carcinoma (Rajasekaran et al., 1999) and bladder carcinoma (Espineda et al., 2004). Previous work from our laboratory (Avila et al., 1997) reported, by western blot technique, that gastric and colon adenocarcinoma showed opposite patterns of β1 isoform expression. While gastric adenocarcinomas showed lower expression levels of β1 than the healthy tissue, colonic adenocarcinomas showed higher expression of this isoform compared to healthy surrounding tissue. In addition, the β2 isoform was neither detected in healthy colon, nor in stomach adenocarcinomas. In the present immunohistochemical study, we detected the β1 and β2 isoforms at the baso-lateral side of the plasma membrane in the healthy colon *mucosae*, but only β1 was found in CRC samples. Which, in a certain manner, resembles our previous findings in Na,K-ATPase in dog and rat prostate cancer where we found a downregulation and a reduced expression of sodium pump (Mobasheri et al., 2000, 2003a,b,c).

Na,K-ATPase β1 and β2 isoforms were detected in the myenteric plexus of healthy colon tissue. It is well-established that the β2 isoform of Na,K-ATPase, is an adhesion molecule on glia (AMOG) (Antonicek et al., 1987; Gloor et al., 1990).

In tumor samples, the β1 isoform presented a less defined pattern of expression. This isoform was detected in some tumor cells but not all, also the subcellular location differed among cells within a given adenocarcinomatous area, while some tumor cells where immunopositive for β1 at the cytoplasmic membrane location (**Figure 2D**) other cells presented immunostaining in a peri-nuclear position (**Figure 2C**).

Research by Rajasekaran and colleagues reported that Na,K-ATPase β subunit is required for epithelial polarization, suppression of invasion, and cell motility (Rajasekaran et al., 2001b), not only presence of Na,K-ATPase in the cell membrane but also Na,K-ATPase activity was important to form proper tight junctions, desmosomes, and induction of polarity in epithelial cells (Rajasekaran et al., 2001b). Further studies suggested that the transcription factor Snail might be repressing the β1 isoform and E-cadherin expression in carcinomas, associating these events to epithelial-mesenchymal transition (EMT) (Espineda et al., 2004).

Taken together, these studies and our results indicate that the level of expression and the location of the β subunit in epithelial cells are important for maintaining their well-differentiated phenotype, which disappears during cancer progression. Research published by our group on sodium pump isoform expression levels in stem cells has confirmed that adipose-derived mesenchymal stem cells express all known Na,K-ATPase isoforms, but some of these genes are turned off along differentiation (Acosta et al., 2011). In CRC cells or its metastases in liver we have never seen expression of all isoforms, rather, we have detected the expression signatures specified in **Table 2**.

Regarding liver metastases, to our knowledge, there have not been any reported studies in reference to Na,K-ATPase isoforms in liver metastasis. In this study the α1 isoform was detected in metastatic tumor cell niches within the liver, exhibiting a cytoplasmic subcellular localization in some cells and a membrane localization in others. The α3 isoform, however, was mainly detected at a peri-nuclear location and was more diffusely expressed across the cytoplasm of tumor metastatic cells. The healthy hepatic tissue presented the α1 isoform at the cytoplasmic membrane where it may establish the functional heterodimer with a β1 isoform and/or β2 isoform. Our observations of the subcellular localization of the α1 isoform are consistent with the first reported immunolocalization of this subunit in hepatocytes of healthy liver tissue (Sztul et al., 1987). However, in healthy liver tissue, the α3 isoform was not detected.

The β2 isoform was detected both at a more peri-nuclear position in some hepatocytes and throughout the cytoplasm in others, but not at the cytoplasmic membrane. The reason for this is unclear at present. It is possible that β2 isoform performs other *moonlighting* protein functions in hepatocytes. In metastasized liver, we detected the β1 isoform in disordered and semi-necrotic tumor tissue. However, β2 isoform was not detected in liver metastases. This may be related to the fact that these metastatic cells arise from CRC tumor cells, which did neither express β2 isoform or at very insignificant levels. Interestingly, apparently in healthy hepatic tissue surrounding the metastatic zone, the hepatocytes expressed the α3 isoform, a phenotype not detected in healthy hepatocytes from non-CRC patient according to our results. It might be possible that the CRC and the FOLFOX-CT affecting this patient could be influencing these hepatocytes driving them to express other genes, *ATP1A3* in this case.

The high levels of peri-nuclear and cytoplasmic α3 isoform in liver metastatic cells is potentially indicative of other *moonlighting* functions of this isoform besides ion transport (Jeffery, 2014; Magpusao et al., 2015; Min et al., 2015). In addition, the α3β1 isozyme may have utility as a novel exploratory biomarker for metastases cells. However, further studies need to be performed in order to confirm both, the moonlighting and biomarker assessments.

AUTHOR CONTRIBUTIONS

Conceived and designed the study and experiments: MM and PV. Patients were selected by: MM. Performed the experiments: MB, DR, MdCM, MG, and JÁ. Analyzed and discussed the data and discussed the written manuscript: All authors. Wrote the manuscript: MB, DR, AM, and PV. Constructed the figures and tables: MB, DR, and JÁ.

ACKNOWLEDGMENTS

This work was supported by grant FIS PI11/00114 to PMV and grant FIS PI12/00729, Spain, to JÁ. Grants MCT-FEDER 2003/2004 (Olympus FV-1000) and IMBRAIN-FP7-REGPOT-2012-31637 awarded to the Institute of Biomedical Technologies and the Center of Biomedical Research of the Canary Islands at ULL.

SUPPLEMENTARY MATERIAL

The Supplementary Material for this article can be found online at: http://journal.frontiersin.org/article/10.3389/fphys.2016.00009

REFERENCES

Abramowitz, J., Dai, C., Hirschi, K. K., Dmitrieva, R. I., Doris, P. A., Liu, L., et al. (2003). Ouabain- and marinobufagenin-induced proliferation of human umbilical vein smooth muscle cells and a rat vascular smooth muscle cell line, A7r5. *Circulation* 108, 3048–3053. doi: 10.1161/01.CIR.0000101919.00548.86

Acosta, E., Avila, J., Mobasheri, A., and Martin-Vasallo, P. (2011). Na+, K+-ATPase genes are down-regulated during adipose stem cell differentiation. *Front. Biosci.(Elite Ed).* 3, 1229–1240. doi: 10.2741/326

Aizman, O., Uhlen, P., Lal, M., Brismar, H., and Aperia, A. (2001). Ouabain, a steroid hormone that signals with slow calcium oscillations. *Proc. Natl. Acad. Sci. U.S.A.* 98, 13420–13424. doi: 10.1073/pnas.221315298

Akopyanz, N. S., Broude, N. E., Bekman, E. P., Marzen, E. O., and Sverdlov, E. D. (1991). Tissue-specific expression of Na,K-ATPase beta-subunit. Does beta 2 expression correlate with tumorigenesis? *FEBS Lett.* 289, 8–10. doi: 10.1016/0014-5793(91)80896-B

Antonicek, H., Persohn, E., and Schachner, M. (1987). Biochemical and functional characterization of a novel neuron-glia adhesion molecule that is involved in neuronal migration. *J. Cell Biol.* 104, 1587–1595. doi: 10.1083/jcb.104.6.1587

Arystarkhova, E., and Sweadner, K. J. (1996). Isoform-specific monoclonal antibodies to Na,K-ATPase alpha subunits. Evidence for a tissue-specific post-translational modification of the alpha subunit. *J. Biol. Chem.* 271, 23407–23417. doi: 10.1074/jbc.271.38.23407

Arystarkhova, E., and Sweadner, K. J. (1997). Tissue-specific expression of the Na,K-ATPase beta3 subunit. The presence of beta3 in lung and liver addresses the problem of the missing subunit. *J. Biol. Chem.* 272, 22405–22408. doi: 10.1074/jbc.272.36.22405

Avila, J., Lecuona, E., Morales, M., Soriano, A., Alonso, T., and Martin-Vasallo, P. (1997). Opposite expression pattern of the human Na,K-ATPase beta 1 isoform in stomach and colon adenocarcinomas. *Ann. N. Y. Acad. Sci.* 834, 653–655. doi: 10.1111/j.1749-6632.1997.tb52341.x

Barwe, S. P., Anilkumar, G., Moon, S. Y., Zheng, Y., Whitelegge, J. P., Rajasekaran, S. A., et al. (2005). Novel role for Na,K-ATPase in phosphatidylinositol 3-kinase signaling and suppression of cell motility. *Mol. Biol. Cell.* 16, 1082–1094. doi: 10.1091/mbc.E04-05-0427

Blanco, G. (2005). Na,K-ATPase subunit heterogeneity as a mechanism for tissue-specific ion regulation. *Semin. Nephrol.* 25, 292–303. doi: 10.1016/j.semnephrol.2005.03.004

Blanco, G., and Mercer, R. W. (1998). Isozymes of the Na-K-ATPase: heterogeneity in structure, diversity in function. *Am. J. Physiol.* 275, F633–F650.

Bleau, A. M., Agliano, A., Larzabal, L., de Aberasturi, A. L., and Calvo, A. (2014). Metastatic dormancy: a complex network between cancer stem cells and their microenvironment. *Histol. Histopathol.* 29, 1499–1510. doi: 10.14670/HH-29.1499

Book, C. B., Wilson, R. P., and Ng, Y. C. (1994). Cardiac hypertrophy in the ferret increases expression of the Na(+)-K(+)-ATPase alpha 1- but not alpha 3-isoform. *Am. J. Physiol.* 266, H1221–H1227.

Charlemagne, D., Orlowski, J., Oliviero, P., Rannou, F., Sainte, B. C., Swynghedauw, B., et al. (1994). Alteration of Na,K-ATPase subunit mRNA and protein levels in hypertrophied rat heart. *J. Biol. Chem.* 269, 1541–1547.

Charlemagne, D., and Swynghedauw, B. (1995). Myocardial phenotypic changes in Na+, K+ ATPase in left ventricular hypertrophy: pharmacological consequences. *Eur. Heart J.* 16(Suppl. C), 20–23. doi: 10.1093/eurheartj/16.suppl_C.20

Chiang, A. C., and Massague, J. (2008). Molecular basis of metastasis. *N. Engl. J. Med.* 359, 2814–2823. doi: 10.1056/NEJMra0805239

Crambert, G., Hasler, U., Beggah, A. T., Yu, C., Modyanov, N. N., Horisberger, J. D., et al. (2000). Transport and pharmacological properties of nine different human Na, K-ATPase isozymes. *J. Biol. Chem.* 275, 1976–1986. doi: 10.1074/jbc.275.3.1976

Espineda, C. E., Chang, J. H., Twiss, J., Rajasekaran, S. A., and Rajasekaran, A. K. (2004). Repression of Na,K-ATPase beta1-subunit by the transcription factor snail in carcinoma. *Mol. Biol. Cell.* 15, 1364–1373. doi: 10.1091/mbc.E03-09-0646

Ewart, H. S., and Klip, A. (1995). Hormonal regulation of the Na(+)-K(+)-ATPase: mechanisms underlying rapid and sustained changes in pump activity. *Am. J. Physiol.* 269, C295–C311.

Ferlay, J., Shin, H. R., Bray, F., Forman, D., Mathers, C., and Parkin, D. M. (2010). Estimates of worldwide burden of cancer in 2008: GLOBOCAN 2008. *Int. J. Cancer* 127, 2893–2917. doi: 10.1002/ijc.25516

Gloor, S., Antonicek, H., Sweadner, K. J., Pagliusi, S., Frank, R., Moos, M., et al. (1990). The adhesion molecule on glia (AMOG) is a homologue of the beta subunit of the Na,K-ATPase. *J. Cell Biol.* 110, 165–174. doi: 10.1083/jcb.110.1.165

Glynn, I. M. (1985). "The Na-K transporting adenosine triphosphatase," in *The enzymes of Biological Membranes*, *2nd Edn.*, eds A. N. Martonosi (New York, NY: Plenum Press), 35–114.

Gonzalez-Martinez, L. M., Avila, J., Marti, E., Lecuona, E., and Martin-Vasallo, P. (1994). Expression of the beta-subunit isoforms of the Na,K-ATPase in rat embryo tissues, inner ear and choroid plexus. *Biol. Cell.* 81, 215–222. doi: 10.1016/0248-4900(94)90003-5

Harwood, S., and Yaqoob, M. M. (2005). Ouabain-induced cell signaling. *Front. Biosci.* 10, 2011–2017. doi: 10.2741/1676

Hess, K. R., Varadhachary, G. R., Taylor, S. H., Wei, W., Raber, M. N., Lenzi, R., et al. (2006). Metastatic patterns in adenocarcinoma. *Cancer* 106, 1624–1633. doi: 10.1002/cncr.21778

Hieber, V., Siegel, G. J., Fink, D. J., Beaty, M. W., and Mata, M. (1991). Differential distribution of (Na, K)-ATPase alpha isoforms in the central nervous system. *Cell Mol. Neurobiol.* 11, 253–262. doi: 10.1007/BF00769038

Hundal, H. S., Marette, A., Mitsumoto, Y., Ramlal, T., Blostein, R., and Klip, A. (1992). Insulin induces translocation of the alpha 2 and beta 1 subunits of the Na+/K(+)-ATPase from intracellular compartments to the plasma membrane in mammalian skeletal muscle. *J. Biol. Chem.* 267, 5040–5043.

Jeffery, C. J. (2014). An introduction to protein moonlighting. *Biochem. Soc. Trans.* 42, 1679–1683. doi: 10.1042/BST20140226

Jemal, A., Bray, F., Center, M. M., Ferlay, J., Ward, E., and Forman, D. (2011). Global cancer statistics. *CA Cancer J. Clin.* 61, 69–90. doi: 10.3322/caac.20107

Jorgensen, P. L., Hakansson, K. O., and Karlish, S. J. (2003). Structure and mechanism of Na,K-ATPase: functional sites and their interactions. *Annu. Rev. Physiol.* 65, 817–849. doi: 10.1146/annurev.physiol.65.092101.142558

Kubben, F. J., Peeters-Haesevoets, A., Engels, L. G., Baeten, C. G., Schutte, B., Arends, J. W., et al. (1994). Proliferating cell nuclear antigen (PCNA): a new marker to study human colonic cell proliferation. *Gut* 35, 530–535. doi: 10.1136/gut.35.4.530

Lavoie, L., Levenson, R., Martin-Vasallo, P., and Klip, A. (1997). The molar ratios of alpha and beta subunits of the Na+-K+-ATPase differ in distinct subcellular membranes from rat skeletal muscle. *Biochemistry* 36, 7726–7732. doi: 10.1021/bi970109s

Lytton, J., Lin, J. C., and Guidotti, G. (1985). Identification of two molecular forms of (Na+,K+)-ATPase in rat adipocytes. Relation to insulin stimulation of the enzyme. *J. Biol. Chem.* 260, 1177–1184.

Magpusao, A. N., Omolloh, G., Johnson, J., Gascon, J., Peczuh, M. W., and Fenteany, G. (2015). Cardiac glycoside activities link Na(+)/K(+) ATPase ion-transport to breast cancer cell migration via correlative SAR. *ACS Chem. Biol.* 10, 561–569. doi: 10.1021/cb500665r

Malik, N., Canfield, V. A., Beckers, M. C., Gros, P., and Levenson, R. (1996). Identification of the mammalian Na,K-ATPase 3 subunit. *J. Biol. Chem.* 271, 22754–22758. doi: 10.1074/jbc.271.37.22754

Martin-Vasallo, P., Wetzel, R. K., Garcia-Segura, L. M., Molina-Holgado, E., Arystarkhova, E., and Sweadner, K. J. (2000). Oligodendrocytes in brain and optic nerve express the beta3 subunit isoform of Na,K-ATPase. *Glia* 31, 206–218. doi: 10.1002/1098-1136(200009)31:3<206::AID-GLIA20>3.0.CO;2-1

McGrail, K. M., Phillips, J. M., and Sweadner, K. J. (1991). Immunofluorescent localization of three Na,K-ATPase isozymes in the rat central nervous system: both neurons and glia can express more than one Na,K-ATPase. *J. Neurosci.* 11, 381–391.

Mercer, R. W., Biemesderfer, D., Bliss, D. P. Jr., Collins, J. H., Forbush, B. III. (1993). Molecular cloning and immunological characterization of the gamma polypeptide, a small protein associated with the Na,K-ATPase. *J. Cell Biol.* 121, 579–586. doi: 10.1083/jcb.121.3.579

Min, K. W., Lee, S. H., and Baek, S. J. (2015). Moonlighting proteins in cancer. *Cancer Lett.* 370, 108–116. doi: 10.1016/j.canlet.2015.09.022

Miyakawa-Naito, A., Uhlen, P., Lal, M., Aizman, O., Mikoshiba, K., Brismar, H., et al. (2003). Cell signaling microdomain with Na,K-ATPase and inositol 1,4,5-trisphosphate receptor generates calcium oscillations. *J. Biol. Chem.* 278, 50355–50361. doi: 10.1074/jbc.M305378200

Mobasheri, A., Avila, J., Cozar-Castellano, I., Brownleader, M. D., Trevan, M., Francis, M. J., et al. (2000). Na+, K+-ATPase isozyme diversity; comparative biochemistry and physiological implications of novel functional interactions. *Biosci. Rep.* 20, 51–91. doi: 10.1023/A:1005580332144

Mobasheri, A., Evans, I., Martin-Vasallo, P., and Foster, C. S. (2003a). Expression and cellular localization of Na,K-ATPase isoforms in dog prostate in health and disease. *Ann. N. Y. Acad. Sci.* 986, 708–710. doi: 10.1111/j.1749-6632.2003.tb07286.x

Mobasheri, A., Fox, R., Evans, I., Cullingham, F., Martin-Vasallo, P., and Foster, C. S. (2003b). Epithelial Na, K-ATPase expression is down-regulated in canine prostate cancer; a possible consequence of metabolic transformation in the process of prostate malignancy. *Cancer Cell Int.* 3, 8. doi: 10.1186/1475-2867-3-8

Mobasheri, A., Pestov, N. B., Papanicolaou, S., Kajee, R., Cozar-Castellano, I., Avila, J., et al. (2003c). Expression and cellular localization of Na,K-ATPase isoforms in the rat ventral prostate. *BJU Int.* 92, 793–802. doi: 10.1046/j.1464-410X.2003.04460.x

Morales, M., Avila, J., Gonzalez-Fernandez, R., Boronat, L., Soriano, M. L., and Martin-Vasallo, P. (2014). Differential transcriptome profile of peripheral white cells to identify biomarkers involved in oxaliplatin induced neuropathy. *J. Pers. Med.* 4, 282–296. doi: 10.3390/jpm4020282

Pachman, D. R., Loprinzi, C. L., Grothey, A., and Ta, L. E. (2014). The search for treatments to reduce chemotherapy-induced peripheral neuropathy. *J. Clin. Invest.* 124, 72–74. doi: 10.1172/JCI73908

Peng, L., Martin-Vasallo, P., and Sweadner, K. J. (1997). Isoforms of Na,K-ATPase alpha and beta subunits in the rat cerebellum and in granule cell cultures. *J. Neurosci.* 17, 3488–3502.

Pietrini, G., Matteoli, M., Banker, G., and Caplan, M. J. (1992). Isoforms of the Na,K-ATPase are present in both axons and dendrites of hippocampal neurons in culture. *Proc. Natl. Acad. Sci. U.S.A.* 89, 8414–8418. doi: 10.1073/pnas.89.18.8414

Rajasekaran, S. A., Ball, W. J. Jr., Bander, N. H., Liu, H., Pardee, J. D., and Rajasekaran, A. K. (1999). Reduced expression of beta-subunit of Na,K-ATPase in human clear-cell renal cell carcinoma. *J. Urol.* 162, 574–580. doi: 10.1016/S0022-5347(05)68629-6

Rajasekaran, S. A., Huynh, T. P., Wolle, D. G., Espineda, C. E., Inge, L. J., Skay, A., et al. (2010). Na,K-ATPase subunits as markers for epithelial-mesenchymal

transition in cancer and fibrosis. *Mol. Cancer Ther.* 9, 1515–1524. doi: 10.1158/1535-7163.MCT-09-0832

Rajasekaran, S. A., Palmer, L. G., Moon, S. Y., Peralta, S. A., Apodaca, G. L., Harper, J. F., et al. (2001a). Na,K-ATPase activity is required for formation of tight junctions, desmosomes, and induction of polarity in epithelial cells. *Mol. Biol. Cell.* 12, 3717–3732. doi: 10.1091/mbc.12.12.3717

Rajasekaran, S. A., Palmer, L. G., Quan, K., Harper, J. F., Ball, W. J. Jr., Bander, N. H., et al. (2001b). Na,K-ATPase beta-subunit is required for epithelial polarization, suppression of invasion, and cell motility. *Mol. Biol. Cell* 12, 279–295. doi: 10.1091/mbc.12.2.279

Sakai, H., Suzuki, T., Maeda, M., Takahashi, Y., Horikawa, N., Minamimura, T., et al. (2004). Up-regulation of Na(+),K(+)-ATPase alpha 3-isoform and down-regulation of the alpha1-isoform in human colorectal cancer. *FEBS Lett.* 563, 151–154. doi: 10.1016/S0014-5793(04)00292-3

Shibuya, K., Fukuoka, J., Fujii, T., Shimoda, E., Shimizu, T., Sakai, H., et al. (2010). Increase in ouabain-sensitive K+-ATPase activity in hepatocellular carcinoma by overexpression of Na+, K+-ATPase alpha 3-isoform. *Eur. J. Pharmacol.* 638, 42–46. doi: 10.1016/j.ejphar.2010.04.029

Shyjan, A. W., Cena, V., Klein, D. C., and Levenson, R. (1990). Differential expression and enzymatic properties of the Na+,K(+)-ATPase alpha 3 isoenzyme in rat pineal glands. *Proc. Natl. Acad. Sci. U.S.A.* 87, 1178–1182. doi: 10.1073/pnas.87.3.1178

Skou, J. C. (1957). The influence of some cations on an adenosine triphosphatase from peripheral nerves. *Biochim. Biophys. Acta* 23, 394–401. doi: 10.1016/0006-3002(57)90343-8

Sztul, E. S., Biemesderfer, D., Caplan, M. J., Kashgarian, M., and Boyer, J. L. (1987). Localization of Na+,K+-ATPase alpha-subunit to the sinusoidal and lateral but not canalicular membranes of rat hepatocytes. *J. Cell Biol.* 104, 1239–1248. doi: 10.1083/jcb.104.5.1239

Wang, X. Q., and Yu, S. P. (2005). Novel regulation of Na, K-ATPase by Src tyrosine kinases in cortical neurons. *J. Neurochem.* 93, 1515–1523. doi: 10.1111/j.1471-4159.2005.03147.x

Woo, A. L., James, P. F., and Lingrel, J. B. (2000). Sperm motility is dependent on a unique isoform of the Na,K-ATPase. *J. Biol. Chem.* 275, 20693–20699. doi: 10.1074/jbc.M002323200

Yang, P., Cartwright, C., Efuet, E., Hamilton, S. R., Wistuba, I. I., Menter, D., et al. (2014). Cellular location and expression of Na+, K+ -ATPase alpha subunits affect the anti-proliferative activity of oleandrin. *Mol. Carcinog.* 53, 253–263. doi: 10.1002/mc.21968

Yuan, Z., Cai, T., Tian, J., Ivanov, A. V., Giovannucci, D. R., and Xie, Z. (2005). Na/K-ATPase tethers phospholipase C and IP3 receptor into a calcium-regulatory complex. *Mol. Biol. Cell* 16, 4034–4045. doi: 10.1091/mbc.E05-04-0295

Zahler, R., Brines, M., Kashgarian, M., Benz, E. J. Jr., and Gilmore-Hebert, M. (1992). The cardiac conduction system in the rat expresses the alpha 2 and alpha 3 isoforms of the Na+,K(+)-ATPase. *Proc. Natl. Acad. Sci. U.S.A.* 89, 99–103. doi: 10.1073/pnas.89.1.99

Zahler, R., Gilmore-Hebert, M., Sun, W., and Benz, E. J. (1996). Na, K-ATPase isoform gene expression in normal and hypertrophied dog heart. *Basic Res. Cardiol.* 91, 256–266. doi: 10.1007/BF00788912

Zhang, S., Malmersjo, S., Li, J., Ando, H., Aizman, O., Uhlen, P., et al. (2006). Distinct role of the N-terminal tail of the Na,K-ATPase catalytic subunit as a signal transducer. *J. Biol. Chem.* 281, 21954–21962. doi: 10.1074/jbc.M601578200

Conflict of Interest Statement: The authors declare that the research was conducted in the absence of any commercial or financial relationships that could be construed as a potential conflict of interest.

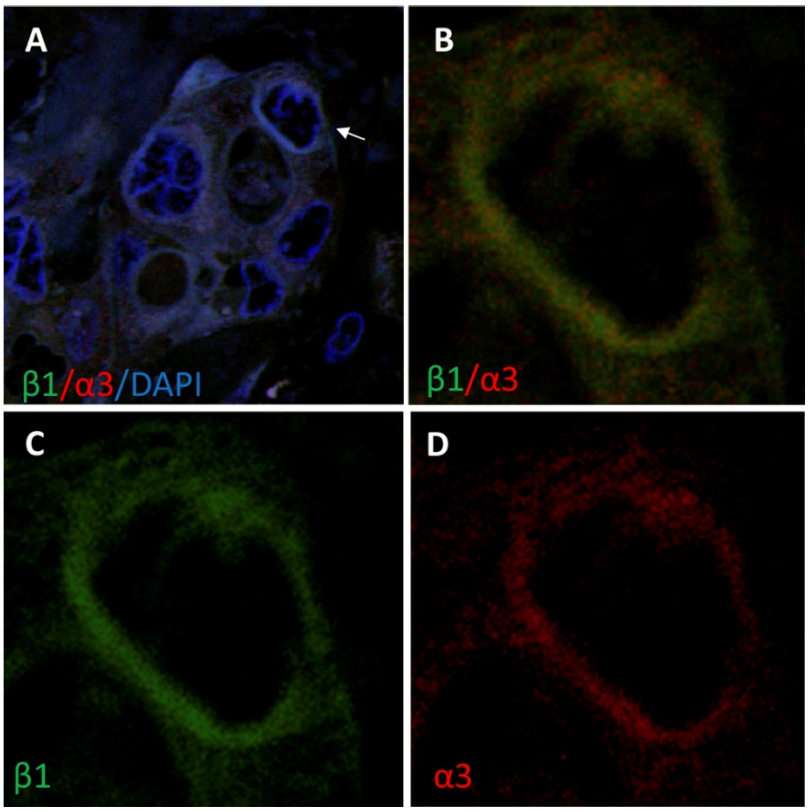

Legend of supplementary Figure S1:

Double immunofluorescence localization of Na,K-ATPase α3 (red) and β1(green) isoforms in liver metastasis. A) α3 and β1 isoforms co-localize at the nuclear envelope in malignant cells. B-D) Magnification of the malignant cell pointed in A; B) α3 and β1 merge. C) β1. D) α3.